University of Babylon
College of Engineering
Department of Civil Engineering

NONLINEAR FINITE ELEMENT ANALYSIS OF REINFORCED CONCRETE BEAM-COLUMN CONNECTION WITH INTERFACE ELEMENTS UNDER CYCLIC LOADING

A Thesis
Submitted to the College of Engineering of the University of Babylon in Partial Fulfillment of the Requirements for the Degree of Master of Science
in
Civil Engineering (Structural Engineering)

By
Israa Khudhair Al-Shimmari

B.Sc. Civil Engineering (١٩٩٩)

Supervisor
Prof. Dr. Husain M. Husain

Assist Prof. Dr. Mustafa B. Dawood

February ٢٠٠٦ **Muhram ١٤٢٧**

جامعة بابل

كلية الهندسة
قسم الهندسة المدنية

تحليل منطقة الربط للعتب والعمود الكونكريتي المسلح تحت تأثير الأحمال الدورية مع استعمال عناصر بينية

اطروحة
مقدمة الى كلية الهندسة في جامعة بابل

وهي جزء من متطلبات نيل

درجة ماجستير علوم في

الهندسة المدنية

(انشاءات)

من قبل
إسراء خضير محسن

بكلوريوس علوم الهندسة المدنية ١٩٩٩
اشراف
أ.د. حسين محمد حسين

أ.م. مصطفى بلاسم داود

شباط ٢٠٠٦ **محرم ١٤٢٧**

الخلاصة

لغرض دراسة الاستجابة اللاخطية لمناطق الربط بين الأعتاب والأعمدة الخرسانية المسلحة بوجود تأثير المفاصل الانشائية للاحمال الدورية المؤثرة عليها ، تمت الاستعانة ببرنامج يعمل أساسا لتحليل المنشاءات تحليلا لاخطيا باستخدام برنامج العناصر المحددة المكتوب من قبل الدكتور احسان الشعرباف. تم تطوير هذا البرنامج ليأخذ تأثير المفاصل الإنشائية بنظر الاعتبار تحت تأثير الأحمال الدورية.

يستخدم البرنامج العنصر الطابوقي ذي العشرين عقدة لتمثيل الخرسانة أما حديد التسليح فقد تم تمثيله بعناصر محورية مطمورة داخل العناصر الطابوقية . تم توضيح أنموذجا خاصاً بالتصرف اللاخطي في حالة تعرض الخرسانة لاجهادات محورية أو اجهادات مسلطة على محاور متعددة . كذلك تم تطوير أنموذجا لاخطياً يأخذ بالحسبان تعرض حديد التسليح إلى أحمال دورية .

اعتبر تصرف الخرسانة تحت تأثير الأحمال الدورية في الانضغاط تصرفا" مرنا" لدنا" يتبعه تصرف تام اللدونة. أما لتمثيل سلوك الخرسانة تحت تأثير اجهادات الشد فقد تم تبني أنموذج التشقق المنتشر (Smeared Crack Model) و استعمل أنموذج تصلب الشد (Tension – Stiffening Model) لاحتساب اجهادات الشد المتبقية في الخرسانة المسلحة بعد تشققها. كذلك اخذ بنظر الاعتبار احتمالية انغلاق و إعادة فتح الشقوق أثناء التحميل الدوري.

حلت معادلات التوازن اللاخطية باستخدام طريقة تزايدية تكرارية (Incremental-Iterative technique) تعمل تحت تحكم الحمل (Load Control) و بالاستعانة بطريقة انيوتن-

رافسن المعدلة. أجريت التكاملات العددية باستخدام قاعدة التكامل ذات ٢٧ نقطة تكامل.

اما سلوك انتقال القص بين خرسانتين تم صبهما باوقات مختلفة فتم تمثيله باستخدام عنصر طبقة بيني ذي العشرين عقدة كما اعتمد نموذجي فرونتيدو و ميلارد لتمثيل صلابة تداخل الركام و توتيد الحديد على التوالي .

تمت المقارنة مع النتائج المختبرية المتوفرة لمفاصل الاعتاب والاعمدة الخرسانية بوجود تأثير المفاصل الانشائية و النتائج المستحصلة كانت مقاربة للنتائج المختبرية المتوفرة. حيث ان اكبر فرق لحمل الفشل ٣.٩% . كانت النتائج تشير الى ان الفشل في كل الحالات حدث في العتب الخرساني كما ان وجود المفصل الانشائي يؤدي الى تناقص ملحوظ في صلابة القص ويؤثر فقط على دوران المفصل ضمن العمود الخرساني وانفعالاته القصية.

كما تم عرض دراسة مقارنة تتعلق بالمفصل الانشائي وذلك باخذ وضعيات مختلفة للمفصل وهي تتضمن مواقع مختلفة للمفصل الانشائي، مقدار الحمل العمودي المسلط على العمود، مقاومة الكونكريت للصبة الثانية، مقدار الحديد المار بالمفصل.

ABSTRACT

To study the nonlinear response of corner beam-column junctions with inclusion of the effect of construction joint between the column and the beam cast at different times and subjected to cyclic and repeated loads, a computer program of three dimensional nonlinear finite element analysis, written by Al-

Shaarbaf, (P۲DNFEA) has been extended to account for the effect of construction joints on the behavior and to deal with concrete behavior under cyclic loads .

The ۲۰-node isoparamatric brick elements have been used to model the concrete, while the reinforcing bars are modeled as axial members embedded within the brick elements. A nonlinear cyclic behavior model for concrete is developed in uniaxial and multiaxial states of stress. Also,

a nonlinear cyclic behavior model for reinforcing bars is presented.

In compression, the behavior of concrete under cyclic loads is simulated by an elasto-plastic work hardening model followed by a perfectly plastic response. In tension, a fixed smeared crack model has been used to simulate the behavior of concrete with a tension-stiffening model to represent the retained post-cracking tensile stresses in concrete. Closing and

reopening of cracks during cyclic loading has been taken into consideration.

The nonlinear equations of equilibrium have been solved using an incremental-iterative technique based on the modified Newton-Raphson method. The convergence of the solution was controlled by a force convergence criterion. The numerical integration has been conducted by using ٢٧-point Gaussian rule.

To represent the shear transfer between two concretes cast at different times, ٢٠-noded interface layer brick elements are used with Fronteddu's and Millard's models to represent the aggregate interlock and the dowel stiffness, respectively. Comparison between the results obtained by the finite elements and the available experimental results is made for two examples. First example is a cantilever loaded by a concentrated cyclic load and the

other is a corner beam-column junction with inclusion of the effect of a construction joint. Good agreement is obtained. The maximum difference in ultimate load is ۳.۹٪.

A parametric study dealing with construction joint is presented by taking various conditions of the junction. These include the axial load on the column, strength of concrete in the second cast and the amount of dowels crossing the joint.

Acknowledgments

In the name of Allah, the most gracious, the most merciful. Before anything, thank to Allah who enabled me to achieve this research.

I wish to express my deep gratitude and great appreciation to Prof. Dr. Husain M. Husain, thesis advisor, whose advise, kindness, generous guidance, valuable suggestions, active interest guidance and help through the time of this research were indispensable.

Assist Prof. Dr. Mustafa B. Dawood, thesis advisor, for his valuable guidance, encouragement, and his help throughout the preparation of this work.

I wish to express my special thanks to Dr. Ihsan Al–Shaarbaf for his appreciable assistance in providing his computer program.

Special thanks to my friends and colleagues for their encouragements and helps to complete this thesis especially Dina M. for her help in providing the computer program.

Finally, I would like to express my sincere thanks and gratitude to my family for their encouragement and support during this work.

Israa

Evaluation of the Flow Vector

The flow vector {a}, is defined as the derivative of the yield function with respect to the stress components, and given by:

$$\{a\} = \left[\frac{\partial f}{\partial \sigma_x}, \frac{\partial f}{\partial \sigma_y}, \frac{\partial f}{\partial \sigma_z}, \frac{\partial f}{\partial \tau_{xy}}, \frac{\partial f}{\partial \tau_{yz}}, \frac{\partial f}{\partial \tau_{zx}} \right] \qquad \text{(B-١)}$$

where,

$$\left.\begin{aligned} a_1 &= \frac{\partial f}{\partial \sigma_x} = c + \left[2\left(c^2 + \beta\right)\sigma_x + \left(2c^2 - \beta\right)\left(\sigma_y - \sigma_z\right) \right] / Q \\ a_2 &= \frac{\partial f}{\partial \sigma_y} = c + \left[2\left(c^2 + \beta\right)\sigma_y + \left(2c^2 - \beta\right)\left(\sigma_x - \sigma_z\right) \right] / Q \\ a_3 &= \frac{\partial f}{\partial \sigma_z} = c + \left[2\left(c^2 + \beta\right)\sigma_z + \left(2c^2 - \beta\right)\left(\sigma_x - \sigma_z\right) \right] / Q \end{aligned}\right\} \qquad \text{(B-٢)}$$

$a_4 = \frac{\partial f}{\partial \sigma_x} = 6.\beta.\tau_{xy}/Q$

$a_5 = \frac{\partial f}{\partial \sigma_y} = 6.\beta.\tau_{yz}/Q$

$a_6 = \frac{\partial f}{\partial \sigma_z} = 6.\beta.\tau_{zx}/Q$

where c and β, are the material constants, and Q is given by:

$$Q = 2\left[\begin{matrix}\left(c^2+\beta\right)\left(\sigma_x^2+\sigma_y^2+\sigma_z^2\right)+\left(2c^2-\beta\right)\left(\sigma_x\sigma_y+\sigma_y\sigma_z+\sigma_z\sigma_x\right)\\ 3\beta\left(\tau_{xy}^2+\tau_{yz}^2+\tau_{zx}^2\right)\end{matrix}\right]^{1/2} \qquad \text{(B-3)}$$

Table (A-1) Weights and Locations of Sampling Points in The 27 and 15 Integration Rules

Points	27 Integration Rule				15a,15b, 14 Integration Rule			
	ξ	η	ζ	Weight	ξ	η	ζ	Weight
1	+A	−A	−A	W1	0.0	0.0	0.0	W1
2	0.0	−A	−A	W2	0.0	−B	0.0	W2
3	−A	−A	−A	W1	0.0	+B	0.0	W2

٤	–A	0	–A	W٢	0.0	0.0	–B	W٢
٥	–A	+A	–A	W١	0.0	0.0	+B	W٢
٦	0	+A	–A	W٢	1.0	0.0	0.0	W٢
٧	+A	+A	–A	W١	–B	0.0	0.0	W٢
٨	+A	0.0	–A	W٢	+C	-C	-C	W٣
٩	٠.٠	٠.٠	-A	W٣	+C	+C	-C	W٣
١٠	+A	-A	٠.٠	W٢	+C	-C	+C	W٣
١١	٠.٠	-A	٠.٠	W٣	+C	+C	+C	W٣
١٢	-A	-A	٠.٠	W٢	-C	-C	-C	W٣
١٣	-A	٠.٠	٠.٠	W٣	-C	+C	-C	W٣
١٤	-A	+A	٠.٠	W٢	-C	-C	+C	W٣
١٥	٠.٠	A	٠.٠	W٣	-C	+C	+C	W٣
١٦	+A	+A	٠.٠	W٢				
١٧	+A	٠.٠	٠.٠	W٣				
١٨	٠.٠	٠.٠	٠.٠	W٤				
١٩	+A	-A	+A	W١				
٢٠	٠.٠	-A	+A	W٢				
٢١	-A	-A	+A	W١				
٢٢	-A	٠.٠	+A	W٢				
٢٣	-A	+A	+A	W١				
٢٤	٠.٠	+A	+A	W٢				
٢٥	+A	+A	+A	W١				
٢٦	+A	٠.٠	+A	W٢				
٢٧	٠.٠	٠.٠	+A	W٣				

where

Symbol	Integration Rule			
	٢٧	١٥a	١٥b	١٤
A	٠.٧٧٤٥٩	-	-	-
B		١.٠	٠.٨٤٨٤٢	٠.٧٩٥٨٢
C		٠.٦٧٤١	٠.٧٢٧٦٦	٠.٧٥٨٧٨
W١	٠.١٧١٤٦٨	١.٥٦٤٤	٠.٧١٢١٣٧	٠
W٢	٠.٢٧٤٣٥	٠.٣٥٥٦	٠.٦٨٦٢٢٧	٠.٨٨٦٤٢٧
W٣	٠.٤٣٨٩٥٧٥	٠.٥٣٧٧٨	٠.٣٩٦٣١٢	٠.٣٣٥١٨
W٤	٠.٧٠٢٣٣٢	-	-	-

CERTIFICATE

We certify that this thesis titled ***NONLINEAR FINITE ELEMENT ANALYSIS OF REINFORCED CONCRETE BEAM-COLUMN CONNECTION WITH INTERFACE ELEMENTS UNDER CYCLIC LOADING,*** was prepared by ***Israa Khudhair Al-Shimmari*** under our supervision at the **University of Babylon** in partial fulfillment of the requirement for the degree of ***Master of Science in Civil Engineering (Structural Engineering).***

Signature **Signature**

Supervisor: ***Prof. Dr. Husain M. Husain*** **Supervisor:** ***Assist Prof.***

Dr.Mustafa.**B.Dawood**

Date*:* **/** **Date*:*** **/**

Date: /

D a t e

CONTENTS

CHAPTER ONE

INTRODUCTION

CHAPTER TWO

LITERATURE REVIEW

CHAPTER THREE

FINITE ELEMENT FORMULATION AND SOLUTION TECHNIQUES

CHAPTER FOUR

MODELING OF MATERIAL PROPERTIES

CHAPTER FIVE

INTERFACE ELEMENT

CHAPTER SIX

APPLICATIONS OF FINITE ELEMENT ANALYSISTO
BEAM - COLUMN JOINTS

Notation

The major part of the symbols used in the text is listed below. Others are defined when they first appear.

General Symbols

$[A]^T$, $\{a\}^T$ Transpose of matrix [A] and vector {a}

$\mathbf{[A]^{-1}}$	Inverse of matrix [A]
$\mathbf{d}$, ∂	Differential symbols
$\mid \mid$, **det.**	Determinant of a Matrix or absolute value
{ }	Vector
[ ]	Matrix

Scalar

$\mathbf{A_s}$	Area of tension reinforcing steel
$\mathbf{C_p}$	Plasticity coefficient
$\mathbf{d\lambda}$	Plastic multiplier
E	Modulus of elasticity
$\mathbf{E_c}$	Modulus of elasticity of concrete
$\mathbf{E_s}$	Modulus of elasticity of steel
f	Function
$\mathbf{f_c'}$	Uniaxial compressive strength of concrete
$\mathbf{f_t}$	Uniaxial tensile strength of concrete
$\mathbf{f_r}$	Modulus of rupture of concrete
H'	Hardening parameter
$\mathbf{I_1}$	First stress invariant
J	Jacobean

$\bar{I}_1$	First strain invariant
J'_2	Second deviatoric strain
J_2	Second deviatoric stress invariant
S	Surface area
V	Volume
W	Weight of a sampling point
u , v, w	Displacement components in x,y and z Cartesian coordinates
x , y , z	Cartesian coordinates
r , s , t	Natural coordinates
α_1 , α_2	Tension-stiffening parameters
β	Shear retention factor
γ	Shear strength
γ_1 , γ_2 , γ_3	Shear retention parameters
ε	Strain
ε_{cu}	Ultimate strain of concrete
ν	Poisson's ratio
σ	Stress
σ_o	Effective stress at onset of plastic deformation
σ^*	Effective stress

ξ, η, ζ	***Natural coordinate system***
$\mathbf{N_i}$	Shape function at the ith node
$\mathbf{W_{int}}$	Internal work
$\mathbf{W_{ext}}$	External work
$\bar{\sigma}$	Equivalent uniaxial stress
$\boldsymbol{\sigma_{cr}}$	Cracking stress of concrete
ε_{cr}	Cracking strain
σ_n	Stress normal to the cracked plane
ε_n	Strain normal to the cracked plane

Matrix

[A]	Displacement gradient matrix
[B]	Strain displacement matrix
[B`]	Strain displacement matrix of the bar element
[D]	Constitutive matrix
[D`]	Constitutive matrix for bar element
$\mathbf{[D]^e}$	Elastic constitutive matrix
[J]	Jacobean matrix
[K]	Stiffness matrix
[K`]	Stiffness matrix for bar element
[N]	Shape function

[T]	Transformation matrix

Vector

{a}	Nodal displacement or flow vector
{f}	External load vector
{P}	Internal load
{r}	Residual load vector
{u}	Displacement vector
{ε}	Strain vector
{σ}	Stress vector

Abbreviation

ACI	American concrete institute
ASCE	American society of civil engineering

CHAPTER ONE

INTRODUCTION

١.١ General

Many concrete structures are subjected to cyclic loads during their life span. These cyclic loads may arise from earthquake ground motion, wind pressure, wave action, blast, machine vibrations, and traffic movement and from other sources of repeated loads.

Experimental investigations to determine the complex effect of cyclic loading behavior of structures are important, but these investigations do not cover all parameter variations.. Analytical models and computer technology allow studying all parameter variations with less time and cost **[Jwad (١٩٩٢)]**. At present, the finite element method offers a powerful and general analytical and research tool to investigate the behavior of reinforced concrete members under cyclic loading. By this method, the complex behavior of reinforced concrete structures including the material nonlinearty such as, cracking, tension-stiffening effect, crushing of concrete and yielding of steel, which were previously ignored or treated in a very approximate way, can be incorporated into the analysis in a more rational manner.

١.٢ Beam-Column Joint

The reinforced concrete beam-column joint is defined as the portion of the column within the depth of the beam framing into the column.

An important result from the research done so far is that the notion of a rigid joint can be discarded forever. Thus, just as beams, columns and other structural elements exhibit flexibility in response to applied loading, so do the joints.

١.٣ Classification of Beam-Column Joint

Structural joints are classified into two categories in accordance with the loading conditions on the joint .

Type ١ : A joint for which the primary design criterion is strength and no significant inelastic deformations are expected .

Type ٢ : A joint connecting members for which the primary design criterion is the sustained strength under reversals in the inelastic range .

The requirements for joints are dependent on the deformations at the joint imposed by the loading condition. Typical applications of each joint type are listed below .

١.٤ Definitions

Cyclic load: is a sequence of loading (or displacements) which acts in the form of successive cycles with constant or variable intensity. Two types of cyclic loading are commonly considered:

a) Repeated loading which means a sequence of loading whose magnitudes vary between zero and a peak load in one direction.
b) Reversed cyclic loading which means a sequence of loading whose magnitudes vary between a peak load in one direction and a peak load in the reversed direction about a neutral point where each cycle contains both tension and compression half-cycle.

١.٥ Failure Modes in Region of Beam-Column Joint

Five different modes of failure are possible in the beam-column connection region, Fig.(١.١).The most desirable failure mode , is a ductile flexural failure of the beams at the connection ,Fig.(١.١.a) . Formation of hinges in the beams outside the connection allows for absorption of energy through large inelastic deformations without loss of strength . Although the mechanism is the same as beam hinging , hinging of the column is less desirable than beam hinging Fig.(١.١.b). Loss of the concrete cover over the reinforcement in the beam-column core,Fig.(١.١.c) , is undesirable since the column compressive load capacity may be reduced . The loss of anchorage of the reinforcement, Fig.(١.١.d),is undesirable because lateral shear can no longer be transmitted by the frame . The consequences of failure of the connection in shear are the same as loss of anchorage , Fig.(١.١.e) .

١.٦ Objective and Scope

Different codes and specifications give rules for design of beam-column joints. Such design rules are usually adequate for all situations. However, on occasions a more detailed method of analysis is required which takes into account most of the principal parameters .

The finite element method is one of the methods widely used to explore the behavior of a beam-column joint which is cast monolithically, but no attempt has been done yet to analyze a beam-column joint which is cast at two stages, as this is complicated by a structural discontinuity due to possible occurrence of slip and vertical separation between the two pours. Finite element representation of those movements is usually achieved by using special interface elements. The

present work is devoted to the study of the behavior of a corner beam-column junction with inclusion of the effect of occurrence of a construction joint when the joint is under cyclic loading by using the finite element method. The computer program was originally written by [**Al-Shaarbaf (١٩٩٠)]**, is developed in the present study to be applicable to analyze reinforced concrete structures with considering the effect of construction joints and the effect of cyclic loading.

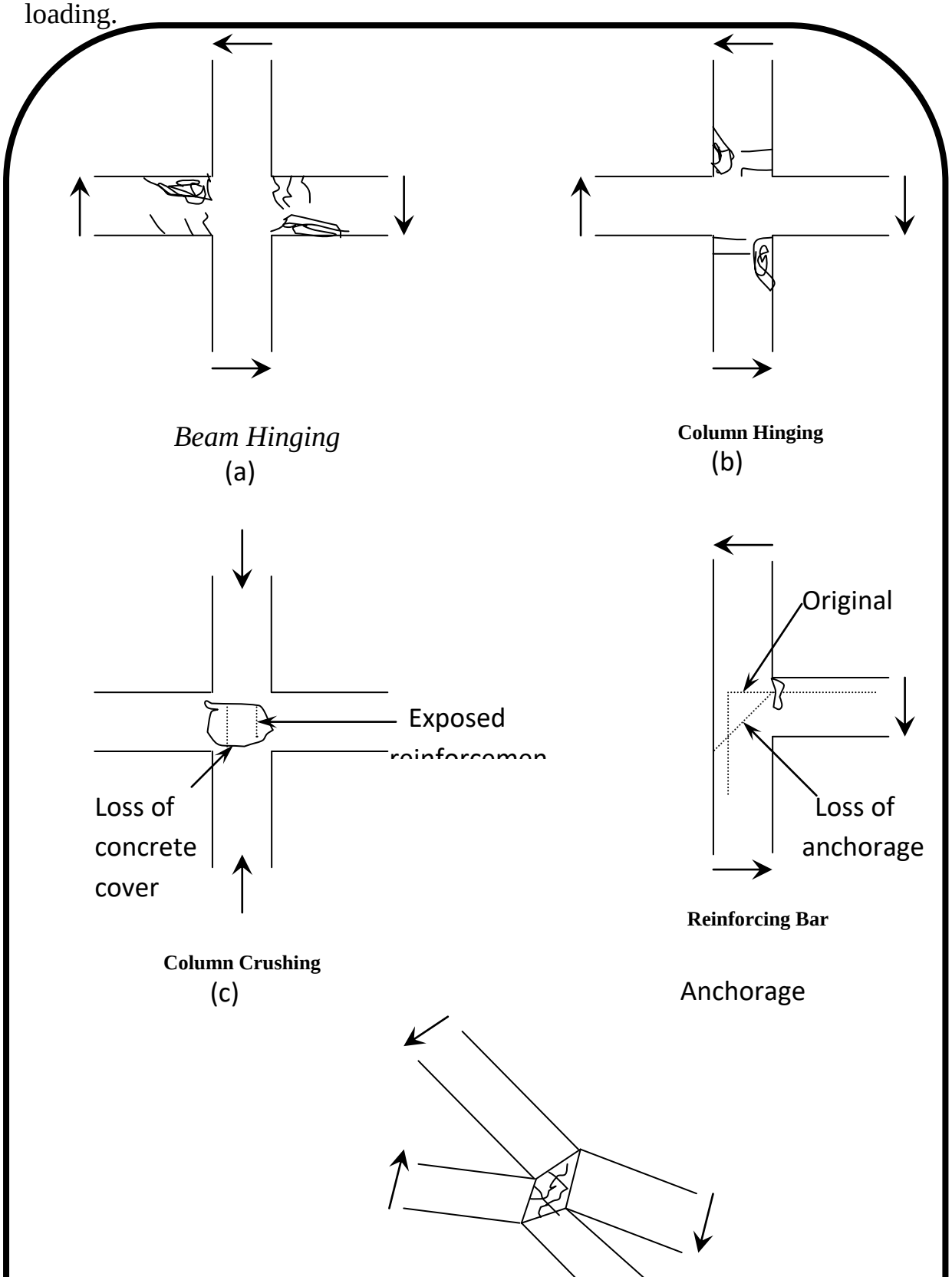

١.٧ Thesis Layout

The thesis contains seven chapters. The present chapter one introduces the problem to be investigated in the present study.

Chapter two gives a review of theoretical and experimental work on the behavior of reinforced concrete under cyclic loads, the available tests on beam-column joints and the effect of interface between two concretes cast at different times (construction joint).

In chapter three, the finite element formulation is illustrated by presenting the derivation of the governing equilibrium equations and the numerical integration rule used to evaluate the stiffness matrix.

Chapter four, deals with the modeling of concrete material properties, which are illustrated in terms of the following constituents; the yield criterion, the hardening rule, the flow rule and the crushing condition. Steel reinforcement properties are also presented.

Chapter five is concerned with the review of the various material models adopted in this study to represent the behavior of interface between two concretes, cast in different times.

In chapter six, the result of the nonlinear analysis of three different examples are presented. The numerical analysis results of two examples are compared with the available experimental results and a parametric study dealing with construction joint is presented.

Finally, a summary of the conclusions drawn from this study and recommendations for future research are given in chapter seven .

CHAPTER TWO
LITERATURE REVIEW

٢.١ General

This chapter is devoted to review the available experimental studies that deal with reinforced concrete beam-column joints, review concerning the use of the finite element method for the analysis of reinforced concrete members and also, behavior of reinforced concrete members under cyclic loads. Shear transfer tests are also reviewed.

٢.٢ Experimental Studies on Reinforced Concrete Beam-Column Joints

Besides the number of experimental investigations about the behavior of reinforced concrete beam-column joints, there is a scarce and limited number of theoretical and analytical studies in this field. The followings are several investigations of reinforced concrete beam-column joints presented chronologically:

Hanson and Connor (١٩٦٧) tested a series of beam-column joint specimens to determine joint reinforcement required for ultimate capacity of cast-in-place beams and columns subjected to multiple reversals of loading of major earthquake magnitudes. The principal variables of this study were column size, column load, and degree of confinement of concrete in the joint. An exterior column and beam joint was selected for the study. This is the most critically loaded joint in a multistory building. A series of six specimens was tested. Two column sizes and two amount of hoop reinforcement in the joint were included. These specimens were tested under two levels of column load. A seventh specimen with short spandrel beam stubs was also tested. This represented a less critical joint, since the connection was confined to two sides by surrounding concrete members. During the tests, they found that joints connecting beam and column need special attention in design :

١.Hoops are required for unconfined (isolated) beam-column joints. A design procedure for hoops based on supplying adequate confinement and shear resistance will provide safe design.

٢.Corner joints with beams on only two column faces should be designed as unconfined joints that require hoops until tests are made for this case.

٣.Hoops are not required for exterior joints confined to at least three sides by beams or spandrels of approximately equal depth and meeting (ACI ٣١٨-٦٣) requirements for concrete strength needed to transfer the column load through the joint.

٤.The cumulative ductility of a test specimen provides a measure of the ability of a structure to withstand seismic deformation, well detailed joints sustained high values of cumulative ductility while they maintain their strength. Omission of important hoop reinforcement reduces the amount of cumulative ductility, which could be sustained

Lee et al (١٩٧٧), tested ٦ reinforced concrete exterior beam-column joints with various design and loading conditions to investigate the behavior of such joints under large load reversals. The design and testing variables were the amount of transverse reinforcement, the magnitude of axial load on the column and the severity of loading. The specimens were tested in horizontal position. During the test of the specimens, the force and deflection at the beam loading point were recorded continuously and used to monitor the progress of the test. Results from this investigation clearly indicate that the "truss analogy" is not a reliable method for determining the contribution of the transverse reinforcement to the shear strength of reinforced concrete beam-column joint.

Meinheit and Jirsa (١٩٨١), tested ١٤ beam-column joint specimens to evaluate the factors that influence shear capacity of the beam-column connection. Several parameters were varied over relatively wide ranges in the investigation. The strength of the connection was governed primarily by the cross-sectional area of the joint. From the tested specimens, the variation of the test parameters can be summarized as follows:

١.Transverse reinforcement in the connection improves the shear capacity.
٢.Column longitudinal reinforcement, if increased, does not produce similar increases in shear strength as seen when transverse reinforcement increases.
٣.Unloaded transverse beams improve the shear capacity, the largest increase, about ٢٠٪, is observed when the transverse beams masked most of the side faces of the columns.
٤.Column axial load has no effect on ultimate shear capacity of the connection, but with higher axial compressive load, the shear at first cracking in the connection is increased.
٥.Connection geometry has no influence on shear strength of the joint, when the shear area of the connection remains constant.

Durrani and Wight (١٩٨٥), studied the performance of interior beam-column joints which had less transverse reinforcement than required by the draft recommendations of ACI-ASCE committee ٣٥٢. They investigated the effect of the level of joint shear stress on strength, stiffness, and energy dissipation of

beam-column joints and examined the slippage of beam and column bars through the joint. To achieve these objectives, three interior beam-column joints were designed according to the provision of Appendix A of the ACI Building code [١٩٧٧] and tested under reversed cyclic loading. From the tests, the following conclusions are drawn:-

١.The joint shear stress appears to have a significant effect on strength and stiffness of joints at larger ductility levels (greater than two). A lower joint shear stress helps to stabilize the loss of strength and stiffness irrespective of the amount of reinforcement in the joint.
٢.The joint hoop reinforcement is more effective for lower ductility levels.
٣.Lower joint shear stress seems to be more effective in reducing the joint shear deformation and slippage of bars than the addition of more joint reinforcement.
٤.For higher energy dissipation, a combination of a lower joint shear stress and a moderate amount of joint reinforcement is found to be more effective than a combination of a higher shear stress level and a heavily reinforced joint.
٥.Minimum column-to-beam flexural strength ratio of (١.٥) is found to be suitable for design.

Sarsam and Phipps (١٩٨٥), reported on tests carried out by the author that there are five high strength exterior beam-column joints. The loading was applied in two stages. In the first stage, the column was loaded to a predetermined concentric load and this was kept constant throughout the test. In the second stage, the beam was loaded near its tip as a cantilever until either the joint failed or the beam failed. The specimens were grouped to examine different parameters. From test results, all five specimens exhibited joint diagonal cracking. Up to the diagonal cracking point, there was no noticeable difference in behavior due to the presence of joint hoops. The restraining influence of hoops was increasingly evident on reaching the yield point of the beam tension steel, and the beam compression concrete crushing point. The specimen without hoops, failed in joint shear, after which it exhibited a rapid rise in joint deformation together with a continuing drop in the joint load-carrying capacity. On the other hand, in the specimens with hoops, the joint remained intact after the first cracking, failure being in the beam. Upon unloading, the presence of joint hoops led to its rebound stiffness being more than twice that of the specimens without joint hoops. The specimen without hoops, exhibited concrete sapling and large joint cracking at failure. In contrast, four other specimens, which had hoops, had only hairline cracks in their joints. This illustrates the importance of horizontal joint hoops. They prevent excessive joint deformation, large joint cracks and joint failure.

Hamil and Scott (٢٠٠٠), investigated the presence (or absence) of column ties (hoops) within the connection zone of a reinforced concrete beam-column joint by using test results from sixteen external connection specimens. Specimens were made using high strength concrete and the results were compared with those from a similar set of normal strength concrete specimens. Two methods of anchoring the beam steel bars within the connection zone were used; bending the bar down into the column and using a U-bar. From their investigation they observed:

١.Initial joint cracking is strongly influenced by the tensile strength of the concrete within the connection zone. Specimens made with high strength concrete have a greater resistance to initial joint cracking due to their greater tensile strength.

٢. The number of connection ties in the joint does not affect the performance of the joint until after cracking occurs.

٣. Bending the main beam steel bars down into the column, rather than using a U-bar, increases the ultimate load at which a specimen fails.

٤.The load-deflection response of specimens made from high strength concrete is seen to be twice as stiff compared with specimens made from normal strength concrete.

٢.٣ Theoretical Studies

In this section, a review of the theoretical studies using the analytical methods to analyze reinforced concrete beam-column joints, by the finite element method is presented :-

٢.٣.١ Theoretical Studies on Reinforced Concrete Beam-Column Joints:

Ueda et al (١٩٨٦), developed a computer program to predict the loaded end deformation and anchorage length requirements for reinforcing bars extending from beams into exterior columns and subjected to large inelastic loading.

The numerical model incorporated several basic elements:
١.A local bond stress-slip relationship.
٢.A stress-strain relationship for the steel.
٣.A failure criterion.
٤.An equivalent embedment length criterion for a hooked bar.

The force displacement relationships were in good agreement with the results obtained in tests on ٢٢ specimens. Consideration should be given to better defining the objective of development length requirement in codes. The objectives should be :

١.To permit a bar to develop a stress at least (١.٢٥) times the specified yield stress for the bar, a requirement that is consistent with recommendation of committee ٣٥٢ [ACI-ASCE ١٩٨٥].

٢.The loaded end displacement for the foregoing condition is not greater than half at which failure is predicted due to bar pullout or bar fracture.

Paulay (١٩٨٩), introduced a procedure to estimate the behavior of reinforced concrete beam-column joints. The purpose of this study was to show that:

١.Critical features of joint behavior stem primarily from large shear forces that need to be transmitted.

٢.With no more than the application of elementary equilibrium criteria, the need for an admissible mechanism capable of transmitting shear forces can be demonstrated.

٣.Satisfying equilibrium criteria indicates immediately the order of magnitudes of internal tension forces that need to be resisted by tension reinforcement.

٤.Confinement of joint cores by means of adjacent plastic hinges in seismically loaded beams is not possible.

٥.Axial compression load on columns beneficially influences the shear resistance of joints.

From this study, he concluded that:

١.Orthogonal tensile forces within the core are necessary to enable shear stresses applied to the boundaries to be transferred by means of a diagonal compression field.

٢.The response of plastic hinges adjacent to a joint may be influenced significantly by the disposition of internal forces within a joint.

٣.After diagonal cracking, diagonal compression forces transmitted by concrete alone are unconditional prerequisites of statically admissible shear transfer within a joint. The purpose of joint shear reinforcement is to sustain such mechanisms.

٤.To restrict excessive joint dilation, orthogonal tensile forces within a joint core must be resisted primarily by reinforcement in addition to beam and column bars that pass through the joint.

٥.Joint forces to be considered are those introduced by means of internal actions from adjacent beams and columns.
٦.Hence, a member such as a beam, which is expected to develop its full strength at an adjacent plastic hinge, cannot be used to supply simultaneously reactive forces.

٢.٣.٢ Theoretical Studies Using Finite Element Method

Al-Niaemi (١٩٩٩), described a three-dimensional nonlinear finite element model suitable for the analysis of high strength fiber reinforced concrete beam-column joint subjected to non-proportional axial and shear loads. The ٢٠-noded isoparametric brick element was used to model the concrete while the reinforcing steel bars were idealized as axial member embedded within the brick elements. The behavior of concrete in compression was simulated by an elastic-plastic work hardening model followed by a perfect plastic response, which was terminated at the onset of crushing. In tension, a smeared crack model with fixed orthogonal cracks was used with the inclusion of model for the retained post-cracking stress and reduced shear modulus. The nonlinear equations of equilibrium were solved by using an incremental-iterative technique operating under load control. Perfect bond between concrete and steel was assumed to occur. Different specimens of high strength fiber reinforced concrete beam-column joints were analyzed and the finite element solutions were compared with the experimental data.

Hamil et al (٢٠٠٠), used two-dimension nonlinear finite element method for the analysis of high strength reinforced concrete beam-column connections. Quadrilateral elements formed from a pair of triangular elements with nodes at each corner were used to represent concrete while the reinforcement was represented by bar element. Perfect bond between concrete and steel was assumed to occur. The developed model was shown to be sensitive to changes in concrete strength, the detailing arrangements of the tension steel and the presence or absence of joint ties. From their investigation, the strength of a

joint without column ties was proportional to the square root of the concrete's compressive strength.

Mohmood (٢٠٠١), used two-dimensional nonlinear finite element method for the analysis of long-term behavior of plane reinforced concrete members. A rectangular eight-noded isoparametric element model was used to idealize concrete while an embedded model was used to simulate the reinforcement bars. A new model for bond slip was included in the analysis by reducing the bond slip stiffness from the steel axial stiffness. The nonlinear behavior of concrete, bond slip, post-cracking, shear transfer were considered. An elastic-plastic one-dimensional behavior of steel was considered. The time-dependent behavior of concrete was considered by adopting a visco-plastic model and a fluidity parameter for concrete was derived. The computer program developed gives complete listing of stresses and deformations and presents the results graphically as deformed shape and cracks development. Also it presents the general deflection curve with time in comparison with experimental or any analytical data.

Hamza (٢٠٠٥) studied the behavior of beam-column joints with nonlinear interface elements. She assumed the interface as a thin brick element with Millard dowel forces.

٢.٤ Behavior of Reinforced Concrete Members Under Cyclic Loads:-

The behavior of reinforced concrete members and structural systems under cyclic loads has been the subject of intensive investigations since the

١٩٦٠s. Because of the complexities associated with the development of rational analytical procedures, present-day design methods continue in many respects to be based on empirical formulae, using the results obtained from the available experimental data.

Verna and Stelon (١٩٦٢), tested reinforced concrete beams to destruction under repeated loading. These beams were simply supported and loaded at the third points. It was concluded that the bond type of failure was more susceptible to fatigue damage and that shear or diagonal tension failures were likely to occur if the specimens were not weak in bond.

History of prior loading and its effect on the ultimate static strength of RC beams was studied also by **Verna and Stelon (١٩٦٣)**. Test results showed that whenever the beam was not susceptible to bond failure, a significant increase in beam strength for a few thousand cycles of repeated load occurred whereas the specimens failing by bond became weaker as more repetitions of load were applied.

Response of simply supported reinforced concrete beam to arbitrary load histories was investigated by **Sinha et al.(١٩٦٤)**. They observed from test results that the behavior of under-reinforced concrete beams under cyclic loading closely resemble that predicted by an elastic-perfectly plastic theory.

Gerstle et al. (١٩٦٥), predicted the response of doubly reinforced concrete beams to variable repeated and reversed loading based on stress-strain relations of steel and concrete under cyclic loading. It was concluded that the concrete stress-strain relations might be approximated by an idealized elastic-plastic curve in the state of reversed loading. While a non-linear stress-strain relationship was suggested to predict the behavior of the steel reinforcement in the state of reversed loading.

Bresler and Bertero (١٩٦٨), studied the influence of load cycling on stress transfer, and stiffness in simple reinforced concrete elements subjected to tension. It was shown that the previous stress history effectively influenced the stress transfer at any given stress level and the contribution of the concrete to the stiffness of the specimen became negligible as the number of load cycles and the magnitude of peak stresses increased.

Brown and Jirsa (١٩٧١), investigated the effect of load history on the strength, ductility and mode of failure of tested RC beams. The results showed that the behavior of the specimens under load reversal was influenced primarily by shear. They also observed that the changes in beam geometry or load history that increased the shear capacity of the beam significantly increased the energy absorbing capacity and the total number of cycles achieved at failure.

Ismail and Jirsa (١٩٧٢), studied experimentally the influence of load history on the deterioration of bond along bars subjected to elastic stresses. The results indicated that the most important factor affecting bond or stress transfer was the peak stress reached in previous cycles. In addition, they found out that repetitions of load cycles with constant peak stress produced only a gradual deterioration of stress transfer capacity.

Darwin and Nmai (١٩٨٦), described the development and application of an "energy index" to characterize reinforced concrete beams under cyclic loads. The effects of flexural reinforcement, transverse reinforcement, concrete strength and load history were considered. From test results, it was concluded

that in order to improve the cyclic performance of RC beams, it was more efficient to increase the shear capacity by increasing the beam width rather than to increase the transverse reinforcement. The analysis also indicated that increasing the ratio of positive to negative reinforcement might not substantially improve the cyclic performance of the tested beam.

Yankelevsky and Reinhardt (١٩٨٧), developed a one-dimensional model for random cyclic behavior of concrete in compression. The model determines a set of focal points that govern the pieced linear branches of the unloading and reloading curves, Fig.(٢.١). The complete unloading-reloading curves, for the developed model, were reproduced graphically for any starting point on the envelope curve. The model laws were also mathematically formulated providing equations of various characteristics, e.g. the common point limit, the residual (plastic) strain locus, etc..

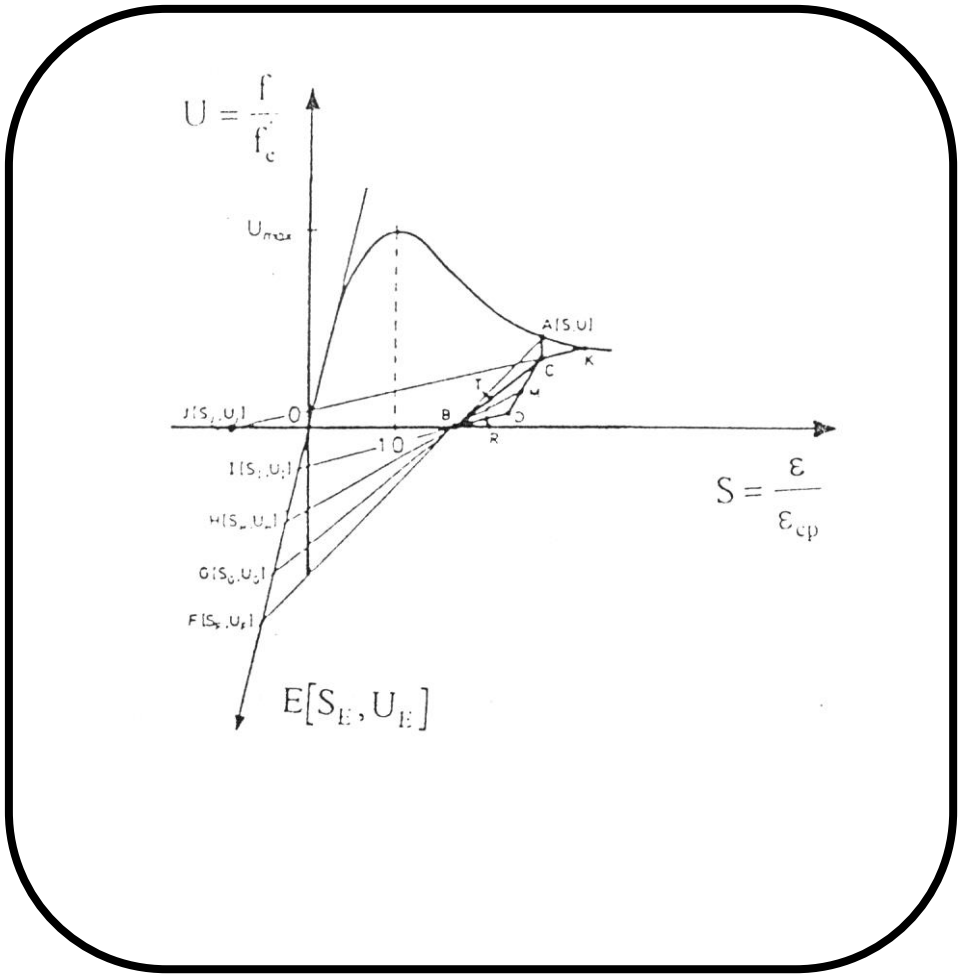

Fig. (٢.١) Scheme of focal points model in compression

(Yankelevsky and Reinhardt ١٩٨٧)

Harajli (١٩٨٨), presented an analytical joint model describing the moment-rotation relationship of partially prestressed beam-column joints. The derived model was based on idealized material models. The stress-strain behavior of concrete under monotonic and cyclic loading adopted in this study is as shown in Fig. .

Yankelevsky and Reinhardt (١٩٨٩), developed a model for stress-strain relationship of concrete subjected to random cyclic tension and compression loads which complement the earlier work of the researchers (١٩٨٧). The model used a set of focal points to compute the piecewise linear branches of the unloading and the reloading curves in the tensile stress domain and in the tension-

compression domain, Fig.(٢.٢) . This model was similar to their earlier model, since both models could be used graphically or mathematically to obtain the stress-strain curve of the concrete in tension and compression.

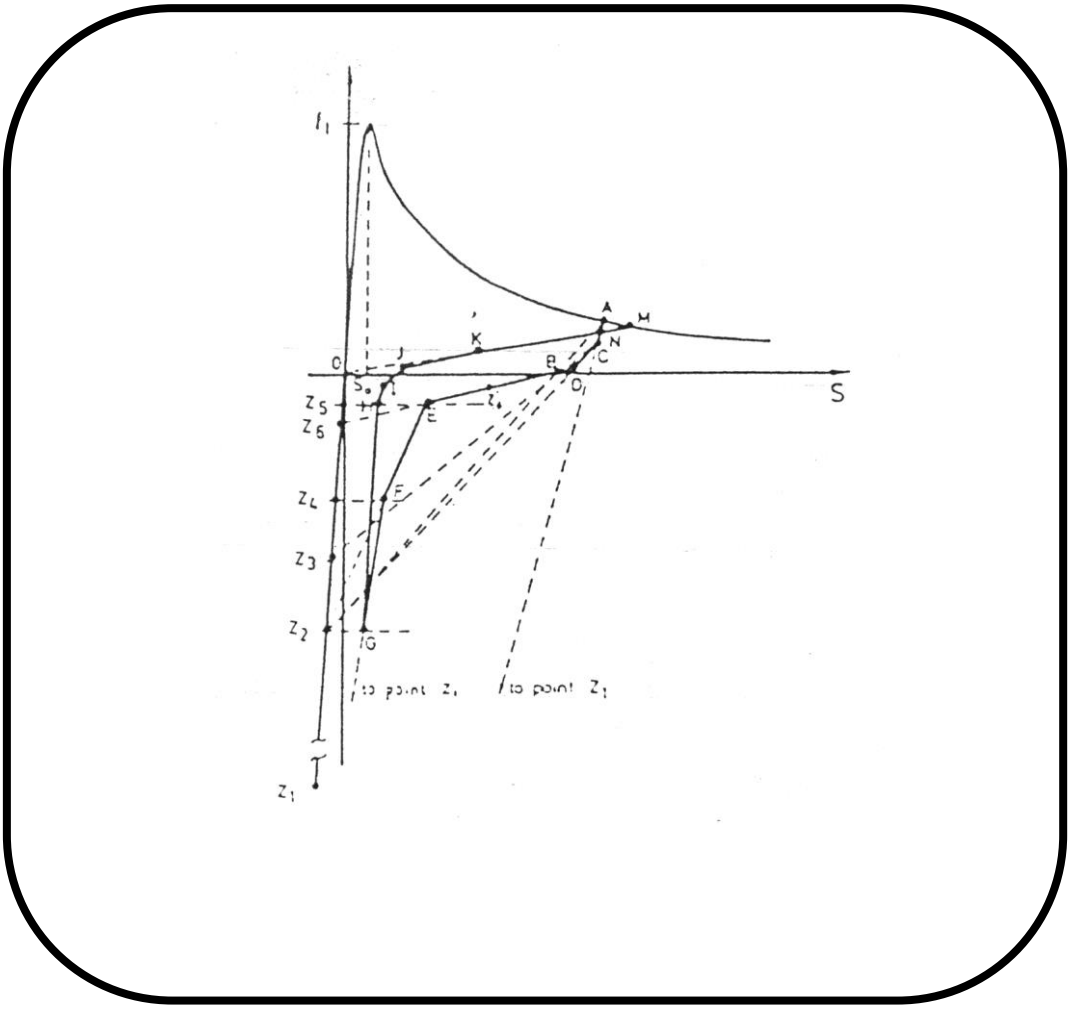

Fig. (٢.٢) Tension-compression model of concrete subjected to Cyclic loads (Yankelevsky and Reinhardt ١٩٨٩)

Taplin and Grundy (١٩٩٨), stated that composite steel and concrete beams rely for their strength and stiffness on the stud shear connection between the steel and the concrete. Tests have been undertaken on composite beams in order to investigate the behavior of the shear connection when it is subjected to repeated loading. In particular, the effect of repeated loading on slip in the shear connection has been studied. The tests show that repeated loading of the beams causes slip damage to accumulate in the shear connection with a consequent loss of stiffness, and an increase in the deflection of the composite beam. An analytical model is presented which enables this effect to be quantified, and comparisons are made between the test results and the analytical model.

٢.٥ Shear Transfer Tests

Several mechanisms exist by which shear is transferred across reinforced concrete sections . Among these mechanisms are the shear stiffness of uncracked concrete, aggregate interlock, dowel action by steel bars and the effect of tension in reinforcement. For the shear transfer across cracked concrete planes crossed by reinforcement, the two major mechanisms in effect are the dowel action and the aggregate interlock . Shear transfer by these two mechanisms is accompanied by slippage or relative movement of cracked faces .

The shear transfer mechanisms across a definite plane have been the object of numerous experimental investigations for many years, some of these investigations are reported herein .

Hofbeck et al.(١٩٦٩) studied the shear transfer in reinforced concrete across a plane, such as at the interface between a pre-cast and cast-in-place concrete elements. Thirty eight push-off specimens were tested , some with, some without a pre-existing crack along the shear plane. The results indicated that a pre-existing crack along the shear plane would both reduce the ultimate shear transfer strength and increase the slip at all levels of load.

The behavior of both smooth and rough interfaces (concrete-to-concrete friction) subjected to monotonically or cyclically imposed shear displacements was investigated by means of several series of tests carried out in the laboratory of reinforced concrete structure, National Technical University of Athens. Some

of these tests are briefly represented by **Tassios and Vintzēleou (١٩٨٧)**, which indicated that , generally , the increasing of concrete compressive strength and / or the normal stress would improve the frictional capacity .

Displacement controlled shear tests on concrete lift joint specimens with different surface preparations were conducted by **Fronteddu et al.**. Experimental results indicated that the coefficient of friction decreases with the increase in normal load .

An experimental study of the factors affecting shear transfer strength was made by Mattock and Hawkins (١٩٧٢) using pull-off , push-off , and modified push-off specimens. **Bass et al.(١٩٨٩)** also made an experimental study to provide information on the surface shear capacities between new cast concrete against an existing concrete surface. A continuing study of the factors affecting shear transfer strength had been made. Some of these factors are as follows:

١. The characteristics of the shear plane .
٢. The characteristics of the reinforcement .
٣. The concrete strength .
٤. Direct stresses acting parallel and transverse to the shear plane .
٥. Direct stresses transverse to the shear plane.

٢.٥.١ Characteristics of the shear plane

Mast (١٩٦٨) pointed out the need to consider the case where a crack may exist along the shear plane before shear is applied. Such cracks occur for a variety of reasons unrelated to shear, such as tension forces caused by restrained shrinkage or temperature deformations or accidental dropping of the member.

A crack in the shear plane reduces the ultimate shear strength of under-reinforced specimens Fig.(٢.٣). The decrease is greater in the push-off specimens than in the pull-off specimens. The shear strength of the initially cracked specimens is not directly proportional to the amount of transverse reinforcement.

٢.٥.٢ Characteristics of the reinforcement

The reinforcement parameter (ρf_y) can be changed by varying either the reinforcement ratio (ρ) the reinforcement yield strength (f_y), or both. Also, for a given shear plane the reinforcement ratio can be changed by changing the bar size and/or the bar spacing. In Fig. (٢.٤),

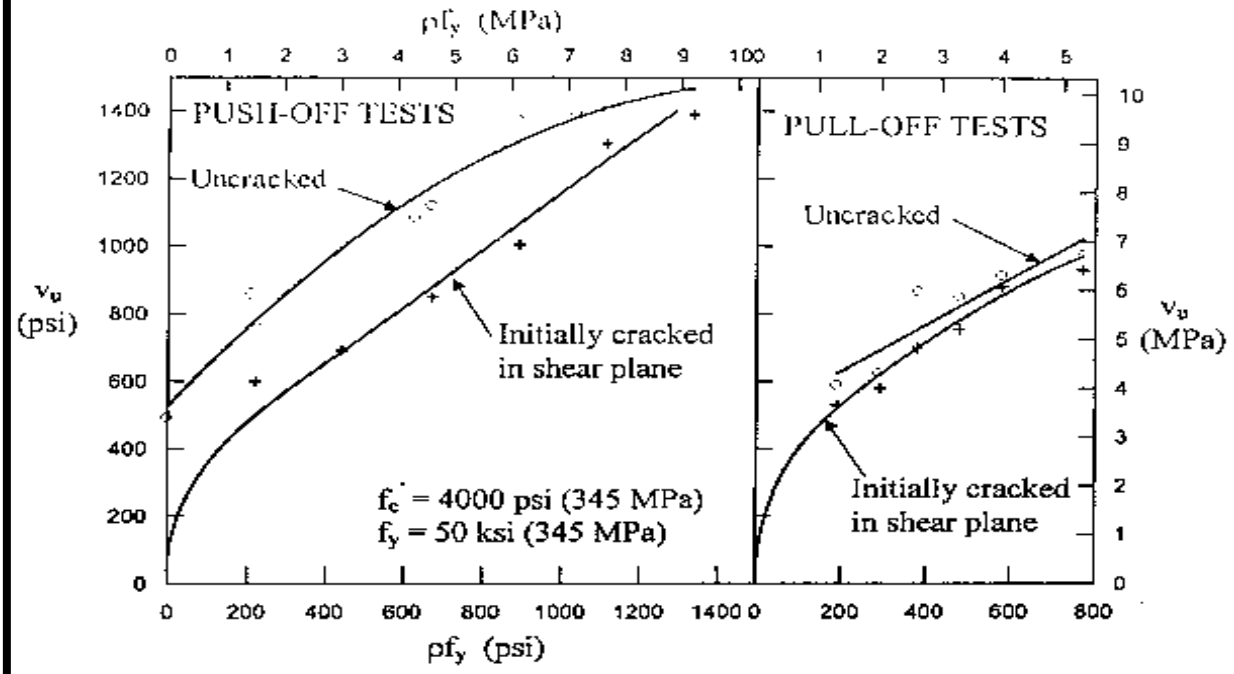

Fig.(٢.٣) Variation of shear transfer strength reinforcement parameter (ρf_y), with and without an initial crack along the shear plane (Mattock and Hawkins (١٩٧٢))

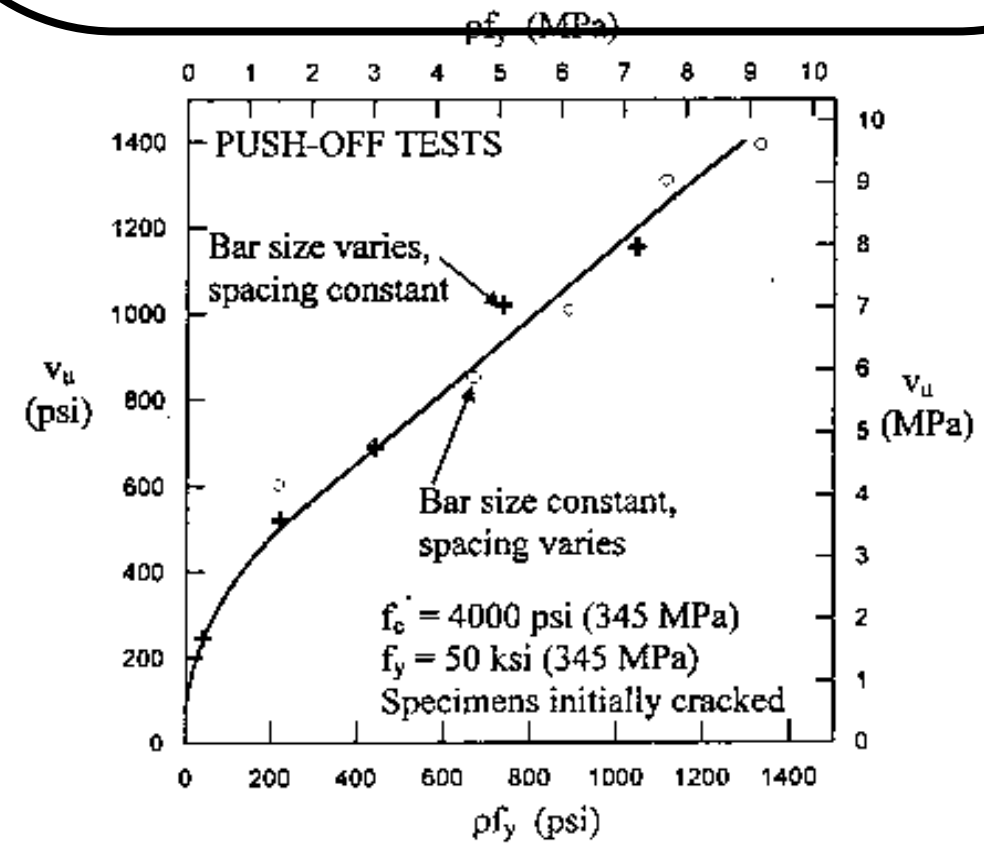

Fig.(٢.٤) Effect of stirrup bar size and spacing on the shear transfer strength of push-off specimens (Mattock, ١٩٧٢).

Mattock and Hawkins (١٩٧٢) showed that the way in which ρ is changed does not affect the relationship between shear strength and the reinforcement parameter ρf_y , Fig.(٢.٢) . Also it was found that the specimens with ٤٥٥MPa(٦٦ksi) steel had slightly higher shear strength than the specimens reinforced with ٣٤٥MPa(٥٠ksi) steel. Therefore the relationship between the reinforcement parameter ρf_y and the ultimate transverse shearing force V_u is the same for higher strength reinforcement as for intermediate grade reinforcement, provided the yield strength does not exceed ٤٦٤MPa(٦٦ksi) .

٢.٥.٣ Concrete Strength

The effect of variation in concrete strength on the shear strength of initially cracked push-off specimens is illustrated in Fig.(٢.٥) . For values of ρf_y below about ٤.١٤MPa(٦٠٠psi) the concrete strength does not appear to affect the shear transfer strength. For higher values of ρf_y the shear strength is lower for the lower strength concrete . The concrete strength therefore appears to set an upper limit value of ρf_y , below which the relationship between V_u and ρf_y established for ٢٧.٥MPa(٤٠٠٠psi) concrete would hold for any strength of concrete equal to or greater than the strength being considered , and above which the shear strength increases at a lesser rate for the concrete strength being considered .

٢.٥.٤ Direct Stresses Parallel to the Shear Plane

By using the method which was proposed for the calculation of the shear transfer strength of initially uncracked concrete **[Zia (١٩٦١]** , an analytical study was made of the influence on shear transfer strength by direct stress parallel to the shear plane . From these calculations it appeared that if a direct tensile stress exists parallel to the shear plane , then the shear transfer strength would increase more slowly , as ρf_y was increased , than in the push-off test where a direct compressive stress exists parallel to the shear plane .

The ultimate shear strengths of the pull-off specimens are compared in Fig.(٢.٦). For initially uncracked specimens , the pull-off tests gave lower shear strengths than the push-off tests . For specimens cracked along the shear plane before being loaded in shear , the shear strengths of the push-off and pull-off specimens are essentially the same for any given value of ρf_y.

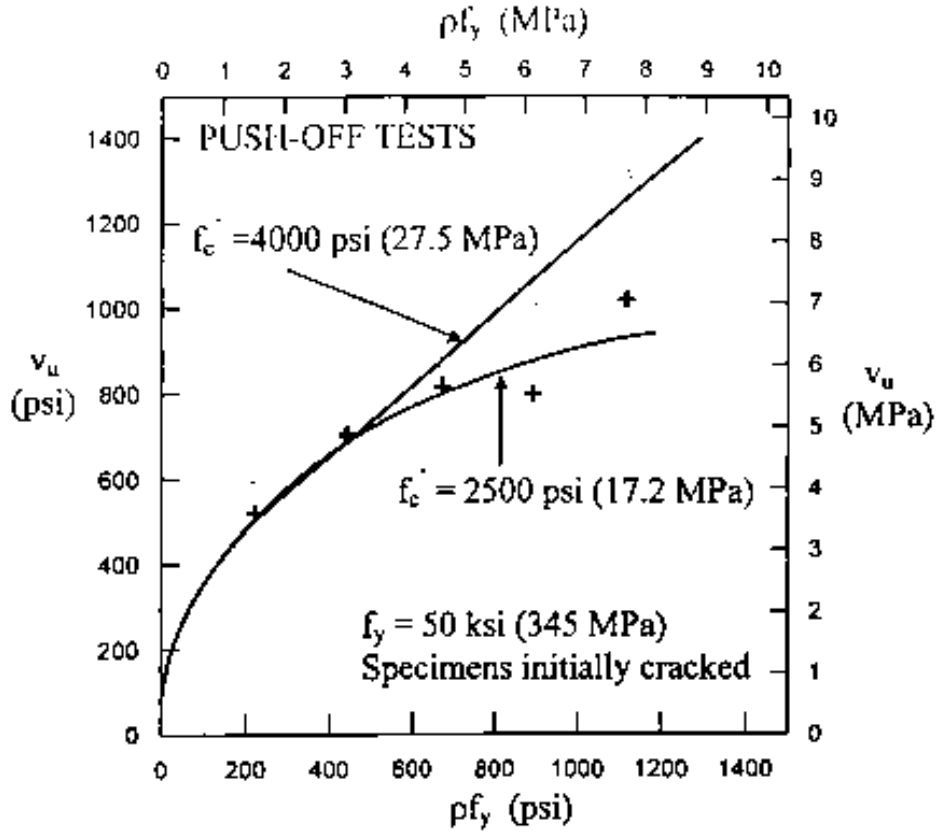

Fig.(٢.٥) Effect of concrete strength on the shear transfer

٢.٥.٥ Direct Stress Transverse to the Shear Plane

The effect of the compressive stresses acting transverse to the shear plane was studied by **Mattock and Hawkins (١٩٧٢)**. Modified push-off specimens were used . The ultimate shear strengths of the modified push-off specimens which had shearing type failures are compared with results of the push-off tests in Fig.(٢.٧) .That if a resultant compressive force acts across a shear plane , the shear transfer strength is a function of the resultant compressive force and the force $A_{vf}f_y$ in the shear friction reinforcement . However , if a resultant tensile force acts across a shear plane , the shear transfer strength will decrease by the amount of a resultant tensile force . Tension may be caused by resraint of deformations due to temperature change ,creep , and shrinkage .

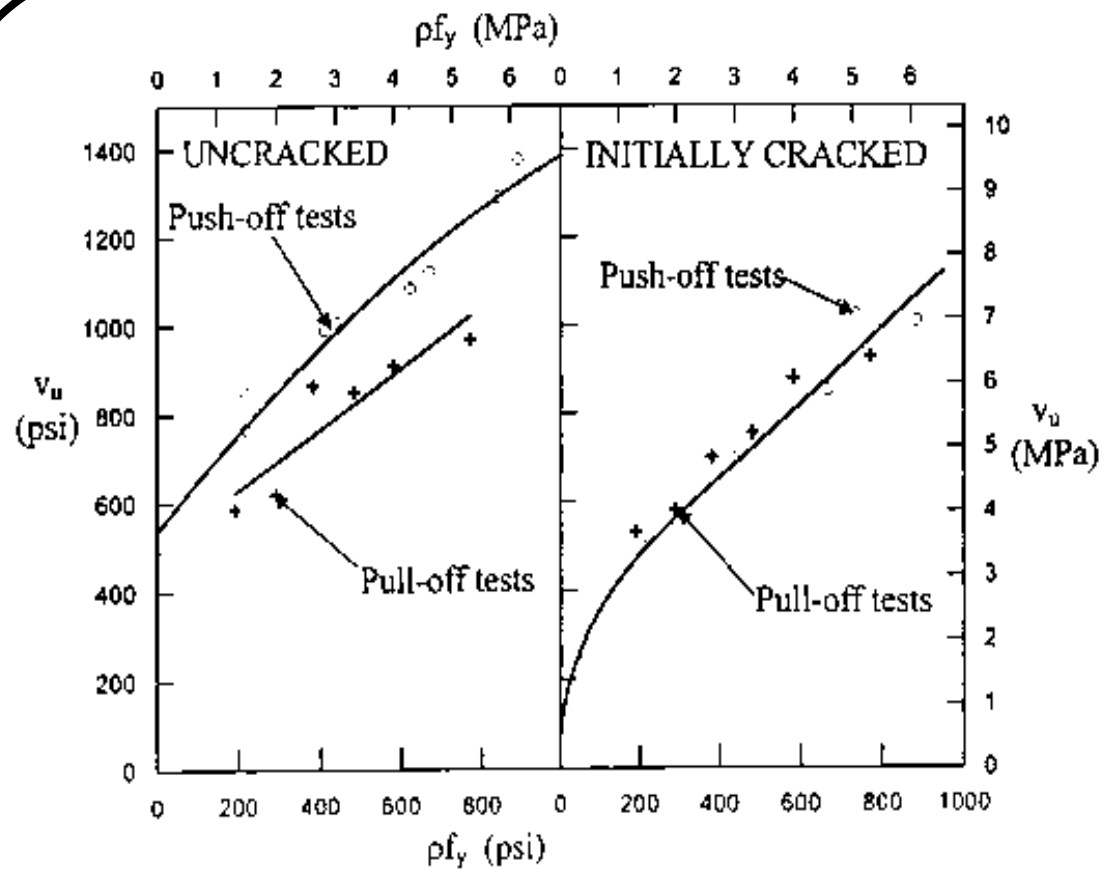

Fig.(٢.٦) Effect on the shear transfer strength of direct stress acting parallel to the shear plane (Mattock, ١٩٧٢).

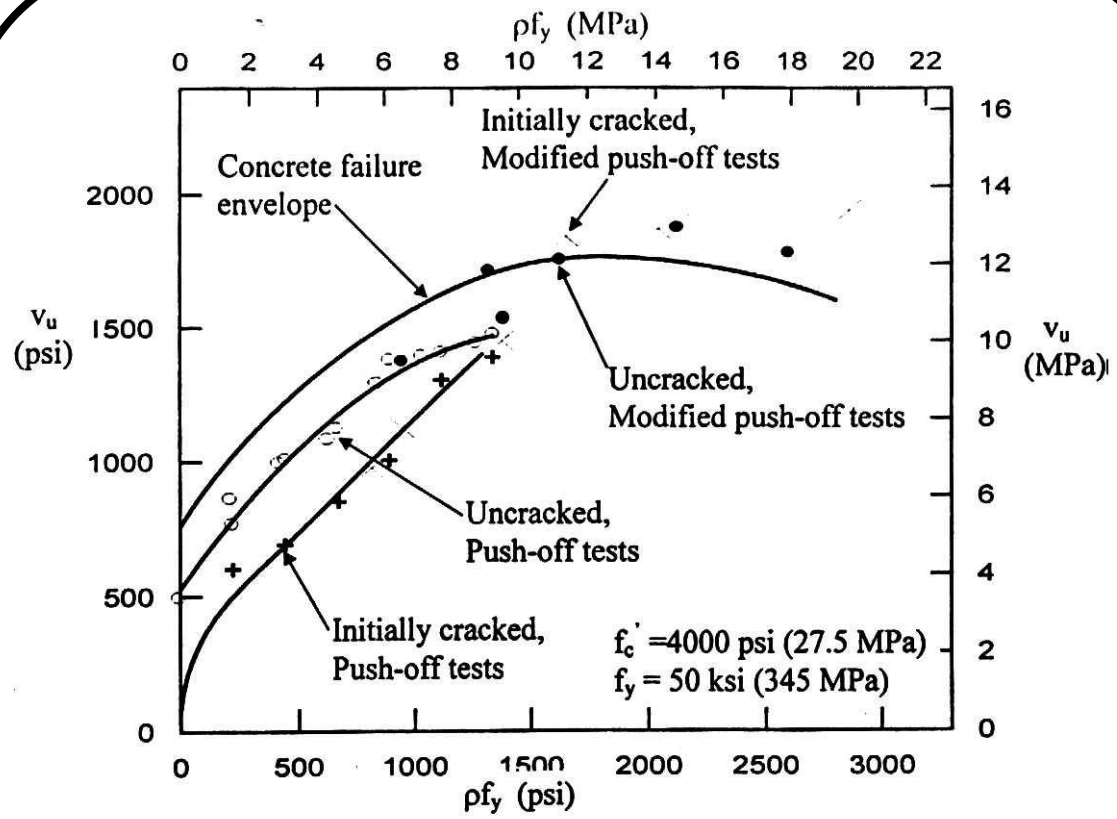

Fig.(٢.٧) Effect on shear transfer strength of direct stress acting transverse to shear plane (Mattock ١٩٧٢)

٢.٥.٦ Cyclic shear transfer

Mattock (١٩٨١) examined the results of cyclically reversing and monotonic shear transfer tests for companion of initially cracked specimens of normal weight and lightweight reinforced concrete. Both composite and monolithic specimens were tested. The interfaces of all composite specimens were roughened as required by Section ١١.٧.٩ of the ACI Building Code ٣١٨-٧٧. In some cases the bond at the interface was deliberately broken. The following conclusions has been obtained from the test results:

١. In the case of a shear plane in normal weight or lightweight monolithic concrete and a rough interface between concretes cast at different times, when good bond has been obtained at the interface, the strength under cyclically reversing shear is about ٨٠ percent of the shear transfer strength under monotonic loading.

٢. If the interface is roughened as specified in Section ١١.٧.٩ of ACI Code and if good bond is obtained at the interface, then after cracking shear transfer behavior under both monotonic and cyclic loading will be essentially the same as in the case of shear transfer across a crack in monolithic concrete.

٣. If bond at the interface between concretes cast at different times is destroyed, shear transfer behavior under cyclic loading deteriorates rapidly and the shear transfer strength is only about ٠.٦ of the shear transfer strength under monotonic loading.

Remarks

After this review, it is noted that no detailed study has been made on RC beam-column connections with construction joints under cyclic loading. The present study will deal with this problem.

CHAPTER THREE
FINITE ELEMENT FORMULATION AND NONLINEAR SOLUTION TECHNIQUES

٣.١ General

The finite element method of analysis is a very powerful, modern computational tool. The method has been used almost universally during the past ٤٥ years to solve very complex problems in the structural engineering, fluid mechanics, thermal analysis, and many other fields.

The finite element idealization of reinforced concrete members should be able to represent the behavior of concrete, the behavior of reinforcement, and the capability of concrete to transfer shear across an interface .

In the present study , to create such an idealization the following element types are used :

١. Brick element to represent concrete under three dimensional stresses .
٢. Line element to represent reinforcement under axial forces .
٣. Interface element to represent shear transfer .

In this chapter, the finite element discretization and formulation of concrete, steel and the nonlinear solution techniques are discussed.

٣.٢ Three – Dimensional Brick Element

In the finite element method, the construction of the stiffness matrix of the brick element has been facilitated by three advances in the finite element technology: natural coordinates, isoparametric definition and numerical integration [**Al–Shaarbaf** ١٩٩٠]. These advances revolutionized the finite element field in mid – ١٩٦٠'s, mainly, when the ٨-node linear and the ٢٠–node quadratic brick elements were used in representing the three dimensional solid bodies.

The quadratic ٢٠ - node brick element shown in Fig. (٣.١) is adopted to represent both concrete in the present study. This type of element is popular due to its superior performance. A major advantage of the quadratic ٢٠ – node brick element over the ٨ – node brick element, when studying complex cases, is that less number of elements can be used, as well as it may have curved sides and therefore provides a better fit to curved sides of an actual structure [**Cook (١٩٧٤)].**

٣.٢.١ Shape Functions

The natural local coordinate system is used to describe the displacement components of a point p (ξ, η, ζ) within the element. These local coordinates (ξ, η, ζ) are emerging from the center of the brick element where the origin point is located as shown in the Fig. (٣.٢)

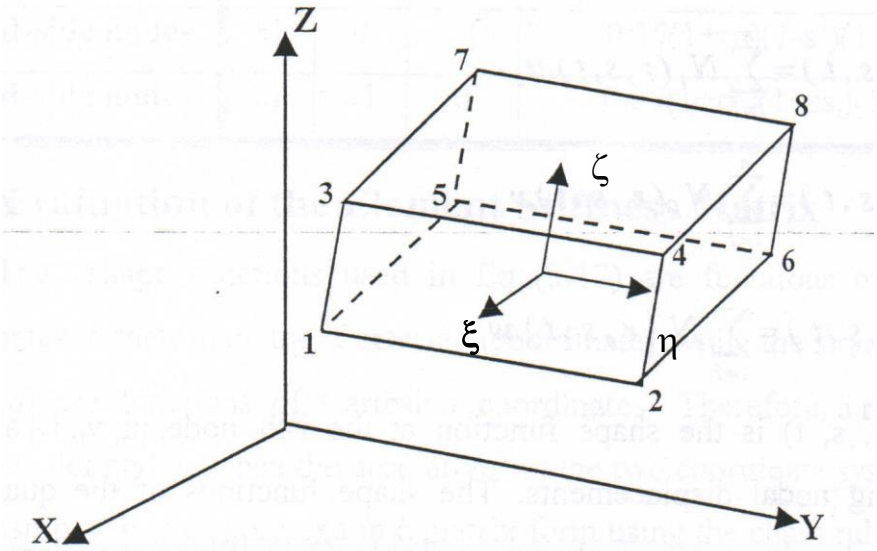

a. Linear 8-node Element

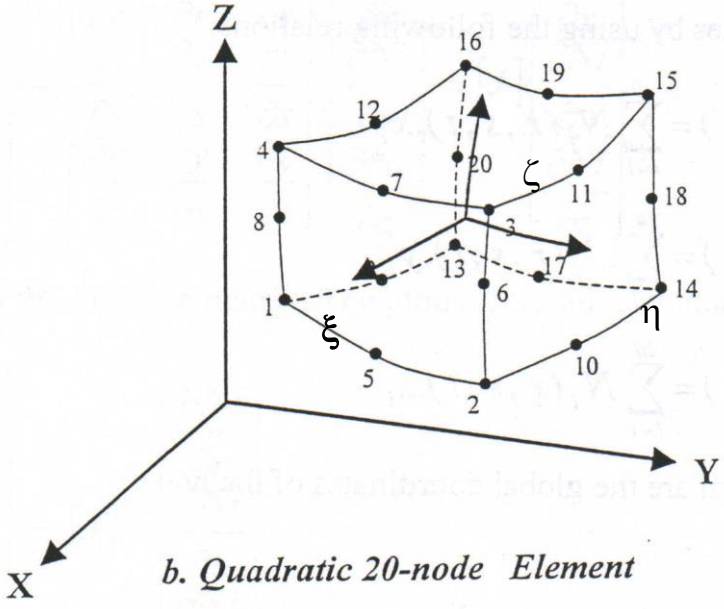

b. Quadratic 20-node Element

Fig. (٢.١) Linear and quadratic isoparamatric solid element

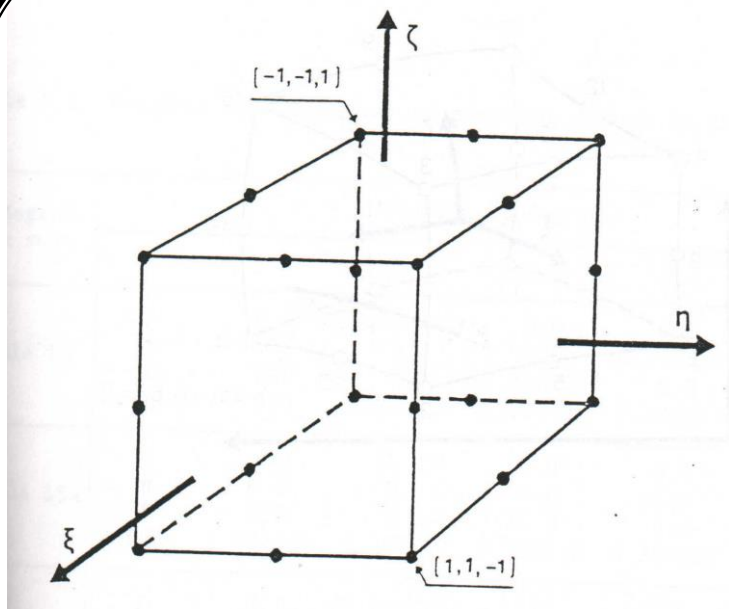

Fig (٣.٢) Local coordinate system

The element has ٢٠ nodes and ٦٠ d.o.f and bounded by planes with ξ, η, and ζ = ± ١ in ξ, η, ζ space. The starting point for the stiffness matrix derivation is the element displacement field. The isoparametric definition of displacement components is:

$$\left.\begin{aligned} u(\xi,\eta,\zeta) &= \sum_{i=1}^{n} N_i\,(\xi,\eta,\zeta)\,u_i \\ v(\xi,\eta,\zeta) &= \sum_{i=1}^{n} N_i\,(\xi,\eta,\zeta)\,v_i \\ w(\xi,\eta,\zeta) &= \sum_{i=1}^{n} N_i\,(\xi,\eta,\zeta)\,w_i \end{aligned}\right\} \qquad (٣.١)$$

where N_i (ξ, η, ζ) is the shape function at the i-th node and u_i, v_i and w_i are the corresponding nodal displacements (with respect to the original (global) coordinate system x,y and z) and n = ٢٠ is the number of nodes. The shape functions of the quadratic ٢٠-node brick element are shown in Table (٣.١)

Table (٣.١) Shape functions of the quadratic ٢٠-node brick element (Cook ١٩٧٤)

Location		η		Ni (ξ, η, ζ)
Corner nodes	١	± ١	١	(١+ ξ ξi)(١+ η ηi)(١+ζζi) (ξ ξi+ η ηi + ζ ζi- ٢)/٨
mid – side nodes		± ١	١	(١- ξ٢)(١+ η ηi)(١+ ζ ζi) /٤
mid – side nodes	١	٠	١	(١- η٢)(١+ ξ ξi)(١+ ζ ζi)/٤
mid – side nodes	١	± ١		(١- ζ٢)(١+ ξ ξi)(١+ η ηi)/٤

To check the above mathematical model, each of its ٢٠ shape functions has a value of unity at its specified node and a value of zero at any of the other ١٩ nodes. These shape functions also satisfy the rigid body displacement of the element.

In the isoparametric group of elements, the interpolation shape functions for displacements are also used to define the geometry (or configuration) of the element where the

global coordinates of any point p(ξ, η, ζ) in terms of the natural local coordinates are given by the relations:

$$x(\xi,\eta,\zeta)=\sum_{i=1}^{20} Ni\,(\xi,\eta,\zeta)x_i$$
$$y(\xi,\eta,\zeta)=\sum_{i=1}^{20} Ni\,(\xi,\eta,\zeta)y_i \qquad (٣.٢)$$
$$z(\xi,\eta,\zeta)=\sum_{i=1}^{20} Ni\,(\xi,\eta,\zeta)z_i$$

where x_i , y_i and z_i are the global coordinates of the node i .

٣. ٢. ٢ *Stress and Strain Fields*

Since the geometrical nonlinerities are not considered in the present work, displacement gradients remain small throughout the loading process and hence the engineering components of strain can be expressed in terms of the first partial derivatives of the displacement components. Therefore, the linearized strain – displacement relationships may be written as:

$$\{\varepsilon\}=\begin{Bmatrix}\varepsilon_x\\ \varepsilon_y\\ \varepsilon_z\\ \gamma_{xy}\\ \gamma_{yz}\\ \gamma_{zx}\end{Bmatrix}=\begin{Bmatrix}\frac{\partial u}{\partial x}\\ \frac{\partial v}{\partial y}\\ \frac{\partial w}{\partial z}\\ \frac{\partial u}{\partial y}+\frac{\partial v}{\partial x}\\ \frac{\partial v}{\partial z}+\frac{\partial w}{\partial y}\\ \frac{\partial w}{\partial x}+\frac{\partial u}{\partial z}\end{Bmatrix}=\sum_{i=1}^{20}\underbrace{\begin{bmatrix}\frac{\partial Ni}{\partial x} & 0 & 0\\ 0 & \frac{\partial Ni}{\partial y} & 0\\ 0 & 0 & \frac{\partial Ni}{\partial z}\\ \frac{\partial Ni}{\partial y} & \frac{\partial Ni}{\partial x} & 0\\ 0 & \frac{\partial Ni}{\partial z} & \frac{\partial Ni}{\partial y}\\ \frac{\partial Ni}{\partial x} & 0 & \frac{\partial Ni}{\partial z}\end{bmatrix}}_{[B]}\underbrace{\begin{Bmatrix}u_i\\ v_i\\ w_i\end{Bmatrix}}_{\{a\}^e} \qquad (٣.٣)$$

Since the shape functions N_i are functions of the local coordinates rather than Cartesian (global) coordinates; a relationship needs to be established between the derivatives in the two coordinates systems. By using the chain rule, the partial differential relation can be expressed in matrix form as:

$$\begin{bmatrix}\frac{\partial \mathrm{Ni}}{\partial \xi}\\ \frac{\partial \mathrm{Ni}}{\partial \eta}\\ \frac{\partial \mathrm{Ni}}{\partial \zeta}\end{bmatrix}=\underbrace{\begin{bmatrix}\frac{\partial \mathrm{x}}{\partial \xi} & \frac{\partial y}{\partial \xi} & \frac{\partial z}{\partial \xi}\\ \frac{\partial \mathrm{x}}{\partial \eta} & \frac{\partial y}{\partial \eta} & \frac{\partial z}{\partial \eta}\\ \frac{\partial \mathrm{x}}{\partial \zeta} & \frac{\partial y}{\partial \zeta} & \frac{\partial z}{\partial \zeta}\end{bmatrix}}_{[J]}\cdot\begin{bmatrix}\frac{\partial \mathrm{Ni}}{\partial \mathrm{x}}\\ \frac{\partial \mathrm{Ni}}{\partial \mathrm{y}}\\ \frac{\partial \mathrm{Ni}}{\partial \mathrm{z}}\end{bmatrix} \qquad (٣.٤)$$

where [J] is the Jacobian matrix and the elements of this matrix can be obtained by differentiation of equation (٣.٢).

The Jacobian matrix can be expressed as:

$$[J]=\begin{bmatrix} \sum \frac{\partial Ni}{\partial \xi} x_i & \sum \frac{\partial Ni}{\partial \xi} y_i & \sum \frac{\partial Ni}{\partial \xi} z_i \\ \sum \frac{\partial Ni}{\partial \eta} x_i & \sum \frac{\partial Ni}{\partial \eta} y_i & \sum \frac{\partial Ni}{\partial \eta} z_i \\ \sum \frac{\partial Ni}{\partial \zeta} x_i & \sum \frac{\partial Ni}{\partial \zeta} y_i & \sum \frac{\partial Ni}{\partial \zeta} z_i \end{bmatrix} \qquad (٣.٥)$$

Then, the derivatives of the shape functions with respect to Cartesian global coordinates can be obtain as:

$$\begin{bmatrix} \frac{\partial Ni}{\partial x} \\ \frac{\partial Ni}{\partial y} \end{bmatrix} = [J]^{-1} \cdot \begin{bmatrix} \frac{\partial Ni}{\partial \xi} \\ \frac{\partial Ni}{\partial \eta} \end{bmatrix} \qquad (٣.٦)$$

where $[J]^{-1}$ is the inverse of Jacobian matrix given by:

$$[J]^{-1} = \begin{bmatrix} \frac{\partial \xi}{\partial x} & \frac{\partial \eta}{\partial x} & \frac{\partial \zeta}{\partial x} \\ \frac{\partial \xi}{\partial y} & \frac{\partial \eta}{\partial y} & \frac{\partial \zeta}{\partial y} \\ \frac{\partial \xi}{\partial z} & \frac{\partial \eta}{\partial z} & \frac{\partial \zeta}{\partial z} \end{bmatrix} \qquad (٣.٧)$$

as $[J].[J]^{-1} = [J]^{-1}.[J] = [I]$ (unit matrix)

The vector of stresses is given by:

$$\{\sigma\} = \begin{Bmatrix} \sigma_x \\ \sigma_y \\ \sigma_z \\ \tau_{xy} \\ \tau_{yz} \\ \tau_{zx} \end{Bmatrix} \qquad (٣.٨)$$

and the stress – strain relationship is represented as:

$$\{\sigma\} = [D].\{\varepsilon\} \qquad (٣.٩)$$

where [D] is the constitutive matrix of order (٦ x ٦) for three dimentions.

٣. ٢. ٣ *Stiffness Matrix Calculation*

In order to establish the governing equations of static equilibrium, which will lead to the derivation of the stiffness matrix, the principle of virtual displacements for a deformable body is used. It simply states that a deformable body is in equilibrium if the total work done by all the external forces plus the total work done by all the internal forces during any kinematically admissible virtual displacement is zero **[Dawe (١٩٨٤)]** or in other words, strain energy is equal to loss of potential work by external forces:

$$\delta W_{int} - \delta W_{ext} = 0 \qquad (٣.١٠)$$

The external work can be expressed as the work done in moving the body forces ***b*** and surface traction ***t*** through the virtual displacement $\{\partial U\}$, as:

$$\delta W_{ext} = \int_V \{\partial u\}^T \{b\}\, dv + \int_S \{\partial U\}^T \{t_S\} ds \qquad (٣.١١)$$

where V is the volume of the body and S is that part of the surface of the body where external tractions are prescribed.

The change in the strain energy, or internal work, due to a set of virtual strains, $\{\partial \varepsilon\}$, corresponding to the virtual displacements $\{\partial u\}$ is:

$$\delta W_{int} = \int_V \{\partial \varepsilon\}^T \{\sigma\} dv \qquad (٣.١٢)$$

By substituting equations (٣.٩) into equation (٣.١٢), then

$$\delta W_{int} = \int_V \{\partial \varepsilon\}^T [D]\{\varepsilon\} dv \qquad (٣.١٣)$$

by substituting equations (٣.١١) and (٣.١٣) into equation (٣.١٠), then:

$$\int_V \{\partial\varepsilon\}^T [D]\{\varepsilon\}dv - \int_V \{\partial u\}^T \{b\} dv - \int_S \{\partial u\}^T \{t_S\}ds = 0 \qquad (٣.١٤)$$

This expression represents the equation of static equilibrium for a general deformable body.

The basic concept of the finite element analysis is to discretize the continuum into arbitrary numbers of small elements connected together at their common nodes. For a finite element, e, of the discretized body, the displacement vector at any point is:

$$\{U\} = [N]\ \{a\}^e \qquad (٣.١٥)$$

where [N] is a matrix containing the interpolation functions which relate the displacement $\{U\}^e$, to the nodal displacements $\{a\}^e$.

By differentiation of the displacements, the corresponding strains, $\{\varepsilon\}^e$, are obtained such that:

$$\{\varepsilon\}^e = [A]\ \{U\}^e \qquad (٣.١٦)$$

where [A] is the matrix, which contains the differential operators. Substituting of equation (٣.١٥) into equation (٣.١٦) yields:

$$\{\varepsilon\}^e = [A]\,[N]\,\{a\}^e \qquad (٣.١٧)$$

or

$$\{\varepsilon\}^e = [B]\,\{a\}^e \qquad (٣.١٨)$$

where [B] is the strain displacement matrix, which represents the values of the strain at any point within the element, due to unit values of nodal displacements. In the discretized body, the equations of equilibrium of the

continuum body may be written as the sum of integration over the volume and surface area for all the finite elements. Therefore, by making use of equation (٣.١٥) and (٣.١٨), equation (٣.١٤) becomes:

$$\partial\{a\}^T\left\{\sum_{n\,v}\int[B]^T[D][B]\,dv^e\{a\}^e-\sum_{n\,v}\int[N]^T\{R\}^e\,dv^e-\sum_{n\,s}\int[N]^T\{T_s\}^e\,ds^e\right\}=0 \qquad (٣.١٩)$$

where $\partial\{a\}$ is the assembled displacements of the body (all elements of the body). Since the relationship must be valid for any set of virtual displacements, and since $\partial\{a_e\}^T$ is arbitrary or $\partial\{a_e\}^T$ not equal ٠, then equation (٣.١٩) is written in brief for one element ***e*** as:

$$\{f\}^e = [k]^e . \{a\}^e \qquad (٣.٢٠)$$

where $[k]^e$ is the stiffness matrix for one element e. the structural stiffness matrix of the assemblage of the elements [k] is given by:

$$[k] = \sum_n [k]^e \qquad (٣.٢١)$$

The element assemblage nodal displacement vector is $\{a\}^e$, and thus {f} is the element assemblage of external nodal force vector given by:

$$\{f\} = \sum_n \int_{v^e} [N]^T \{b\}^e \, dv^e + \sum_n \int_{s^e} [N]^T \{T_S\}^e \, ds^e \qquad (٣.٢٢)$$

For an element of volume V^e, the stiffness matrix is presented implicitly in equation (٣.٢١) as:

$$[K]^e = \int_{v^e} [B]^T.[D].[B]\, dv^e \qquad (٣.٢٣)$$

For three–dimension elements, the differential volume dv^e, may be written as:

$$dv^e = dxdydz \qquad (٣.٢٤)$$

Equation (٣.٢٤) can be transformed into the natural coordinates as:

$$dv^e = |J| d\xi d\eta d\zeta \qquad (٣.٢٥)$$

where $|J|$ is the determinant of the Jacobian matrix. The limits of integration in the natural coordinates become –١ an +١ and the element stiffness matrix can therefore be written as:

$$[K]^e = \int_{-1}^{+1}\int_{-1}^{+1}\int_{-1}^{+1} [B]^T [D][B]|J|d\xi d\eta d\zeta \qquad (٣.٢٦)$$

In general it is not possible to evaluate the element stiffness matrix explicitly. Thus, numerical integration has to be used.

٣.٣ Reinforcement Idealization

In developing a finite element model for reinforced concrete members, at least three alternative representations of reinforcement have been used:

a) Distributed Representation

In this representation, Fig. (٣.٣a), the steel is assumed to be distributed in the concrete element with a particular orientation angle θ. In the composite concrete, reinforcement constitutive relation is used in this case **[ASCE (١٩٨١), Chen (١٩٨٢)].** To derive such a relation, perfect bond is usually assumed between the concrete and steel.

b) Discrete Representation

A discrete representation of the reinforcement by using independent one – dimensional elements has been also used, Fig. (٣.٣b). Axial force members, or bar links, may be used and they are assumed to be pin connected with two – degrees of freedom at the nodal points. Beam elements may also be used, and they are assumed to be capable of

resisting axial force, shearing forces, and bending moment, with three degrees of freedom assigned at each node. In either case, the one – dimensional reinforcement elements are easily superimposed on the multi – dimensional finite element mesh representing the concrete. A significant advantage of the discrete representation is that it can account for possible displacement of the reinforcement with respect to the surrounding concrete**.** **[Cook (١٩٨١), Chen (١٩٨٢)].**

c) Embedded Representation

An embedded representation, Fig. (٣.٣c), may be used in connection with higher order isoparametric concrete elements [**ASCE (١٩٨١), Al-Mahaidi (١٩٧٩)]**. The reinforcement bar is considered to be an axial member built into the isoparametric concrete element such that its displacements are consistent with those of the element. Perfect bond between the steel and the concrete has been assumed in this case. A major advantage of this approach is that the steel bars can be placed in their correct positions without imposing any restrictions on mesh choice and hence the finite element analysis can be carried out with a smaller number of brick elements compared to the discrete

representation of reinforcement. Therefore, the embedded representation is adopted in the present work.

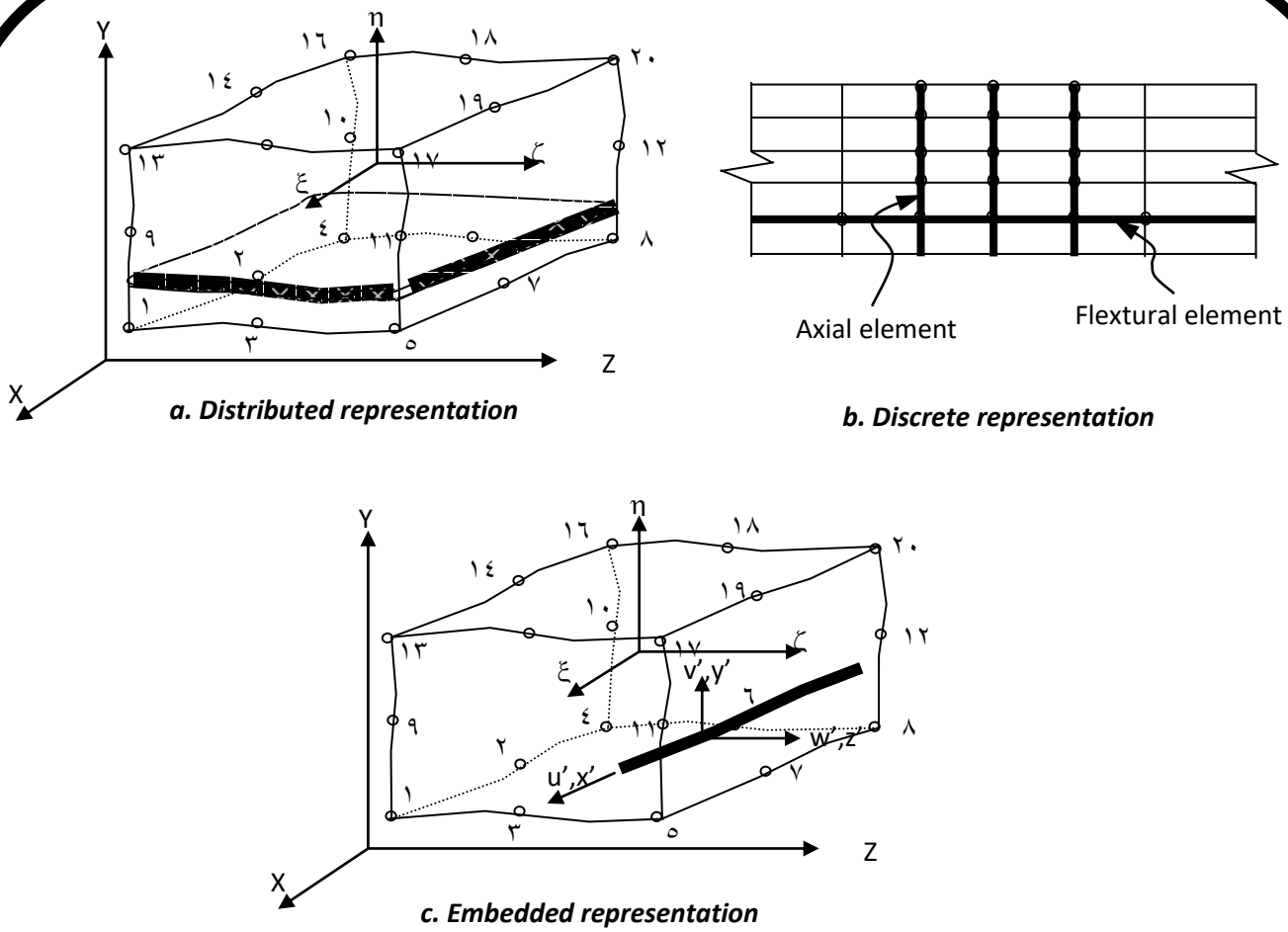

a. Distributed representation

b. Discrete representation

c. Embedded representation

Fig. (٣.٣) Alternative representations of steel reinforcement

For particular types of problems, a combination of representations may be used. As an example, discrete beam elements may be used for main reinforcement in beams while axial bar elements for stirrups. Or a distributed model can be used for the steel throughout the surface of curved shell and discrete bar or beam elements for special reinforcement along the edge.

A derivation is presented in this section for a bar parallel to the local coordinate axis ξ. A similar derivation can be used for bars parallel to η and ξ axes [**Phillips and Zienkiewicz (١٩٧٦), Mohamed (١٩٨٦)].**

For a bar lying inside a hexahedral brick element and parallel to the local coordinate axis ξ, with $\eta = \eta_c$ and $\zeta = \zeta_c$, the displacement representations are:

$$\left.\begin{aligned} u &= \sum_{i=1}^{n} N_i(\xi) u_1 \\ v &= \sum_{i=1}^{n} N_i(\xi) v_1 \\ w &= \sum_{i=1}^{n} N_i(\xi) w_1 \end{aligned}\right\} \qquad (٣.٢٧)$$

The strain-displacement relationship can be expressed in the local coordinate system as:

$$\varepsilon' = \sum_{i=1}^{n} \left[\frac{1}{h^2} \begin{bmatrix} c_1 & c_2 & c_3 \\ c_2 & c_4 & c_5 \\ c_3 & c_5 & c_6 \end{bmatrix} \begin{bmatrix} \frac{\partial N_i}{\partial x} \\ \frac{\partial N_i}{\partial y} \\ \frac{\partial N_i}{\partial z} \end{bmatrix} \right] \begin{bmatrix} u_i \\ v_i \\ w_i \end{bmatrix} \qquad (٣.٢٨)$$

where:

$$c_1 = (\partial x / \partial \xi)^2,$$
$$c_2 = (\partial x / \partial \xi)(\partial y / \partial \xi),$$
$$c_3 = (\partial x / \partial \xi)(\partial z / \partial \xi)$$
$$c_4 = (\partial y / \partial \xi)^2,$$
$$c_5 = (\partial y / \partial \xi)(\partial z / \partial \xi),$$
$$c_6 = (\partial z / \partial \xi)^2$$

and

$$h = \sqrt{c_1^2 + c_4^2 + c_6^2} \qquad (٣.٢٩)$$

Eq. (٣.٢٨) is expressed in a compact form as:

$$\{\varepsilon'\} = [B']\{a\}^e \qquad (٣.٣٠)$$

where [B′] is the strain-displacement matrix of the bar element. Then the stiffness matrix of an axially loaded bar element may be expressed as:

$$[K']^e = \int_{v`} [B']^T [D'] [B'] dv^e \qquad (٣.٣١)$$

The constitutive matrix [D′] represents the modulus of elasticity of the steel bar for the case of one-dimensional bar element lying in the direction parallel to the natural coordinate lineξ, and the volume differential dv^e can be written as:

$$dv^e = As\, dx' = As\, h\, d\xi \qquad (٣.٣٢)$$

where As **is the cross-sectional area of the bar. By substitution of Eq. (٣.٣٢) into Eq. (٣.٣١), the stiffness matrix of the embedded bar can be expressed as:**

$$[K']^e = As \int_{-1}^{+1} [B]^T [D'] [B'] h\, d\xi \qquad (٣.٣٣)$$

٣.٤ Numerical Integration

To perform the integration required to set up the element stiffness matrix, suitable scheme of numerical integration has to be made. In finite element work, the Gauss-Legendre quadratic scheme has been found to be accurate and efficient. The finite integral of the element stiffness matrix given in Eq. (٣.٢٦), can be expressed in the form **[Robinson (١٩٧٣), Dawe (١٩٨٤)]:**

$$I = \int_{-1}^{1}\int_{-1}^{1}\int_{-1}^{1} F(\xi,\eta,\zeta)\,d\xi\,d\eta\,d\zeta \qquad (٣.٣٤)$$

which may be rewritten numerically as:

$$I = \sum_{i=1}^{ni}\sum_{j=1}^{nj}\sum_{k=1}^{nk} Wi.Wj.Wk\,F(\xi_i,\eta_j,\zeta_k) \qquad (٣.٣٥)$$

where ***ni, nj, nk*** are the number of Gaussian points in the ξ_i,η_j,ζ_k direction respectively. The function $\boldsymbol{F(\xi_i,\eta_j,\zeta_k)}$ represents the matrix multiplication $(\boldsymbol{[B]^T.[D].[B].det[J]})$ at sampling points ξ_i,η_j,ζ_k.

In a similar manner, the integral of the stiffness matrix of the embedded reinforcement can be written as:

$$I = \sum_{i=1}^{ni} Wi\, F(\xi_i) \qquad (٣.٣٦)$$

The application of the three-dimensional finite element analysis in connection with the non-linear behavior of reinforced concrete structures needs a large amount of computation time, due to the frequent evaluation of the stiffness matrix. Therefore, it is necessary to choose a suitable integration rule that minimizes the computation time with sufficient accuracy. Several types of integration rules can be used such as the eight (٢ *x* ٢ *x* ٢), and the twenty-seven (٣ *x* ٣ *x* ٣) Gaussian rules are integrate the stiffness matrix of the eight-node linear and the twenty node quadratic

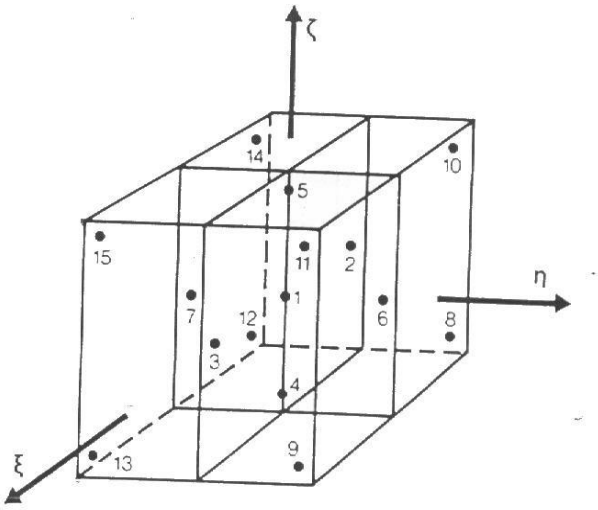

a. ١٥ Point rule

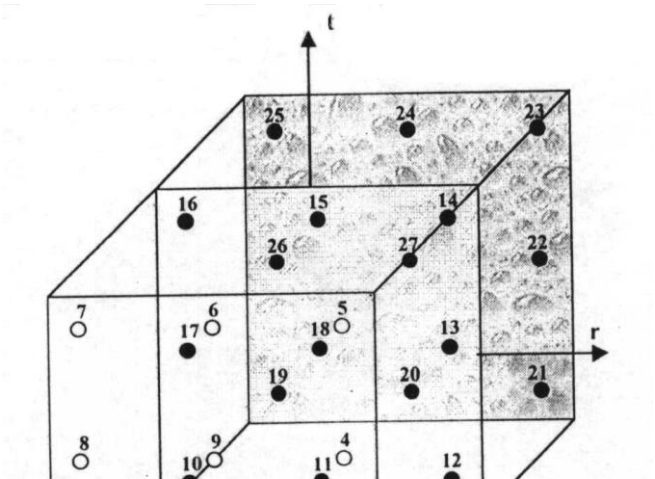

brick elements **[Bathe, ١٩٩٦].** Also, there is the fifteen - node Gauss type integration rule which evaluates the integration for the twenty node quadratic brick element **[Irons ١٩٧١].**

The integration rules, which exist in the program of the present study, are the ٨(٢ *x* ٢ *x* ٢) and ٢٧ (٣ *x* ٣ *x* ٣) Gauss quadratures and also the ١٥ point integration rule. The weights and abscissa of the sampling points are listed in Appendix (A) .The relative distribution of the Gaussion points over the element is given in Fig. (٣.٤).

In the present study, ٢ ٧ Gauss points are used for the numerical integration, as this procedure gives better accuracy **[AL-Shaarbaf, ١٩٩٠]**.

٣.٥ Nonlinear Solution Techniques

A non-linear solution is usually obtained by making a succession of linear approximations until the constitutive laws and conditions of equilibrium are satisfied with an

acceptable error *[Zienkiewiez and Taylor]*.

Using finite element methods leads in general to a set of algebraic equations in the form:

$$\{p\} = [k]\{a\}$$

This can not be achieved directly in the cases of nonlinear system where the stiffness matrix [k] is a function of structure displacement.

$$[k] = [k\{a\}]$$

Therefore, it cannot be calculated before determining the unknown nodal displacements {a}. While in a simple linear elastic problem, the

solution for these equations can be obtained directly.

٣.٥.١ *Survey of Numerical Methods*

The most widely used numerical methods can be classified into three categories:

١. ***Incremental techniques.***
٢. ***Iterative techniques.***
٣. ***Incremental- Iterative techniques.***

In the present study, Incremental-Iterative techniques are used.

٣.٥.١.١ *Incremental- Iterative techniques*

In the present study, the solution of nonlinear problems has been achieved by using the incremental-iterative techniques, in which the load is applied incrementally, but after each increment, successive iterations are performed in order to obtain a converged solution [Al-Shaarbaf ١٩٩٠]. This method yields higher accuracy but a large cost of computational effort, Fig. (٣.٥)

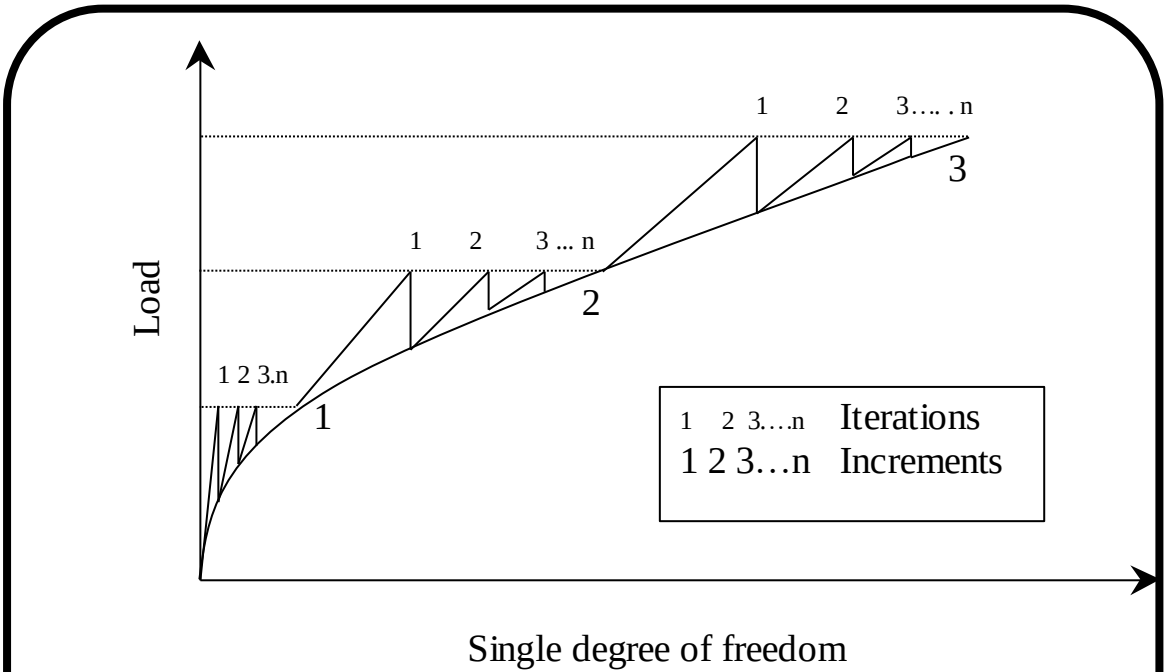

The computer program used in this study incorporates the following incremental-iterative methods .

١. *The standard Newton- Raphson method: In this method the tangential stiffness matrix is updated at each iteration. This is an expensive computational procedure [Ma and May ١٩٨٦].*

٢. *The modified Newton- Raphson method: In this method the stiffness matrix is updated only once for each load increment. Fig.(٢.٦b) shows that the stiffness matrix is updated at the beginning of the first iteration of each load increment, (the KT١ method), while Fig. (٢.٦c) shows that the stiffness matrix is updated at the beginning of the second iteration. (the KT٢ method). But the developed program incorporates a modified Newton- Raphson*

method, in which the stiffness matrix is updated at the 2^{nd} ,…., iterations of each increment of loading. This method is designated as KT٢a at stiffness method.

٣. The initial stiffness method: In this method the stiffness matrix is formulated only once for the analysis. The computation cost per iteration is significantly reduced. However, the solution requires many more iterations compared with those required by the previous methods.

٥.٦ Convergence Criteria

The convergence criterion is an indication for the control of the

level of accuracy of the solution . It terminates the equilibrium iteration as soon as the desired accuracy is achieved .

For nonlinear structural analysis , several convergence criteria can be used to monitor equilibrium. These criteria are usually based on out of balance forces, displacements or internal energy .

In the present work , a displacement convergence criterion is adopted. For this convergence , the criterion employed is :

$$\frac{\sqrt{\sum_{j=1}^{N}\left(\left\{\Delta U j_n^i\right\}\right)^2}}{\sqrt{\sum_{j=1}^{N}\left(\{Uj\}\right)^2}} * 100\% \leq \text{Tolerance} \qquad (٥.١٧)$$

where N denotes the total number of nodal points in the problem , n and i are the number of load increments and iterations , respectively. $\{\Delta U\}$ is the incremental displacement vector, and $\{U\}$ is the displacement vector during the previous iteration. In the present study a tolerance of ٥٪ is used .

٤.٦.٤ Shear Retention Models

In the finite element analysis of reinforced concrete members, a shear retention model is usually used to take into account the capacity of the cracked concrete to transfer shear across the crack. In the present study, a reduction factor has been used across the crack plane, to reduce the shear stiffness at the cracked sampling points. Before cracking a value of unity is assigned to the shear reduction factor. As the crack propagates, the shear reduction factor is taken to be linearly decreasing with the strain normal to the cracked plane, which represents the crack width. When the cracks have sufficiently opened, a constant value is assigned to to account for dowel action. The shear retention model can be expressed as:

١) For $\varepsilon_n < \varepsilon_{cr}$

$$\beta = ١.٠ \qquad (٤.٢٦)$$

٢) For $\varepsilon_{cr} \le \varepsilon_n \le \gamma ١\ \varepsilon_{cr}$

$$\beta = \frac{\gamma 2 - \gamma 3}{\gamma 1 - 1.0}\left[\gamma 1 - \frac{\varepsilon_n}{\varepsilon_{cr}}\right] + \gamma 3 \qquad (٤.٢٧)$$

٣) For $\varepsilon_n > \gamma ١\ \varepsilon_{cr}$

$$\beta = \gamma ٣ \qquad (٤.٢٨)$$

Fig. (٤.٤) shows schematically the value of ***(β)*** for different stages. γ_1, γ_2 ***and*** γ_3 are shear retention parameters. γ_1 represents the rate of decay of shear stiffness as the crack widens, γ_3 is the sudden loss in shear stiffness at the instant of cracking and γ_2 is the residual shear stiffness due to the dowel action. When the crack at a sampling point is closed because of application of cyclic or repeated loading, it is assumed that the original shear modulus is retained, as shown in Fig. (٤.٤) and thus a value of unity is assigned to the shear reduction factor β.

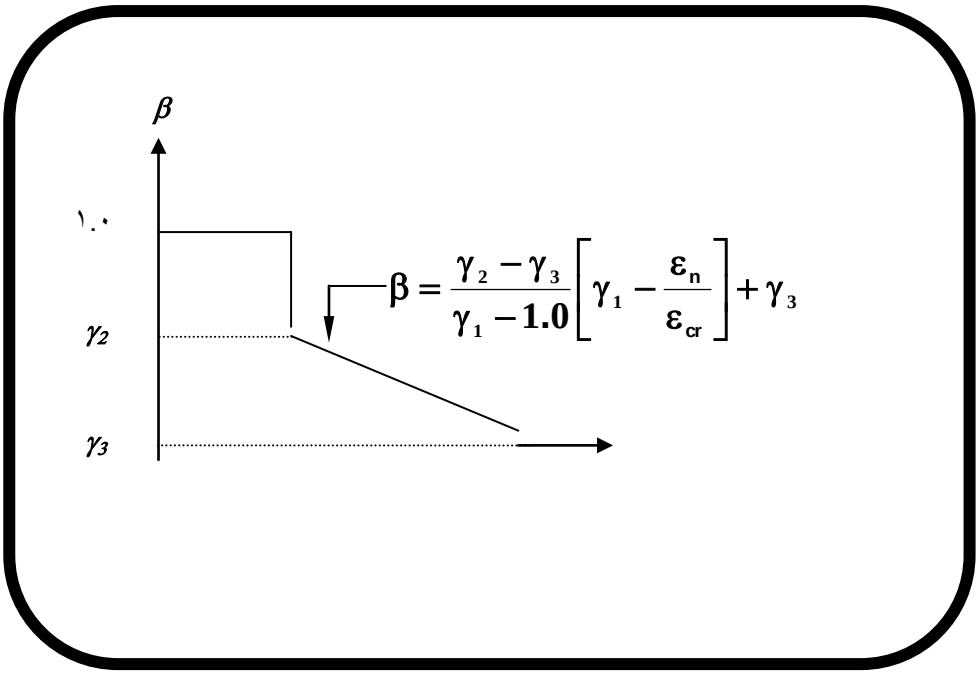

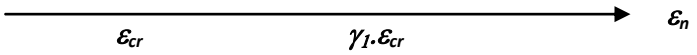

Fig (٤.٤) Shear retention for concrete

٤.٧ Modeling of Reinforcement

In this study the reinforcing steel is modeled as a linear elastic, homogeneous material that can be assumed to have the same strength in tension and compression behavior and its mechanical properties in comparison to the properties of concrete are well known and well understood. Reinforcing bars are usually long and slender and therefore can be generally assumed to be capable of transmitting axial forces only.

In the current study, an elastic-linear work hardening model, as shown in Fig.(٤-٤), simulates the uniaxial stress-strain behavior of steel bars **[Raid Ahmed ٢٠٠٥]**.

In this figure, if the load is released before failure in cyclic or repeated loading, the response curve for unloading from any stress state is approximately a straight line parallel to the initial elastic response. Reloading results in a response path approximately parallel to the original elastic shape.

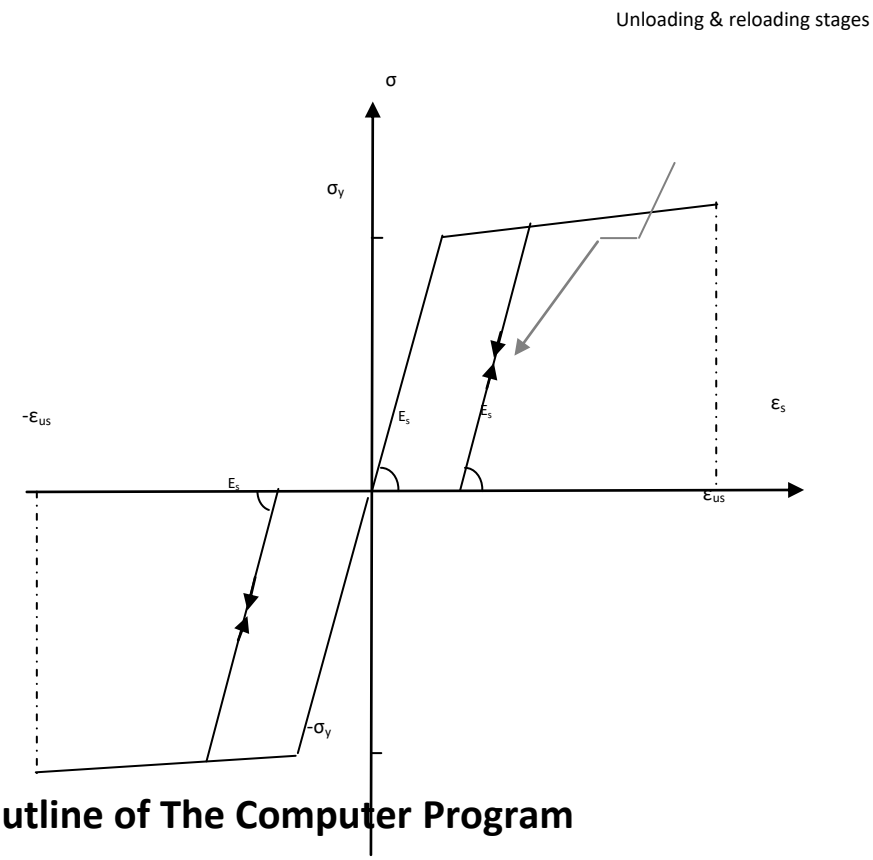

Fig (٤-٥) Idealized elastic-plastic stress-strain relationship for reinforcing steel

٤.٨ Outline of The Computer Program

The computer program P٣ DNFEA (three-dimensional nonlinear finite element analysis) has been used in the present work. This program is originally developed by Al – Shaarbaf. The main objective of the program is to analyze reinforced concrete members under general three-dimensional states of loading up to failure.

In the present research work, the computer program has been modified to analyze beam-column joints under cyclic loading. A nonlinear cyclic behavior model for concrete is used for uniaxial and multiaxial states of stress. Also, a nonlinear cyclic model for reinforcing bars is presented. Closing and reopening of cracks during cyclic loading has been taken into consideration.

In the present study, the numerical analysis has been carried out on ١.٧ GH_z Pentium (IV) processor of a computer that is provided with an ٢٥٦ MB RAM, using the virtual memory technique that utilizes a strong capacity of ٤٠ GB.

٤.٩ Termination of the Analysis

The finite element analysis is terminated when any of the following criteria is satisfied.

١. The stiffness matrix is no longer positive definite .
٢. A reinforcing bar has been fractured .
٣. Excessive concrete crushing takes place .
٤. The number of increments exceeds a maximum specified number .
٥. The number of iterations exceeds a maximum specified number .

Since steel-reinforcement elements in concrete construction are mostly one-dimensional, it is generally not necessary to introduce the complexities of multiaxial constitutive relationships for steel. For simplicity, it is often necessary to idealize the one-dimensional stress-strain curves for steel.

٤.٥ Stress-Strain Models for Concrete in Compression

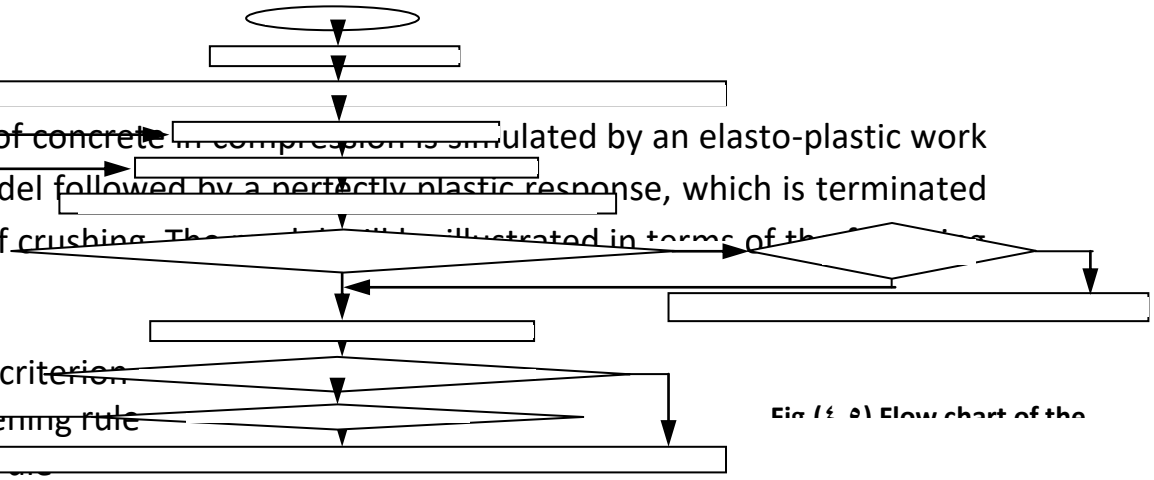

Fig (٤.٩) Flow chart of the

The behavior of concrete in compression is simulated by an elasto-plastic work hardening model followed by a perfectly plastic response, which is terminated at the onset of crushing. The model will be illustrated in terms of the following constituents

(a) The yield criterion
(b) The hardening rule
(c) The flow rule
(d) The crushing condition

٤.٥.١ Yield Criterion

The strength of concrete under multidimensional states of stress is a function of the state of stress and cannot be predicted by limitations of simple tensile, compressive, and shearing stresses independently of each other. Therefore, a proper evaluation of concrete strength can be achieved by considering the interaction of the various components of the state of stress. Many researchers have successfully used a yield criterion which is also used in the present work **[Al-Shaarbaf],[Owen, and Hinton] and [Naji]**. It can be expressed as:

$$f(\sigma) = f(I_1, J_2) = [(\alpha I_1)^2 + 3\beta J_2]^{0.5} = \sigma_o \qquad (٤.١)$$

where α and β are material parameters, I_1 is the first stress invariant given by,

$$I_1 = \sigma_x + \sigma_y + \sigma_z \qquad (٤.٢)$$

J_2 is the second deviatoric stress invariant given by ,

$$J_2 = 1/3\,[(\sigma_x^2 + \sigma_y^2 + \sigma_z^2) - (\sigma_x\sigma_y + \sigma_y\sigma_z + \sigma_z\sigma_x)] + [\tau_{xy}^2 + \tau_{yz}^2 + \tau_{zx}^2] \qquad (٤.٣)$$

and $\sigma_o > 0.0$ is the equivalent effective stress at the onset of plastic deformation which can be determined from the uniaxial compression test as:

$$\sigma_o = Cp\, f'_c \qquad (٤.٤)$$

where C_p is the plasticity coefficient which is used to mark the initiation of the plastic deformation.

The parameters (α) and (β) are determined by using the uniaxial and biaxial compression tests. Then for a uniaxial compression state, the yield stress is given by:

$$\sigma_X = -\sigma_O \qquad (٤.٥)$$

and for the equal biaxial compression state, the yield stress is given by:

$$\sigma_X = \sigma_y = -\gamma\sigma_0 \qquad (٤.٦)$$

If the results obtained by **[Kupfer et. al. (١٩٦٩)]** for the failure envelope is employed for initial yield, the value of the constant ***(γ)*** is equal to (١.١٦). Fro Eq. (٤.١) and using Eqs. (٤.٥) and (٤.٦), the material constants can be found to be:

$$\alpha = 0.35468\ \sigma_0 \quad \text{and} \quad \beta = 1.35468 \qquad (٤.٧)$$

Writing $C = \dfrac{\alpha}{(2\sigma_0)} = 0.17734$ then Eq. (٤.١) can be written as:

$$f(\sigma) = (2C\sigma_o\ I_1 + 3\beta J_2)^{1/2} = \sigma_0 \qquad (٤.٨)$$

This can be solved for σ_o as:

$$C.I_1 + \{(C.I_1)^2 + 3\beta J_2\}^{1/2} = \sigma_o \qquad (٤.٩)$$

٤.٥.٢ The Hardening Rule

The hardening rule is necessary to define the change of position of the loading surface during plastic deformation. A relationship between the accumulated plastic strain and the effective stress is required to control the position of the current "loading surface". A number of hardening rules has been proposed to describe the growth of the subsequent loading surfaces for a work hardening material. The isotropic hardening rule has been adopted in the present study to simulate concrete behavior. This rule assumes that the yield surface expands uniformly without distortion as plastic deformation occurs. Therefore, the subsequent loading surfaces may be written as:

$$f(\sigma) = f(I_1, J_2) = [(\alpha I_1)^2 + 3\beta J_2]^{0.5} = \bar{\sigma} \qquad (٤.١٠)$$

where the effective stress or equivalent uniaxial stress $\bar{\sigma}$ represents the level at which further plastic deformation will occur. The uniaxial stress-strain curve is assumed to be linear up to stress level equal to Cpf'_c followed by a parabolic shape up to peak compressive stress f'_c.

a) For $\bar{\sigma} \leq Cp\, f'_c$

$$\bar{\sigma} = E\, \varepsilon_c \qquad (٤.١١)$$

b) For $Cp\, f'_c \leq \bar{\sigma} \leq f'_c$

$$\bar{\sigma} = Cp\, f'_c + E\left[\varepsilon_c - \frac{Cp\, f'_c}{E}\right] - \frac{E}{2\varepsilon'_\circ}\left[\varepsilon_c - \frac{Cp\, f'_c}{E}\right]^2 \qquad (٤.١٢)$$

c) For $\varepsilon_c \geq (2 - Cp) f'_c / E$

$$\bar{\sigma} = f'_c \qquad (٤.١٣)$$

where $\varepsilon'_\circ$ the total strain corresponding to the parabolic part of the curve given by:

$$\varepsilon'_{o} = ٢ (١ - Cp) f'_{c} / E \qquad (٤.١٤)$$

A value of ٠.٥ is assumed for the plastic coefficient C_p in the present study and hence plastic yield begins at stress level that equals (٠.٥ f'_c) Fig.(٤.٢) .

In cyclic loading or repeated loading, when the load is released before failure the response curve for unloading part is approximately a straight line parallel to the initial elastic response. Reloading follows the same path of unloading stage.

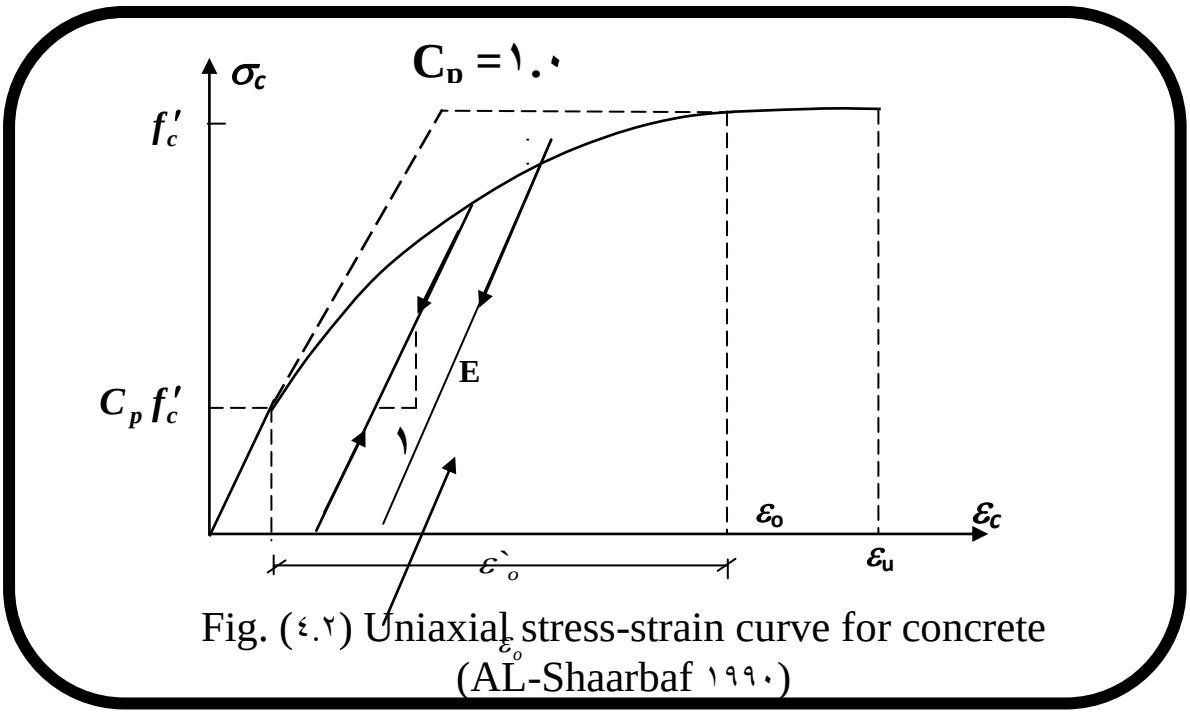

Fig. (٤.٢) Uniaxial stress-strain curve for concrete (AL-Shaarbaf ١٩٩٠)

By substituting the value of total strain component, which is the sum of the elastic and plastic strains in Eq (٤.١٢), the effective stress – plastic strain relationship can be expressed as:

$$\bar{\sigma} = Cp\, f'_c - E\,\varepsilon_p + (٢\, E^2\ \varepsilon'_\circ \varepsilon_p)^{0.5} \qquad (٤.١٥)$$

The hardening coefficient, which is the slope of the effective stress – plastic strain curve, is used in the formulation of the hardening coefficient H' which is obtained by differentiating Eq. (٤.١٥) with respect to the effective plastic strain.

$$H' = \frac{d\bar{\sigma}}{d\varepsilon_p} = E\left[\left(\frac{\varepsilon'_\circ}{2\,\varepsilon_p}\right)^{0.5} - ١.٠\right] \qquad (٤.١٦)$$

4.5.3 Flow Rule

In plasticity theory, a flow rule must be defined so that the plastic strain increment can be determined for a given stress increment. The associated flow rule has been widely used for concrete models mainly because of its simplicity. This approach is adopted in the current study. The plastic strain increment is expressed as:

$$d(\varepsilon_p) = d\lambda\ \frac{\partial f(\sigma)}{\partial \sigma} \qquad \ldots(٤.١٧)$$

The normal to the current loading surface $\frac{\partial f(\sigma)}{\partial \sigma}$ is termed as the flow vector {a} which is, the yield function derivatives with respect to the stress components:

$$\{a\} = \left[\frac{\partial f}{\partial \sigma_x}, \frac{\partial f}{\partial \sigma_y}, \frac{\partial f}{\partial \sigma_z}, \frac{\partial f}{\partial \tau_{xy}}, \frac{\partial f}{\partial \tau_{yz}}, \frac{\partial f}{\partial \tau_{zx}} \right]^T \quad \ldots(٤.١٨)$$

These derivatives are given in Appendix [B]:

4.5.4 The Crushing Condition

Crushing indicates the complete rupture and disintegration of the material under compressive stress state. After crushing, the current stresses drop rapidly to zero and the concrete is assumed to lose its resistance completely against further deformation.

In the adopted model, concrete is considered to crush when the strain reaches a specified ultimate value. Hence, rewriting the yield condition from Eq. (٤.٩) in terms of the peak strain, the following crushing criterion is obtained:

$$C\ \bar{I}_1 + \sqrt{\left(C\bar{I}_1\right)^2 + \beta\bar{J}_2} = \varepsilon_{cu} \qquad (٤.١٩)$$

where $\bar{I}_1$: is the first strain invariant

$\overline{J_2}$: is the second deviatoric strain invariant

ε_{cu} : is the ultimate concrete strain that can be obtained from the uniaxial compression test ($\varepsilon_u = \varepsilon_{cu}$).

٤.٦ Crack Model for Concrete in Tension

A smeared fixed-cracking model is used to represent the crack model and it is widely used in connection with the finite element analysis. This implies that the cracks are distributed at a cracked sampling point **[Al-Shaarbaf]**. It is assumed that the concrete becomes orthotropic after the first crack has occurred. Cracks are assumed to form in a plane perpendicular to the direction of the maximum principal tensile stress.

٤.٦.١ The Cracking Criterion

Tensile failure occurs if the tensile stress in a principal stress direction exceeds the limiting tensile strength of concrete. Also a plane of fracture is assumed to develop perpendicular to the principal stress direction. The limiting tensile stress required to define the onset of cracking can be calculated for states of triaxial tensile stress and for combinations of tension and compression principal stresses as follows[**Bathe and Ramaswamy ١٩٧٩**].

a) For triaxial tension zone $(\sigma_1 \geq \sigma_2 \geq \sigma_3 \geq 0)$ (٤.٢٠)

$$\sigma_i = \sigma_{cu} = f_t \qquad i = 1,2,3$$

b) For the tension-tension-compression zone $(\sigma_1 \geq \sigma_2 \geq 0, \sigma_3 \leq 0)$

$$\sigma_i = \sigma_{cr} = f_t\left[1+\frac{0.75\,\sigma_3}{f'_c}\right] \qquad i = 1,2 \qquad (٤.٢١)$$

For the tension-compression-compression zone $(\sigma_1 \rangle 0, \sigma_3 \leq \sigma_2 \leq 0)$

$$\sigma_1 = \sigma_{cr} = f_t\left[1+\frac{0.75\sigma_2}{f'_c}\right]\left[1+\frac{0.75\sigma_3}{f'_c}\right] \qquad (٤.٢٢)$$

where

σ_{cr} is the cracking stress and both f_t and $f`_c$ are given positive values. Eq. (٤.٢١) incorporates the fact that compression in one direction favors cracking in the others and thus reduces the tensile capacity of the material.

When the major principal stress σ_1 violates the cracking criterion, planes of failure develop perpendicular to its direction. Concrete behavior is no longer isotropic, it becomes orthotropic with the direction of orthotropy coinciding with the direction of σ_1. Therefore, the normal and shear stresses across the plane of failure and the corresponding normal and shear stiffness are reduced, and the concrete is assumed to be transversely isotropic with axes of isotropy being perpendicular to the direction of σ_1 or parallel to the plane of crack . Thus, the incremental stress-strain relationship in the local axes can be expressed as:

$$\begin{Bmatrix} \Delta\sigma_1 \\ \Delta\sigma_2 \\ \Delta\sigma_3 \\ \Delta\tau_{12} \\ \Delta\tau_{23} \\ \Delta\tau_{31} \end{Bmatrix} = \begin{bmatrix} E_1 & 0 & 0 & 0 & 0 & 0 \\ 0 & E/\left(1-\nu^2\right) & \nu E/\left(1-\nu^2\right) & 0 & 0 & 0 \\ 0 & \nu E/\left(1-\nu^2\right) & E/\left(1-\nu^2\right) & 0 & 0 & 0 \\ 0 & 0 & 0 & \beta_1 G & 0 & 0 \\ 0 & 0 & 0 & 0 & G & 0 \\ 0 & 0 & 0 & 0 & 0 & \beta_1 G \end{bmatrix} \begin{Bmatrix} \Delta\varepsilon_1 \\ \Delta\varepsilon_2 \\ \Delta\varepsilon_3 \\ \Delta\gamma_{12} \\ \Delta\gamma_{23} \\ \Delta\gamma_{31} \end{Bmatrix} \qquad (٤.٢٣)$$

or in a condensed from:

$$\{\Delta\sigma\} = [D_{cr}]\{\Delta\varepsilon\} \qquad (٤.٢٤)$$

where E' is the reduced modulus of elasticity in the direction of σ', and $\beta\backslash G$ is the reduced shear modulus across the failure plane. $[D_{cr}]$ is the material stiffness in the local axes. The stress increments in the global axes (x, y, z) may be obtained by using the coordinate transformation matrix such that:

$$\{\Delta\sigma\} = [T]^T [D_{cr}][T]\{\Delta\varepsilon\} \qquad (٤.٢٥)$$

where ***[T]*** is the transformation matrix expressed in terms of the direction cosines as:

$$[T] = \begin{bmatrix} l_1^2 & m_1^2 & n_1^2 & l_1 m_1 & m_1 n_1 & n_1 l_1 \\ l_2^2 & m_2^2 & n_2^2 & l_2 m_2 & m_1 n_1 & n_1 l_1 \\ l_3^2 & m_3^2 & n_3^2 & l_3 m_3 & m_1 n_1 & n_1 l_1 \\ 2l_1 l_2 & 2m_1 m_2 & 2n_1 n_2 & l_1 m_2 + l_2 m_1 & n_2 m_1 + n_1 m_2 & l_2 n_1 + l_1 n_2 \\ 2l_2 l_3 & 2m_2 m_3 & 2n_2 n_3 & l_2 m_3 + l_3 m_2 & n_3 m_2 + n_2 m_3 & l_3 n_2 + l_2 n_3 \\ 2l_3 l_1 & 2m_3 m_1 & 2n_3 n_1 & l_3 m_1 + l_1 m_3 & n_1 m_3 + n_3 m_1 & l_1 n_3 + l_3 n_1 \end{bmatrix}$$

where l_i, m_i and n_i represent the direction cosines of the local coordinate axes (i=١, ٢ and ٣ for x, y and z) direction respectively. For the tension – tension – compression and the triaxial tension states of stress, the cracking criterion may be violated by the major principal stress σ_1, and the second principal stress σ_2, simultaneously. Thus, two sets of orthogonal cracked planes may develop and the constitutive matrix in the local material axes becomes diagonal:

$$[D]_{cr} = \begin{bmatrix} E_1 & 0 & 0 & 0 & 0 & 0 \\ 0 & E_2 & 0 & 0 & 0 & 0 \\ 0 & 0 & E_3 & 0 & 0 & 0 \\ 0 & 0 & 0 & \beta_1 G & 0 & 0 \\ 0 & 0 & 0 & 0 & \beta_2 G & 0 \\ 0 & 0 & 0 & 0 & 0 & \beta_1 G \end{bmatrix} \qquad (٤.٢٧)$$

In the current model, a maximum of three sets of cracking are allowed to form at each sampling point.

4.6.2 Tension- Stiffening Model

The tensile stresses normal to the cracked planes are gradually released, and represented by an assumed average stress-strain curve. In the present study such a relationship is obtained by using the tension-stiffening model. This is specified by a linear descending

stress-strain curve similar to that shown in Fig. (٤.٣) and this is given by: [**Scanlon (١٩٧١), Bathe and Ramsawamy (١٩٧٩)]**

a) for $\varepsilon_{cr} \leq \varepsilon_n \leq \alpha_1 \varepsilon_{cr}$

$$\sigma_n = \alpha_2 \sigma_{cr} \left[\frac{\alpha_1 - \frac{\varepsilon_n}{\varepsilon_{cr}}}{\alpha_1 - 1.0} \right] \qquad (٤.٢٨)$$

b) For

$$\varepsilon_n > \alpha_1 \varepsilon_{cr}$$

$$\sigma_n = 0.0 \qquad (٤.٢٩)$$

where σ_n and ε_n are the normal stress and strain normal to the cracked plane, ε_{cr} is the cracking strain associated with the cracking stress σ_{cr} and α_1 and α_2 are the tension-stiffening parameters. α_1 represents the rate of stress release as the crack widens, while α_2 represents the sudden loss of stress at instant of cracking.

٤.٦.٣ Closing and Re-Opening of Cracks

For a member under cyclic or repeated loading, cracks at sampling points may close. For a closing crack it is assumed that the orthotropy of the sampling point under consideration is maintained. Unloading and re-opening of cracks are assumed to follow a secant path, Fig. (٤.٣) . The secant modulus, $E_{\backslash}$, can be evaluated from the previously stored maximum strain developed normal to the cracked plane. This secant modulus may be used to calculate the retained stress as:

$$\sigma_n = E_{\backslash}. \ \varepsilon_n \qquad (٤.٣٠)$$

where ε_n is the maximum strain developed normal to the cracked plane.

CHAPTER FOUR

MODELING OF MATERIAL PROPERTIES

٤.١ Introduction

Concrete and reinforcing steel have very different material properties ,the behavior of the composite reinforced concrete is usually simulated by considering the constitutive relations of the constituents independently. Full interaction between the two materials has been assumed to exit throughout the present work.. The stress–strain relationship for steel is very well defined. Concrete, however, is heterogeneous but assumed homogeneous for macroscopic behavior and has completely different properties in tension and compression .

٤.٢ Uniaxial Behavior of Concrete

٤.٢.١ Uniaxial Behavior of Concrete in Compression

The stress-strain relation is composed of an almost straight line up to about ٠.٣ f'_c for normal strength concrete then a strain-hardening portion extending to the maximum compressive stress (f'_c), which is of the same shape for various testing conditions, followed by a strain-softening portion extending to the ultimate compressive strain (E_{cu}), Fig. (٤.١).

The shape of the stress-strain curve is similar for concrete of low, normal, and high strength .A high strength concrete behaves in a linear fashion to a relatively higher

stress level than the low strength concrete, but all peak points are located close to a strain value of (٠.٠٠٢).On the descending portion of the stress-strain curve ,higher strength concretes tend to behave in a more brittle manner ,the stress dropping off more sharply than it does for concrete with lower strength. The essential features defining the stress-strain relation are :

١.Compressive strength (f'_c) .

٢. Initial elastic modulus (E).

٣. The strain corresponding to the maximum stress (E_o).

٤.٢.٢ Uniaxial Behavior of Concrete in Tension

Fig. (٤.١) shows the stress-strain curve for concrete in uniaxial tension and compression. The curve for tension is nearly linear up to a relatively high stress level equal to the tensile strength. The shape of the curve shows some

similarities to the uniaxial compression curve. This is not surprising since the role of microcraking must be even more important for tensile states of stress. There are, however, some differences between the two states of stress.

There are several forms of models which are used to represent the post-cracking behavior such as linear descending branches, bilinear and trilinear descending branches, and nonlinear descending branch.

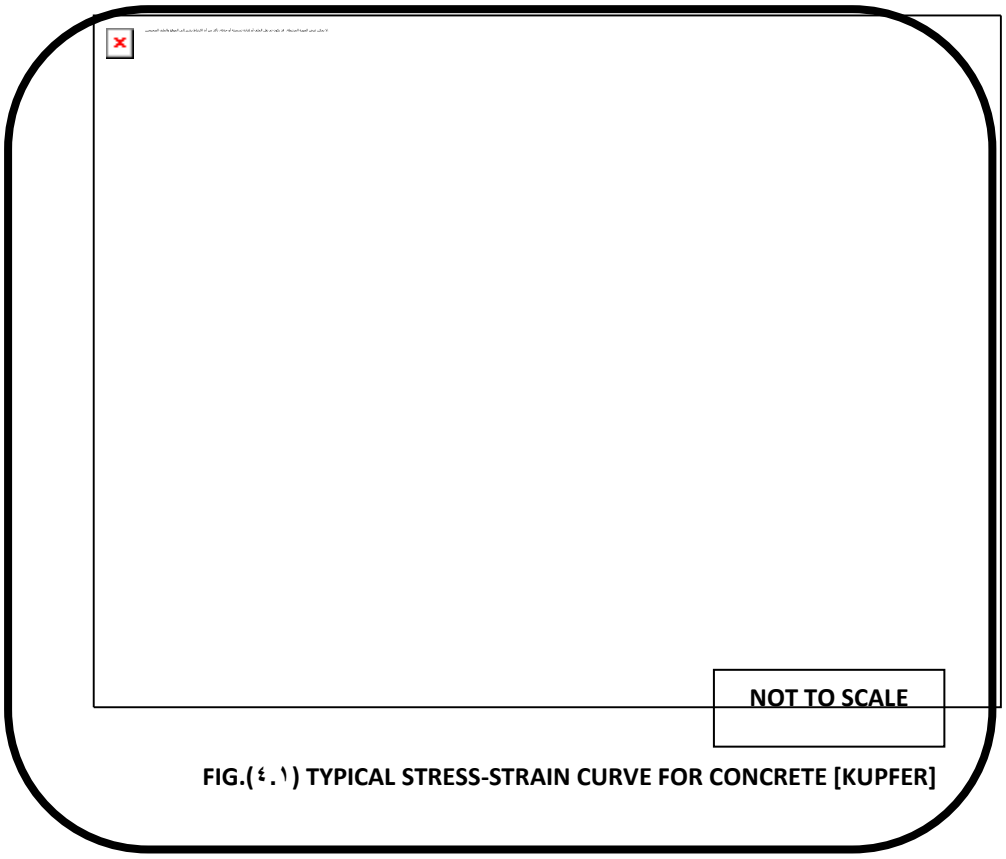

FIG.(٤.١) TYPICAL STRESS-STRAIN CURVE FOR CONCRETE [KUPFER]

٤.٣ Multiaxial Behavior of Concrete

Under multiaxial states of stress, concrete exhibits strength, stiffness and stress-strain behavior somewhat different from that of uniaxial state. Based on experimental results [Kupfer et al.(١٩٦٩)], the concrete ductility under biaxial stresses has different values depending on whether the stress states are compressive or tensile. Under biaxial compression state, the compressive strength increases approximately by ٢٥ percent for principal stress ratio of ٠.٥ and by ١٦ percent for principal stress ratio of ١.٠ .Under biaxial compression-tension ,the compressive strength decreases almost linearly as the applied tensile stress is increased .Under biaxial tension ,the strength is almost the same as that of uniaxial tensile strength . When subjected to triaxial compressive stress, concrete exhibits strength which increases with the increasing confining pressures .

٤.٤ Stress-Strain Behavior of Reinforcing Steel

Typical stress-strain curves for steel are composed of three distinctive parts: a linear elastic part, a yield plateau and a strain-hardening part which is terminated by ultimate value. The stress-strain curves for steel are generally assumed to be identical in tension and compression. The essential properties defining the stress-strain curves are:

١. Elastic modulus (E_s).
٢. Yield strength (f_y).
٣. Yield plateau.
٤. Strain-hardening region.
٥. Ultimate steel strain(ε_{su}).

٥.٥ Shear Transfer Across the Crack

For the shear transfer across cracked concrete planes crossed by reinforcement , the two major mechanisms in effect are the dowel action and the aggregate interlock. Shear transfer by these two mechanisms is accompanied by slippage or relative movement of crack faces . When the concrete interface is subjected to a shear displacement, this relative displacement causes some deformation and/or cut-off of protruding asperities . Due to this overriding , a lateral dilatancy is produced . To this dilatancy the reinforcing bar responds by a pullout force . For the purpose of equilibrium this tensile force is equal to a compressive force acting on the concrete at the vicinity of the bar . It is precisely due to this compressive force that a shear resistance is developed at the interface.

٥.٥.١ Aggregate Interlock

Several models have been proposed to explain or predict the aggregate interlock behavior. The two-phase model by [**Walraven** and **Reinhardt (١٩٨١)]** is an example of a physical model . That type of model gives a better understanding of the mechanism involved at the crack interface. The [**Yoshikawa et al. (١٩٨٩)]** model is an example of an empirical model , in which a free slippage occurs in the initial shear load on the cracked planes which are not in close contact , and further application of the shear stress makes the cracks stiffer due to firm contact (aggregate interlock). Finally , the shear

stress levels are approaching the ultimate shear strength . The [**Tassios** and **Vintzeleou (١٩٨٧)]** model is another example of empirical model . It covers two types of interfaces , the rough interface and the smooth interface , for normal stresses ranging up to ٢ MPa .

In this model , the frictional resistance is roughly equal to the tensile strength of concrete , taking into account the tensile strength reduction due to a transverse compressive stress as follows :

$$\tau_u = [\ ٠.٣\ (\ ١٠+٩\ (\ \sigma_c/f_t\ ) - (\ \sigma_c/f_t\ )^{٢}\ )^{٠.٥}\ ]\ f_t \qquad (٥.٦)$$

[Fronteddu et al. (١٩٩٨)] utilized their experimental results from displacement controlled shear tests on concrete lift joint specimens with different surface preparations, to propose an empirical interface constitutive model based on the concept of basic friction coefficient (μ_b) and roughness friction coefficient (μ_i) :

$$\tau_u = \frac{\lambda_d \mu_b + \chi_i \mu_i}{1 - \lambda_d \chi_i \mu_b \mu_i} \qquad (٥.٧)$$

where $\mu_b = ٠.٩٥٠ - ٠.٢٢٠\ \sigma_n$ for $\sigma_n \leq ٠.٥$ MPa

$\mu_b = ٠.٨٦٥ - ٠.٠٥٠\ \sigma_n$ for $٠.٥ \leq \sigma_n \leq ٢.٠$ MPa

μ_i is defined by the equations in Table (٥.١). Two correction factors were introduced: (١) λ_d, the dynamic reduction factor equal to ١.٠٠ for static loading, and ٠.٨٥ for dynamic loading ; and (٢) χ_i,the interface roughness factor equal to ١.٠٠ for cracked homogeneous concrete , ٠.٨ for water blasted joints, ٠.١٥ for untreated joints, and ٠.٠٠ for flat independent concrete surfaces.

*Based on the experimental results presented by [**Fronteddu et al. (١٩٩٨)**], a bilinear relationship between shearing stress and slip, Fig. (٥.٣), is adopted, which is multiplied by the effective thickness at the Gaussian point of interface element to convert it to a relationship between shearing stress and strain. From Eqs.(٥.٦ and ٥.٧) a good prediction of aggregate interlock stiffness can be obtained.*

Table (٥.١) Roughness coefficient for concrete interface model
[Fronteddu et al. (١٩٩٨)]

Interface type	σ_n (MPa)	Peak μ_{ib}
Homogeneous	$\sigma_n \leq$ ٠.٤	٠.٩٠- ١.٣٦٧ σ_n
	٠.٤ $\leq \sigma_n \leq$ ١.٥	٠.٤٠- ٠.١١٦٧ σ_n
	١.٥ $\leq \sigma_n \leq$ ٢	٠.٣٠- ٠.٠٥٠ σ_n
Water- blasted	$\sigma_n \leq$ ٠.٢٧٥	٠.٨٧٥- ١.٧٥ σ_n
	٠.٢٧٥ $\leq \sigma_n \leq$ ١.٢	٠.٤٤- ٠.١٨٥ σ_n
	١.٢ $\leq \sigma_n \leq$ ٢	٠.٢٥- ٠.٠٣٧٥ σ_n
Untreated	$\sigma_n \leq$ ١.٠	٠.١٥- ٠.١٥ σ_n
	١.٠ $\leq \sigma_n \leq$ ٢.٠	٠.٠٥- ٠.٠٠٥ σ_n

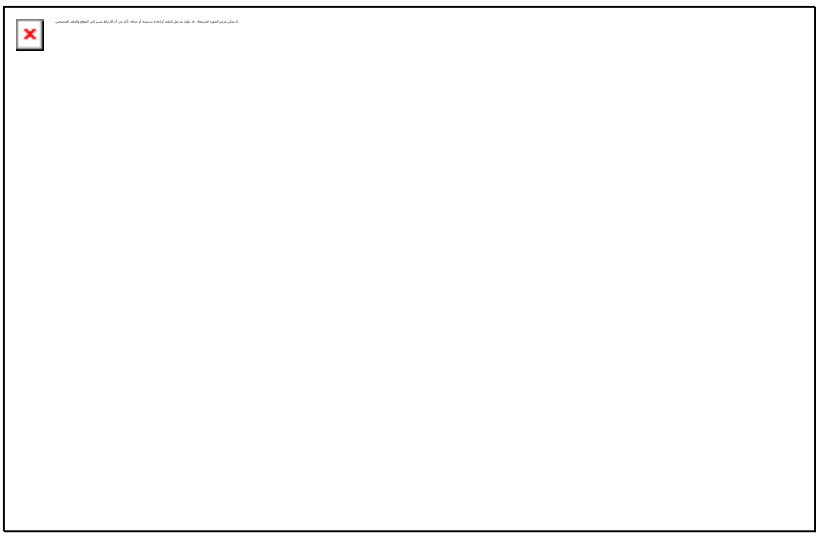

Fig. (٥.٣) Adopted shearing stress-slip relationship

٥.٥.٢ Dowel Action

Shearing forces can be transmitted across a crack in the reinforced concrete by the reinforcement crossing the crack . If the reinforcement is
normal to the plane of cracking, dowel action (shearing and flexure of the bars) will contribute to the overall shear stiffness .

It has been suggested **[Paulay et al. (١٩٧٤)]** that there are three mechanisms of shear transfer through the dowel action in cracked reinforced concrete, i.e. direct shear, kinking and flexure of the bars . If the concrete supporting each bar were considered to be rigid , the first two mechanisms would predominate. However, it has been recognized **[Mills (١٩٧٥)]** that significant deformation of the concrete does occur , so that flexure of the dowel bar within the concrete is a principal action . This has been modeled **[Millard (١٩٨٤)]** by considering the dowel bar as a beam on elastic foundation. This model is adopted, according to this model the dowel force , $F_{d,}$ is given by :

$$F_d = ٠.١٦٦\ \Delta_t\ G_f^{٠.٧٥}\ \Phi^{١.٧٥}\ E_s^{٠.٢٥} \qquad (٥.٨)$$

where the constant term is dimensionless

G_f : foundation modulus for concrete , A typical value for ٣٥ MPa concrete has been found to be ٧٥٠ N/mm^{٣} (ACI Committee ٣٢٥). For the high strength mix, it has been assumed that G_f is proportional to $f_{cu}^{٠.٥}$.

Φ : diameter of the bar.

E_s : elastic modulus of steel.

Δ_t : slip or relative displacement across the crack .

Only the initial dowel stiffness can be predicted using this equation .

The nonlinear shear stiffness of the dowel action may be attributed to one or both of the following two causes .

١) Crushing or splitting of the concrete supporting the bar .

٢) Plastic yielding of the reinforcement .

A good prediction of the ultimate shearing force in a bar with an axial stress of $f_s = \alpha f_y$ is given by:

$$F_{du} = ١.٣ \Phi^{٢} f_{cu}^{٠.٥} (f_y (١- \alpha^{٢}))^{٠.٥} \quad (٥.٩)$$

where F_{du} is the ultimate dowel force and $\alpha = f_s / f_y$.

An exponential function was used to describe the overall dowel action behavior. The dowel force , F_d , is as follows :

$$F_d = F_{du} (١-\exp(-ki\ \Delta_t / F_{du})) \quad (٥.١٠)$$

where $k_i = F_d / \Delta_t$ is the initial dowel stiffness obtained from Eq.(٤.٨).By simplifying Eq.(٥.١٠), the shear stiffness of the dowel action which is used in the present study as a relationship between the shearing stress and the shear strain can be found as follows :

$$k_d = (k_i - \frac{ki^2 \Delta_t}{2 F_{du}}) t / A_c \quad (٥.١١)$$

٥.٦ Interface Element

The behavior of a composite concrete specimen depends upon the interaction between the two concerts cast at different times . There can be separation , closing of gap , and slipping between the two parts .In the present study a thin layer element is used to represent this behavior .

٥.٦.١ Thin Layer Element

An isoparametric finite element formulation , which is treated essentially like a solid element , can be used to represent the behavior of the interface region **[Desai and Zaman (١٩٨٤)]** , Fig.(٥.٤) . Since the element is treated essentially like any other solid element , its incremental stress-strain relationship is expressed as :

$$\{d\sigma\} = [D]_i \{d\varepsilon\} \qquad (٥.١٢)$$

where $[D]_i$ is the constitutive matrix for the interface region . The behavior of the interface material is assumed to be like the concrete of the softer material properties for all stages of loading, described in Chapter four , except the shear component which represents the shear behavior specified for the interface region, described in Chapter four (G_t), thus the constitutive matrix for the interface element can be written as :

$$[D]_i = \begin{bmatrix} (1-\nu)E' & \nu E' & \nu E' & 0 & 0 & 0 \\ \nu E' & (1-\nu)E' & \nu E' & 0 & 0 & 0 \\ \nu E' & \nu E' & (1-\nu)E' & 0 & 0 & 0 \\ 0 & 0 & 0 & G_t & 0 & 0 \\ 0 & 0 & 0 & 0 & G_t & 0 \\ 0 & 0 & 0 & 0 & 0 & G_t \end{bmatrix} \qquad (٥.١٣)$$

$$\text{Where } E' = \frac{E}{(1+\nu)(1-2\nu)}$$

where G_t is obtained from Eq. (٥.١١) for dowel action and from Eq. (٥.٧) besides the contribution to the dowel action, the steel reinforcement crossing the interface is treated as axial members embedded in the concrete (interface) brick elements.

$G_t = K_i + K^*$

$K^* = (\tau_u)(t_{efc.})$

The interface behavior depends on the properties of the surrounding media . However, it also depends on the thickness of the thin-layer element .If the thickness is too large in comparison with the average contact dimension (B) of the surrounding element , the thin-layer element will behave essentially as a solid element. On the other hand, if it is too small, computational difficulties may arise .Based on the available experimental results, the satisfactory simulation of the interface behavior can be obtained for (t / B) ratios in the range from (٠.٠١) to (٠.١). This conclusion may need modification if the nonlinear behavior of solids and interfaces were simulated .The ٢٠-noded isoparametric brick element is used to describe the interface brick element in this study.

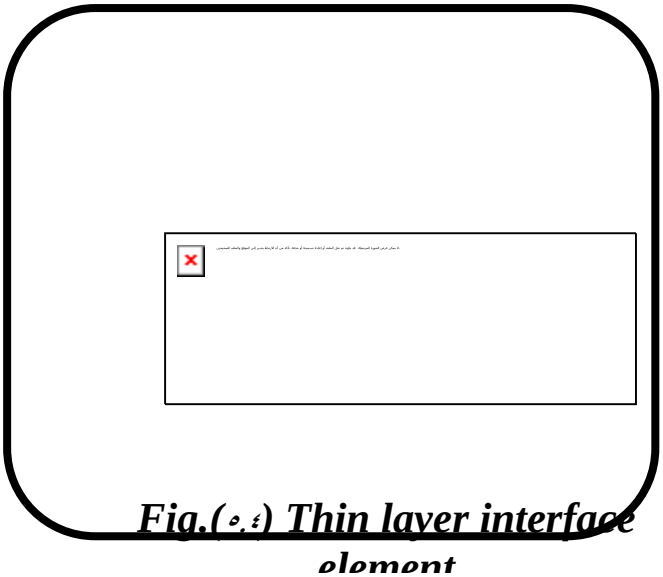

Fig.(٤.٥) Thin layer interface element

CHAPTER FIVE

INTERFACE ELEMENT

٥.١ Introduction:

In many cases, the assumption of complete compatibility in the contact interface between two bodies or two materials is a coarse simplification which may lead to unrealistic results in a finite element analysis .The contact interface is a special region of a structure, which behaves nonlinearly causing stress concentration and relative displacement like crack opening or slip. The adequate modeling of the interaction between two concretes cast at different ages including the definition of the stress transfer in the interface requires an interface element which is compatible to the three-dimensional elements used in concrete modeling. An isoparametric solid element has has been used to meet these requirements.

This solid element called a thin-layer element, developed by [Desai et.al. (١٩٨٤)] is used in the present study. The twenty-node isoparametric brick element with small thickness is used to model the interface, Fig.(٥.١). The formulation of the thin-layer element is essentially the same as for the brick element used for representing concrete, but a special constitutive model is

used and various deformation modes such as no slip, slip, debonding and rebonding are incorporated. The normal and shear stiffnesses are assumed to be composed of participation of the thin-layer element and the adjoining solid elements.

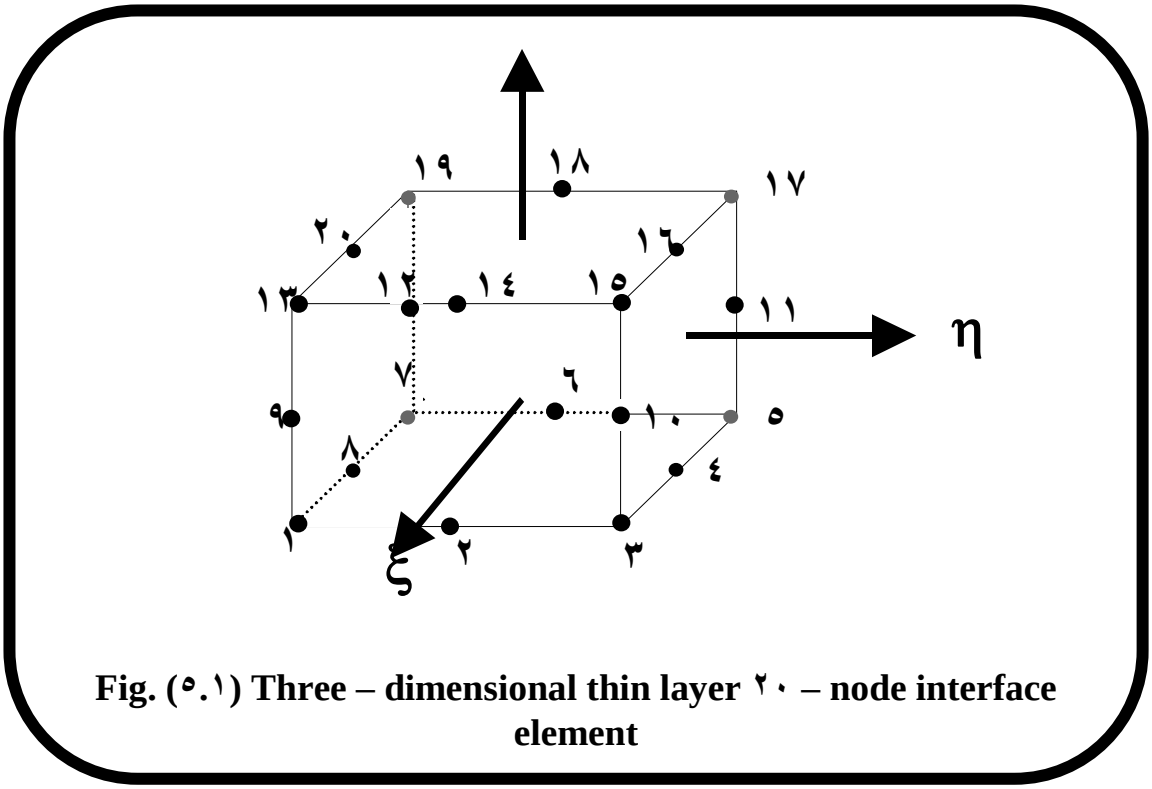

Fig. (٥.١) Three – dimensional thin layer ٢٠ – node interface element

٥.٢ *Shear-Friction Concept*

The shear-friction concept provides a convenient tool for the design of members for direct shear where it is inappropriate to design for diagonal tension , as in precast connections, and brackets or (corbels) . The approach is to assume that a crack has formed at an expected location , as illustrated in

Fig.(٥.٢). As slip begins to occur along the crack , the roughness of the crack surface forces the opposite faces of the crack to separate . This separation is resisted by reinforcement (A_{vf}) across the assumed crack . The tensile force ($A_{vf}f_y$) developed in the reinforcement by this strain induces an equal and opposite normal clamping force , which in turn generates a frictional force ($A_{vf}f_y\mu$)parallel to the crack to resist further slip , where μ is the coefficient of friction .

Shear-friction design is to be used where direct shear is being transferred across a given plane. Situations where shear-friction design is appropriate include the interface between conceretes cast at different times , an interface between concrete and steel , and connections in precast constructions . Successful application of the concept depends on proper selection of the location of the assumed slip or crack .

٥.٣ Shear-Friction Design Method

As with other design applications , the code provisions for shear-friction are presented in terms of shear-transfer strength (V_n) for direct application in the basic shear strength relation :

$$V_u \leq \Phi V_n \qquad (٥.١)$$

where Φ is ٠.٨٥ for shear (ACI Code ٣١٨M-٩٥) . The required shear-transfer strength for shear-friction reinforcement perpendicular to the shear plane is :

$$V_u \leq \Phi A_{vf} f_y \mu \qquad (٥.٢)$$

The required area of shear-friction reinforcement (A_{vf}) can be computed directly from :

$$A_{vf} = V_u / \Phi f_y \mu \qquad (٥.٣)$$

The condition where shear-friction reinforcement crosses the shear plane at an angle α_f other than ٩٠ degrees , the tensile force ($A_{vf} f_y$) is inclined to the crack and must be resolved into two components : ١)a clamping component ($A_{vf} f_y \sin\alpha_f$), and ٢) a component parallel to the crack that directly resists slip equal to (A_{vf} fy $\cos\alpha_f$) . The shear transfer strength requirement becomes :

$$Vu \leq \Phi(A_{vf} f_y \sin\alpha_f \mu + A_{vf} f_y \cos\alpha f) \qquad (٥.٤)$$

The required area of shear-friction reinforcement can be computed directly from:

$$A_{vf} = V_u / \Phi f_y (\mu \sin\alpha_f + \cos\alpha_f) \qquad (٥.٥)$$

The shear-friction method assumes that all shear resistance is provided by friction between crack faces. The actual mechanics of resistance to direct shear is more complex, since dowel action and the apparent cohesive strength of the concrete both contribute to direct shear strength. It is , therefore, necessary to use artificially high values of the coefficient of friction (μ) in the shear friction equations so that the calculated shear strength will be in reasonable agreement with test results . Use of these high coefficients gives predicted strengths that are a conservative lower bound to test data .

٥.٤ Coefficient of Friction

The effective coefficient of friction (μ) for the various interface conditions includes a parameter λ which accounts for the somewhat lower shear strength of all lightweight and sand lightweight concretes . For example , μ value for all lightweight concrete (λ= ٠.٧٥) and when placed against hardened concrete not intentionally roughened it is ٠.٦ (٠.٧٥)= ٠.٤٥ .

CHAPTER SIX

APPLICATION OF FINITE ELEMENT ANALYSIS TO BEAM-COLUMN JOINTS

٦.١ Introduction

In this chapter, a three dimensional nonlinear finite element analysis has been carried out on corner beam-column joints by implementing the modified computer program. The three-dimensional model describe the behavior of the analyzed corner beam-column joint under cyclic loading. In this chapter, two of these examples have been chosen from the available experimental studies for the numerical analyses.

The first example is a cantilever loaded by a concentrated cyclic load applied at the free end, which was tested by **[Kwak** and **Kim (٢٠٠١)]**. While the second example is a corner beam-column joint , which was tested by [**Sarsam (١٩٨٣)].** The third example is a corner beam-column joint subjected to cyclic load.

٦.٢ Kwak and Kim Reinforced Concrete Cantilever Under Cyclic Load

A cantilever of ordinary reinforced concrete was analyzed to investigate the validity and accuracy of the finite element models and solution techniques adopted in this study. This was designated as R٦ and chosen from the two beams tested by [**Kwak** and **Kim].**

٦.٢.١ Description of Beam (R٦)

The beam (R٦) was a cantilever over ١٥٨٩ mm span. It had a rectangular cross-section ٢٢٨.٦ mm wide and ٤٠٦.٤ mm deep. The longitudinal steel ratio was ١.٥٢٪. Loading arrangement, reinforcement details and geometry of the beam are shown in Fig.(٦.١).

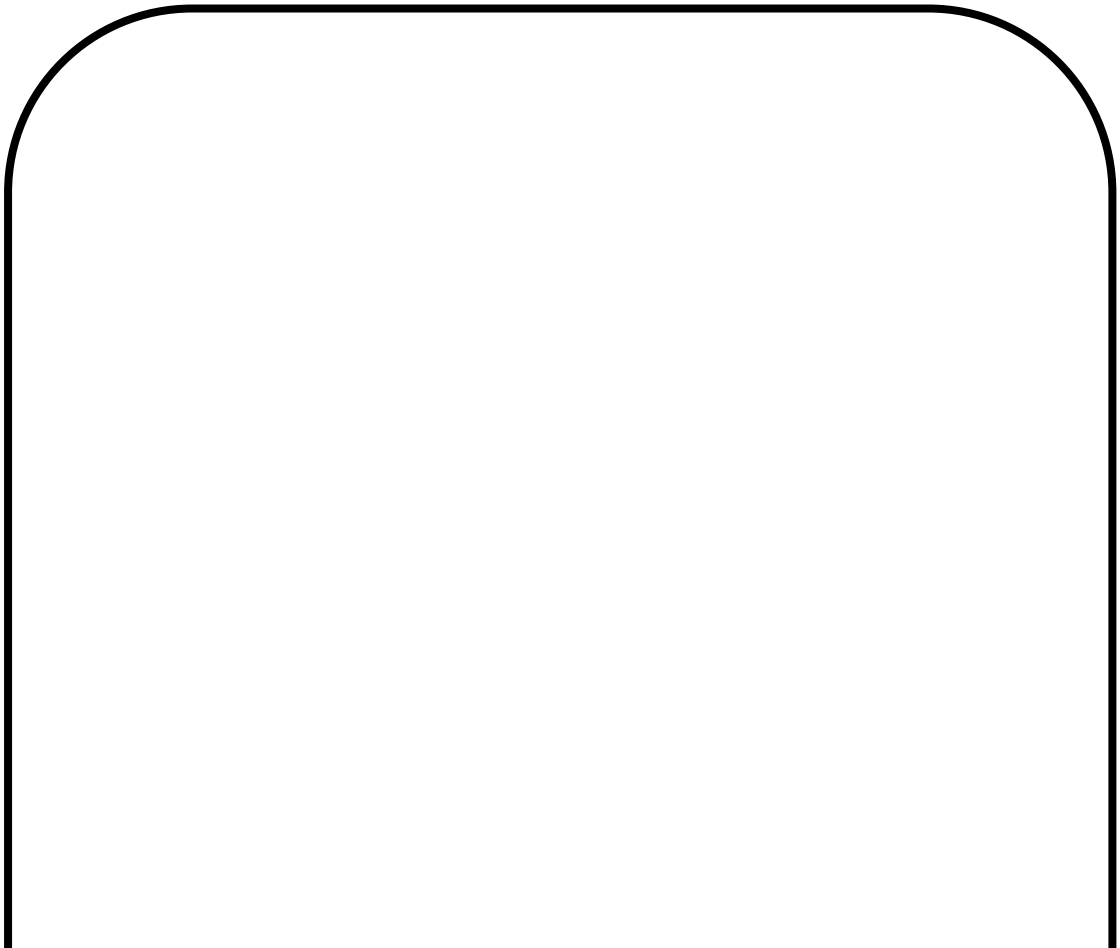

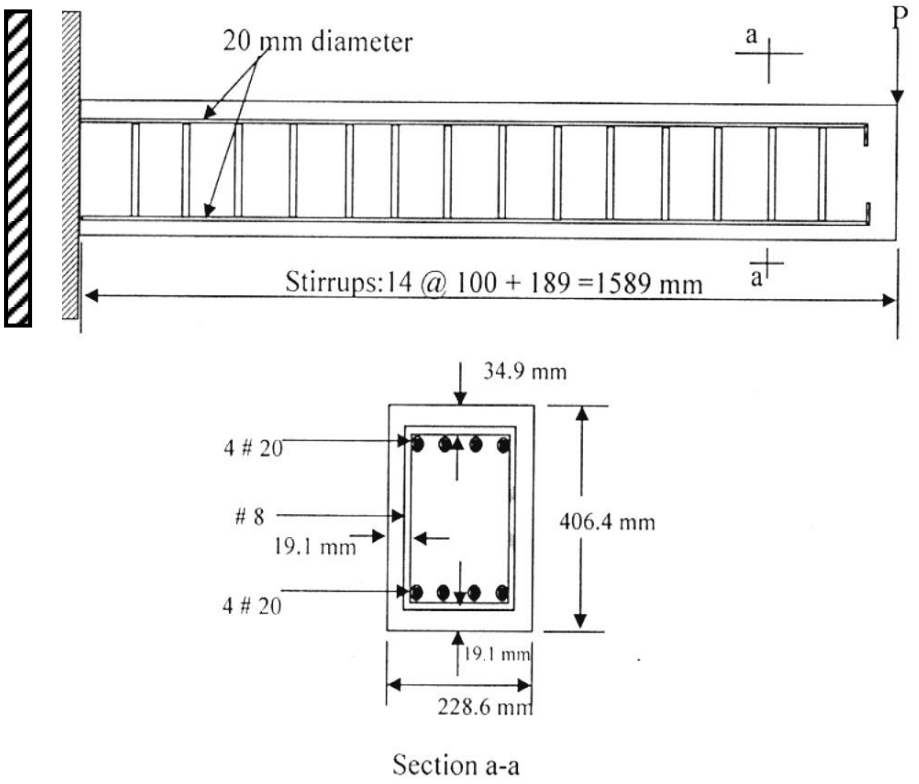

Fig. (٦.١) Dimensions and reinforcement details of beam (R٦)

٦.٢.٢ Finite Element Idealization and Material Properties

By taking into consideration the advantage of the loading and geometric symmetry, only one-half of the beam has been used in the finite element analysis. The half considered was modeled using ٥٠ brick elements. The finite element mesh, boundary and symmetry conditions and loading arrangement used are shown in Fig (٦.٢).

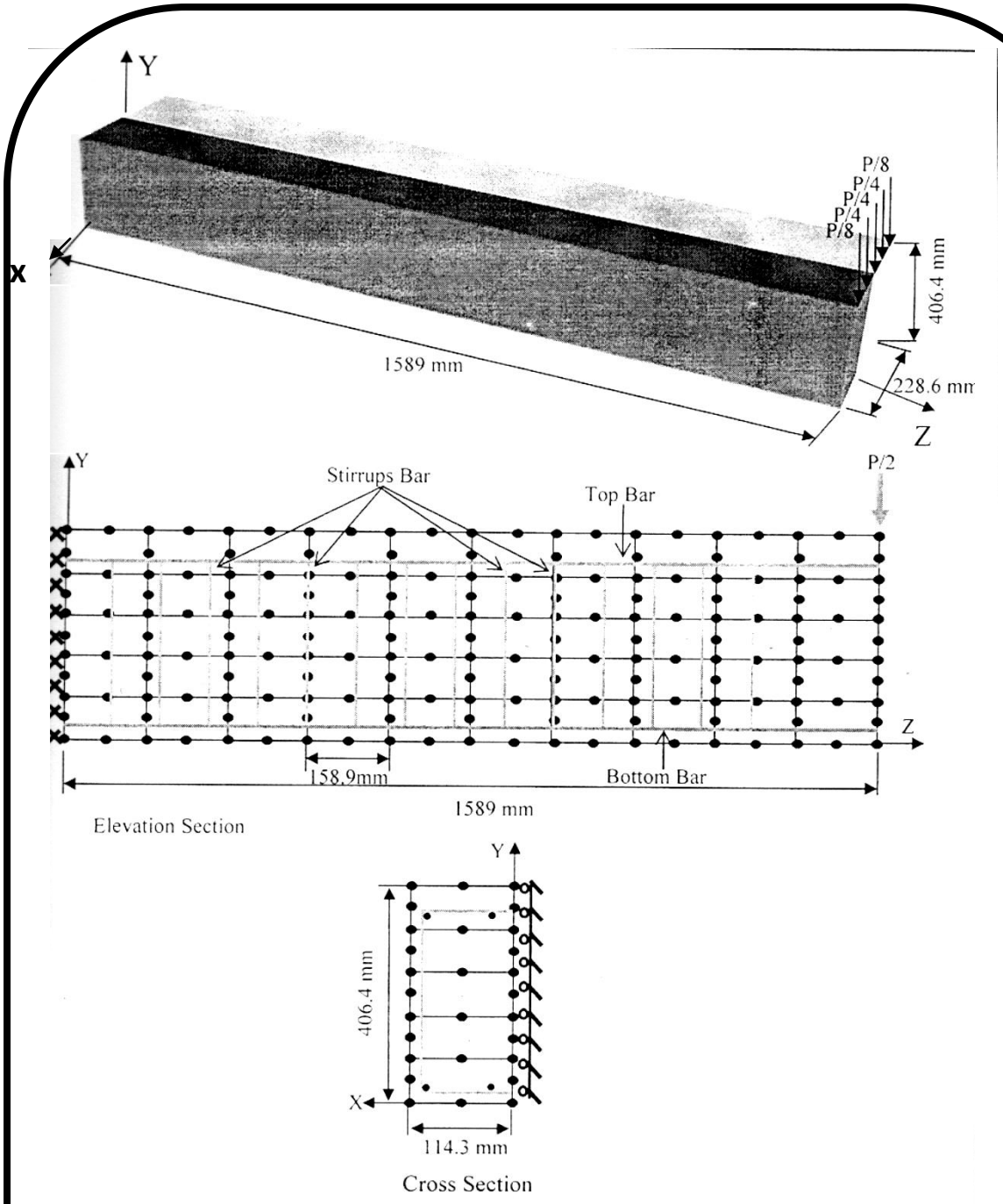

Fig. (٦.٢) Finite element mesh, boundary and symmetry conditions for beam (one-half of the beam)

or this ordinary reinforced concrete beam the tension-stiffening parameters α ١ and α ٢ was set equal to ٥٥ and ٠.٥ respectively. While the shear-retention parameters γ ١,γ٢ and γ ٣ was set equal to ١٠, ٠.٥ and ٠.١ respectively. Material properties adopted in the analysis are shown in Table (٦.١).

Table (٦-١) Material properties used for beam (R٦)

CONCRETE		
E_c	Modulus of elasticity (GPa)	٢٤.٠
f'_c	Compressive strength (MPa)	٢٩.٨
f_t	Tensile strength (MPa)	٣.٢
	Uniaxial crushing strain	٠.٠٠٤
N	Poisson's ratio*	٠.٢
LONGITUDINAL REINFORCEMENT		
E_s	Young's modulus (GPa)	٢٠٠
f_y	Yield strees (MPa)	٤٥١
A_s	Area of top steel ($mm^٢$)	١٢٥٦.٦
	Area of bottom steel ($mm^٢$)	١٢٥٦.٦

* Assumed value

٦.٢.٣ Results of Analysis of Beam (R٦)

The experimental and numerical cyclic load-deflection curves obtained for this beam are shown in Fig.(٦.٣). Good agreement is obtained by using the finite element model compared with the experimental results throughout the entire range of the behavior. During the experimental tests, unloading of the beam was started after the yielding of reinforcement took place. A relatively stiffer numerical response has been observed and the peak load was slightly higher than the experimental value. Table (٦-٢) presents a comparison between the peak experimental and numerical peak load.

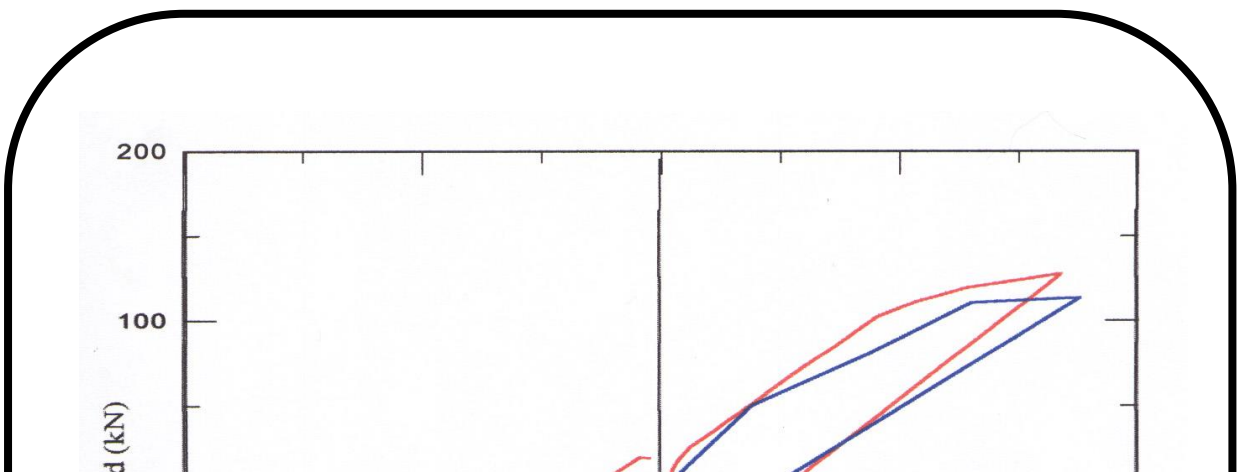

Fig. (٦.٣) load-deflection curve

Table (٦.٢) Comparison between the peak experimental and numerical peak loads for beam (R٦)

NUMBER OF HALF-CYCLIC	EXP. PEAK LOAD $P_{U١}$(KN)	NUM. PEAK LOAD $P_{U٢}$(KN)	$P_{U٢}/P_{u١}$
١st half cyclic	١١٣.٣	١٢٧.٣	١.١٢٣
٢nd half cyclic	-١٠٥.٣	-١٢٥.٠٤	١.١٨٧

٦.٣ Beam-Column Joint Specimen (under monotic loads)

Nine specimens of beam-column joints (٥ exterior and ٤ interior) were tested by **[Sarsam (١٩٨٣)].** The plane exterior ones – EX series were made of two pours. The first pour was made on one day. This pour included the specimen up to the level of the top of the joint. The second pour was made on the next day for the top column. Thus, a horizontal construction joint existed at top of joints.

٦.٣.١ Description of Beam-Column Joint Specimen

The column was reinforced with four ١٦mm longitudinal bars and ٨mm closed links at ٨٥mm center to center spacing , giving three joint links . The beam was reinforced with two ١٦mm bars on the tension side and two ١٢mm bars on the compression side . Beam links were ٨mm of closed type and spaced at ١٣٠mm center to center .

EX١ specimen is used in the present study , its dimensions are shown in Table(٦.٣) and Fig.(٦.٤) .Material properties and additional material parameters of this specimen are shown in Table (٦.٤) .The column was first loaded to a predetermined value of (Nc) , prior to any beam loading , the next stage involved loading the beam up to ultimate load .

Table (٦.٣) Dimensions of Sarsam's specimens

Dimensions/ *Specimens*	Beam		Column		Lc (mm)	av (mm)	Column Load (kN)
	h (mm)	b (mm)	h (mm)	b (mm)			
Specimen EX١	٣٠٣	١٥٢	٢٠٥	١٥٢	١٥٣١	١٤٢٢	٢٩٢.٦

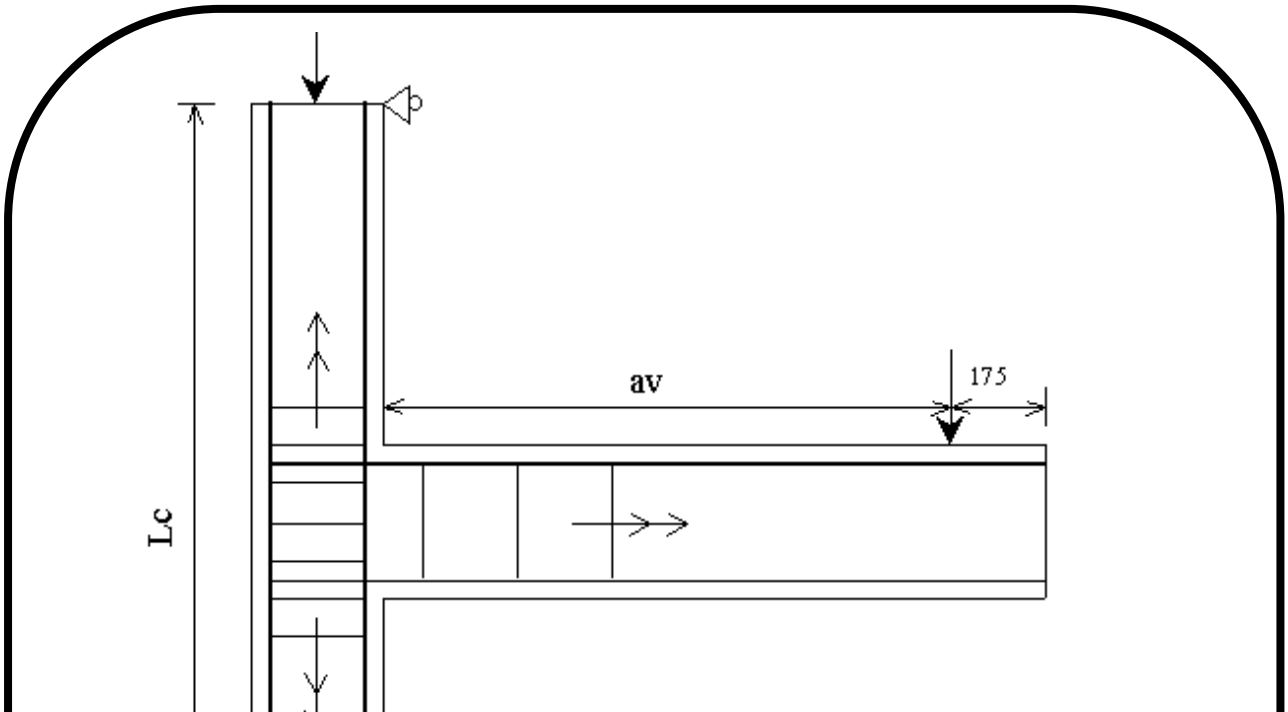

Fig. (٦.٤) Experimental corner beam-column joint specimens of Sarsam (١٩٨٣

Table (٦.٤) Material properties and additional material parameters of Sarsam's specimen EX١

First pour (age= ٦٤ days)		
Material properties		**Material parameters**
Modulus of elasticity , E (MPa)	٣٥٥٠٠	Tension-stiffening parameters : α_1=٣٥ , α_2=٠.٣٥ Shear-retention parameters : γ_1=٢٥,γ_2=٠.٥, γ_3=٠.١
Compressive strength, f'_c(MPa)	٥٦.٣	
Tensile strength , f_t (MPa)	٤.٥	
Poisson's ratio , ν	٠.٢*	
Uniaxial crushing strain	٠.٠٠٢٣٨	
Second pour (age= ٦٣ days)		
Material properties		Material parameters
Modulus of elasticity , E (MPa)	٣٠٦٠٠	Tension-stiffening parameters : α_1=٢٥ , α_2=٠.٢٥ Shear-retention parameters : γ_1=٢٥,γ_2=٠.٥, γ_3=٠.١
Compressive strength, f'_c (MPa)	٤٥.٨	
Tensile strength , f_t (MPa)	٣.٩٣	
Poisson's ratio , ν	٠.٢*	
Uniaxial crushing strain	٠.٠٠٣*	

Steel reinforcement				
Longitudinal bar Φ١٦	Young's modulus (MPa)	٢٠٨٠٠٠	Yield stress (MPa)	٥٠٤
Longitudinal bar Φ١٢		١٩٨٠٠٠		٥٠٧
Stirrup bar Φ٨		١٩٧٠٠٠		٥١٧

* Assumed value

٦.٣.٢ Finite Element Idealization

The concrete of specimen EX١is idealized by using ٥٨ ٢٠-noded brick elements (including ١ interface element at the top level of the joint), (for half of this specimen) , Fig.(٦.٥) . To simulate the procedure of loading that occurred during the experimental test , the column axial load has been firstly applied in equal increments of ١٠٪ of the maximum column load for this specimen . Later ,for EX١ two different sizes of increments have been used for beam loading. The beam was loaded initially by increments of ٣٧.٥kN up to ٧٥٪ of the expected collapse load (٤٠ kN) . Then reduced increments of ١.٤٣kN each were applied until the failure load has been reached . Both the initial and post-cracking stiffness are reasonably predicted, Table (٦.٤). For this ordinary reinforced concrete beam the tension-stiffening parameters α ١ and α ٢ was set equal to ٥٥ and ٠.٥ respectively. While the shear-retention parameters γ ١,γ٢ and γ ٣ was set equal to ١٠,٠.٥ and ٠.١ respectively.

٦.٣.٣ Analysis of EX١ Specimen (under static loads)

In order to analyze the specimen, the effect of the thickness of interface element must be examined . For EX١ specimen, numerical tests with values of the thickness (t) equal to ٠.٠١٤mm ,٠.١٤mm , and ١.٤mm have been carried out . The results show that the type of failure of the specimen EX١ is beam hinging for the range of (٠.٠١٤-٠.١٤)mm for thickness of interface element, Fig.(٦.٣). A response stiffer than the experimental results was obtained when the thickness is reduced within the range , and the best fit to the experimental results was obtained at t=٠.١٤mm with effective thickness of Gaussian point of ٠.٠٣٨mm , in which the effect of nonlinearities along the loading stages is clear . The failure load of numerical results is ٣٧.٥kN while the failure load of experimental results is ٣٦.٠٤kN , so that the error ratio is ٣.٩٪. In the present study the value of thickness of the interface element equal to ٠.١٤mm is fixed for EX١ specimen, Fig.(٦.٥) .

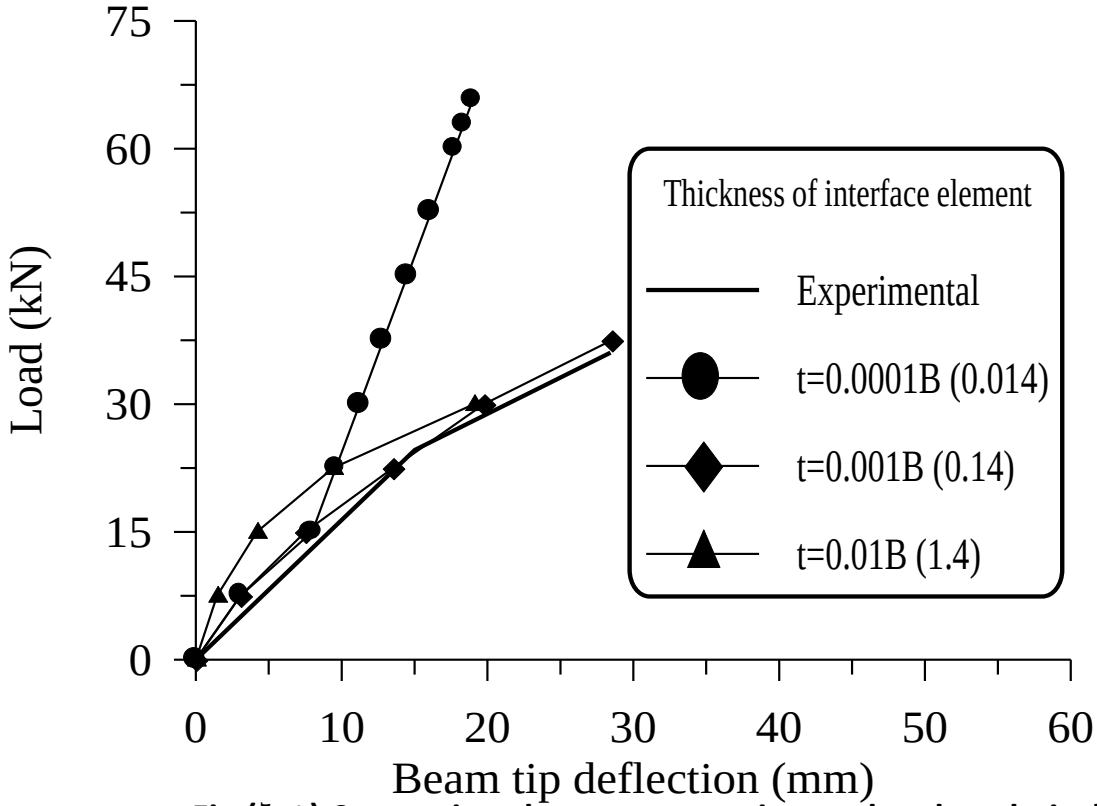

Fig.(٦.٥) Comparison between experimental and analytical response for different interface thickness values for EX١

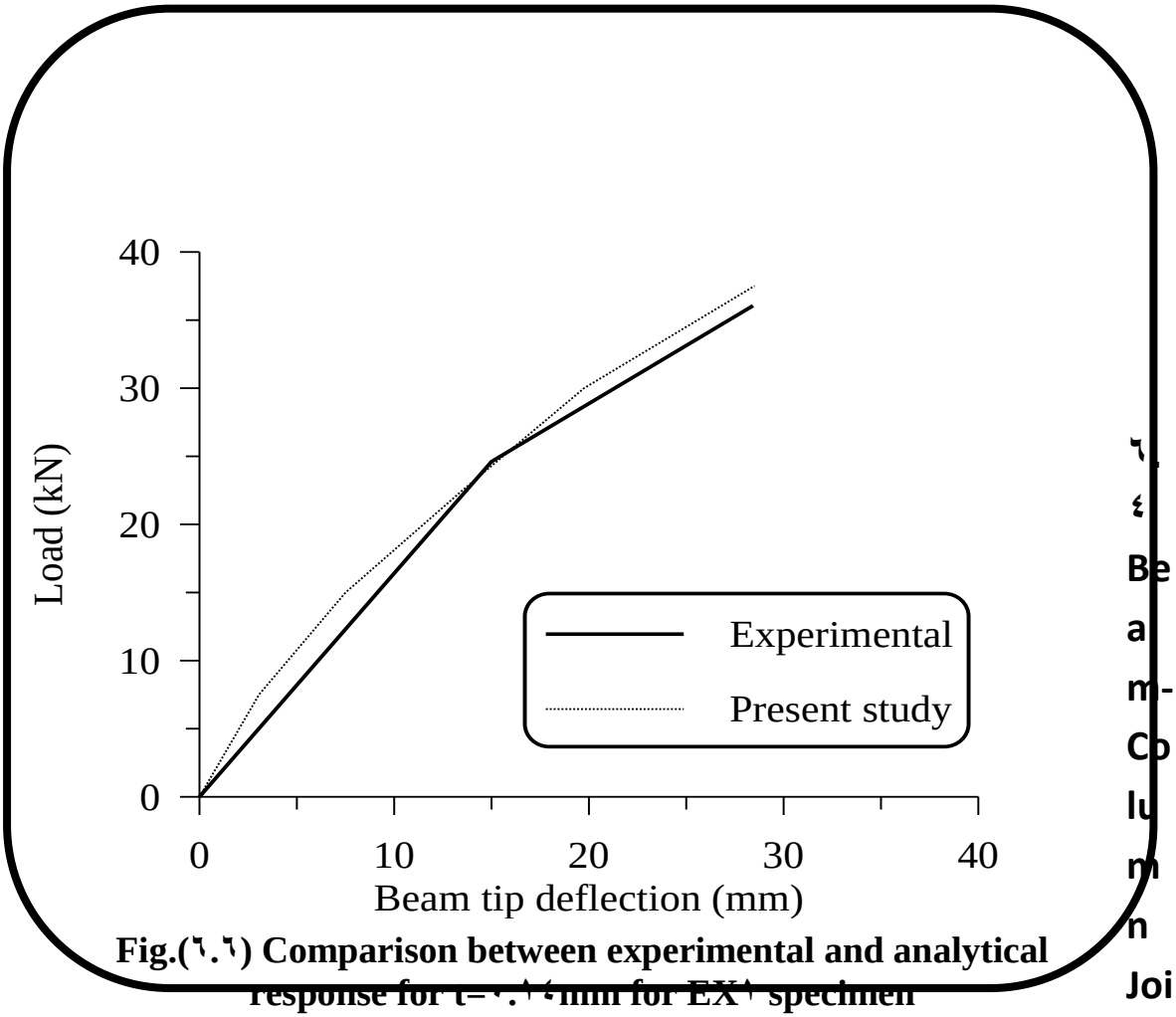

Fig.(٦.٦) Comparison between experimental and analytical response for t=٠.٢٤mm for EX٢ specimen

٦.٤ Beam-Column Joint

Specimen (under cyclic loads)

Also Ex١ has been taken. This was made of two pours. The first pour was made on one day. This pour included the specimen up to the level of the top of the joint. The second pour was made on the next day for the top column. Thus, a horizontal construction joint existed at top of joints.

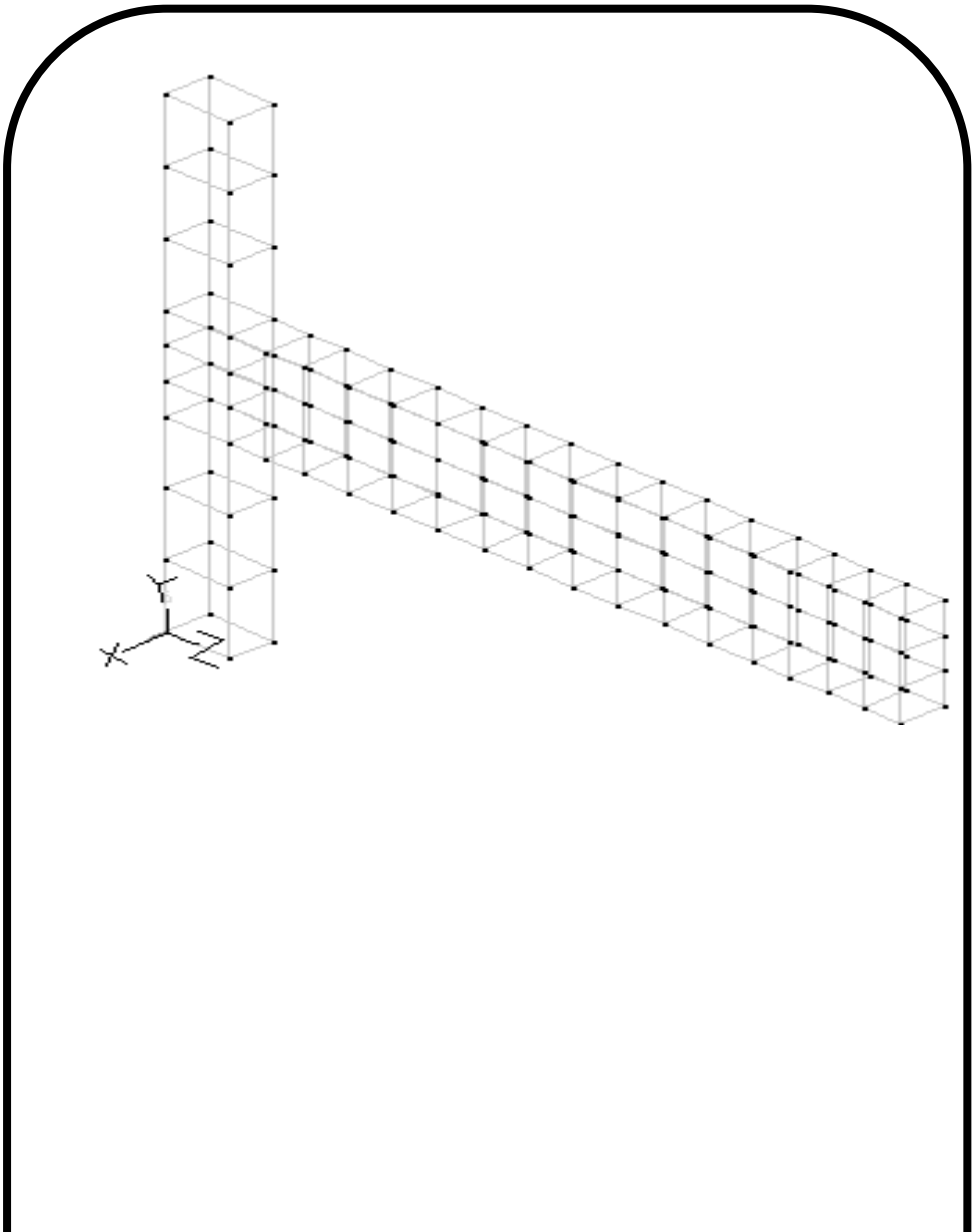
Y
X
Z

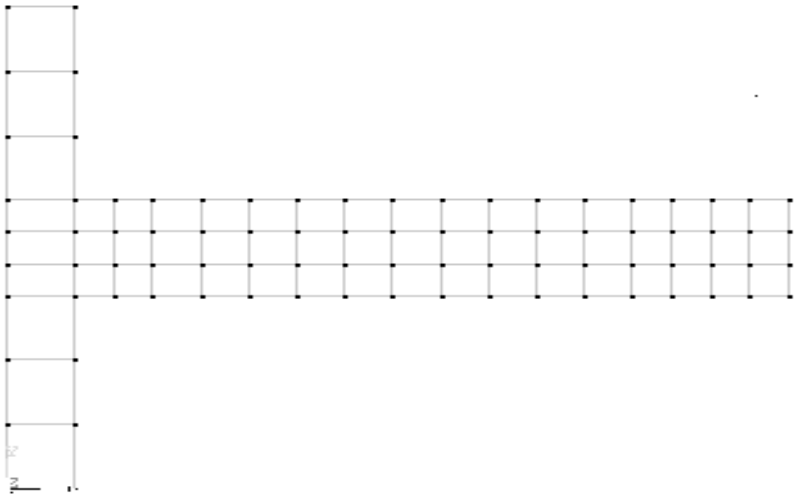

Fig.(٦.٧) Finite element discretization of half of EX١

٦.٤.١ Finite Element Idealization

By making use of the geometric and loading symmetry, a segment, which represents one-half of the beam-column joint, has been used for the finite element analysis. This segment has been discretized into ٥٨٢٠ -noded brick elements (including ١ interface element at the top level of the joint) . The column axial load has been firstly applied in equal increments of ١٠٪ of the maximum column load for this specimen . Later ,four different sizes of increments have been used for beam loading.

As in Table (٦.٤). for this ordinary reinforced concrete beam the tension-stiffening parameters α_1 and α_2 were set equal to ٥٥ and ٠.٥ respectively, while the shear-retention parameters γ_1, γ_2 and γ_3 were set equal to ١٠,٠.٥ and ٠.١ respectively.

٦.٤.٢ Analysis of EX ١ (under cyclic loads)

Fig. (٦.٨) shows the numerical repeated load-beam tip deflection curve. Also the figure reveals that the first half-cyclic, a tri-segmental curve was usually recognized. The first segment represents the elastic-uncracked stage of behavior. The second represents the elastic-cracked stage. While, the third stage represents the yielding of main reinforcment. During the sequence of half cycles, these segments will disappear and a smooth behavior is seen which is characterized by cracking and post-yielding stages.

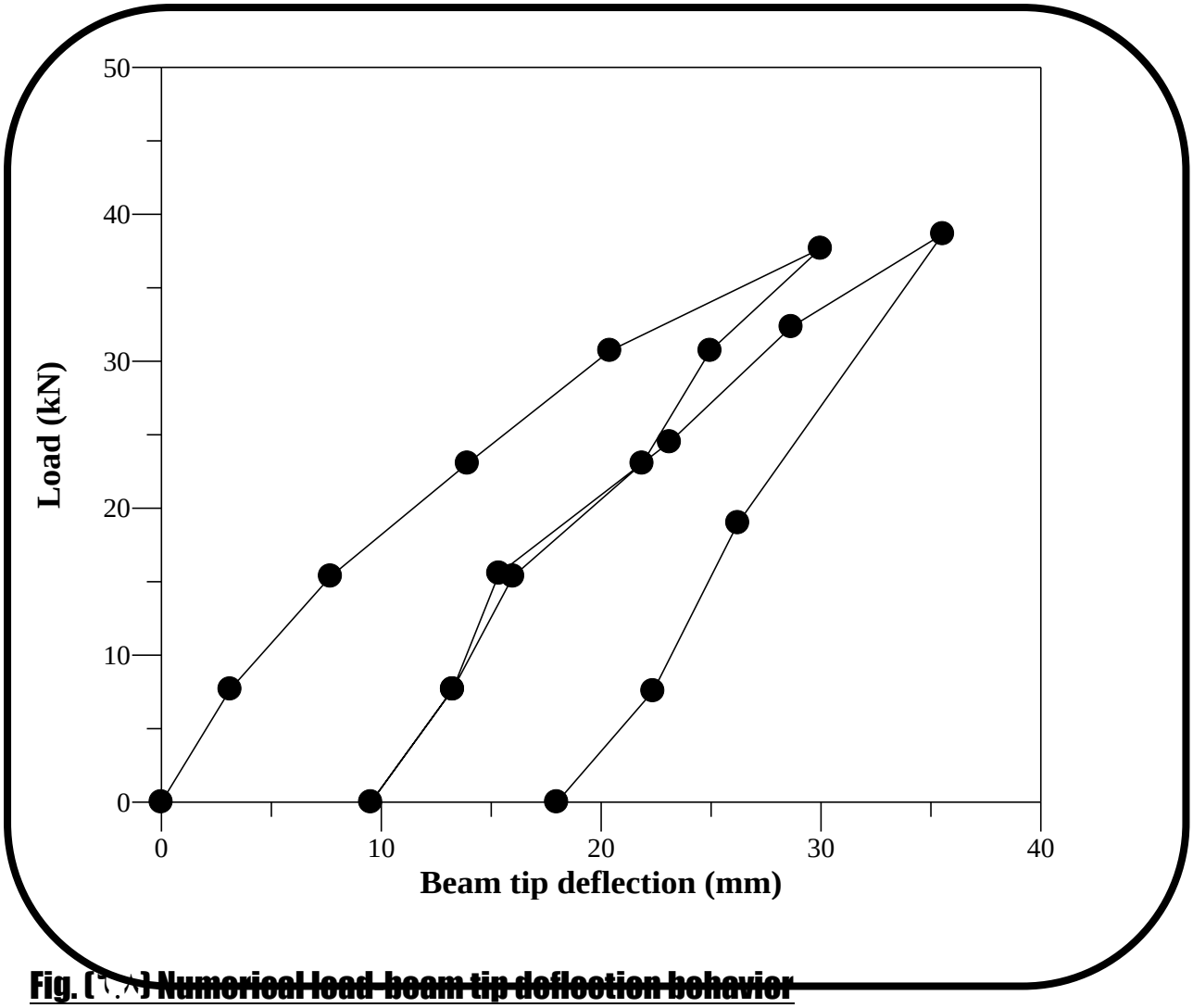

Fig. (٦.٨) Numerical load-beam tip deflection behavior

٦.٤.٣ The Effect of Column Axial Load

In order to inspect the effect of column axial load on the behavior of construction joint, a numerical study has been carried out, one with experimental column axial load (Nc=٢٩٢.٦kN), and the other with half column axial load (Nc/٢) for the case of construction joint at the top level of the beam-column joint. It can be observed from Figs.(٦.١٠) and (٦.١١) that the shear and normal strains in the joint for Nc/٢ are less than the strains for Nc=٢٩٢.٦kN . A possible explanation of this

feature may be the following : Higher compressive stresses (at Nc=٢٩٢.٦kN),in spite of the more intimate interlocking they secure, produce a shortening of the protruding asperities and subsequently reduce overriding resistance . This mechanism is less apparent at Nc/٢. On the contrary , due to loss of some confinement for Nc/٢, the response of the specimen at Nc/٢ is softer than the response for Nc=٢٩٢.٦kN , Fig.(٦.٩) .

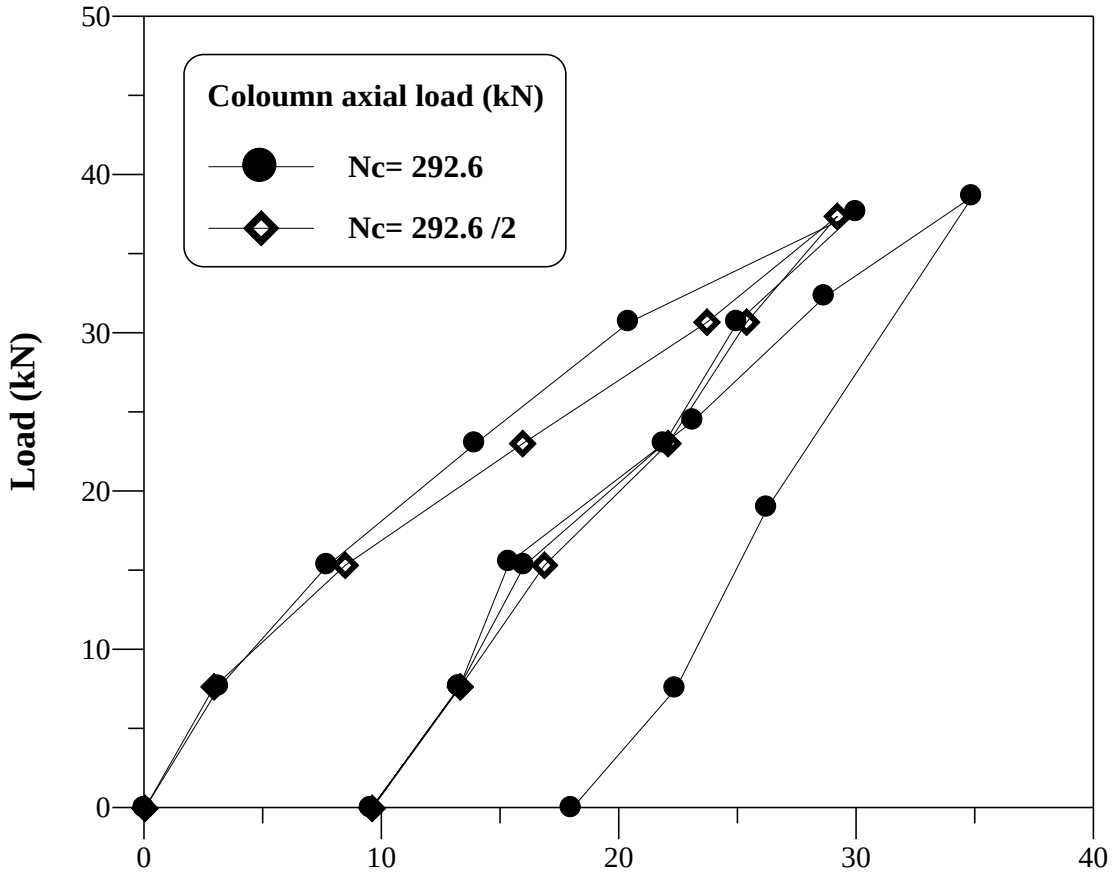

Fig. (٦.٩) Load-beam tip deflection curve

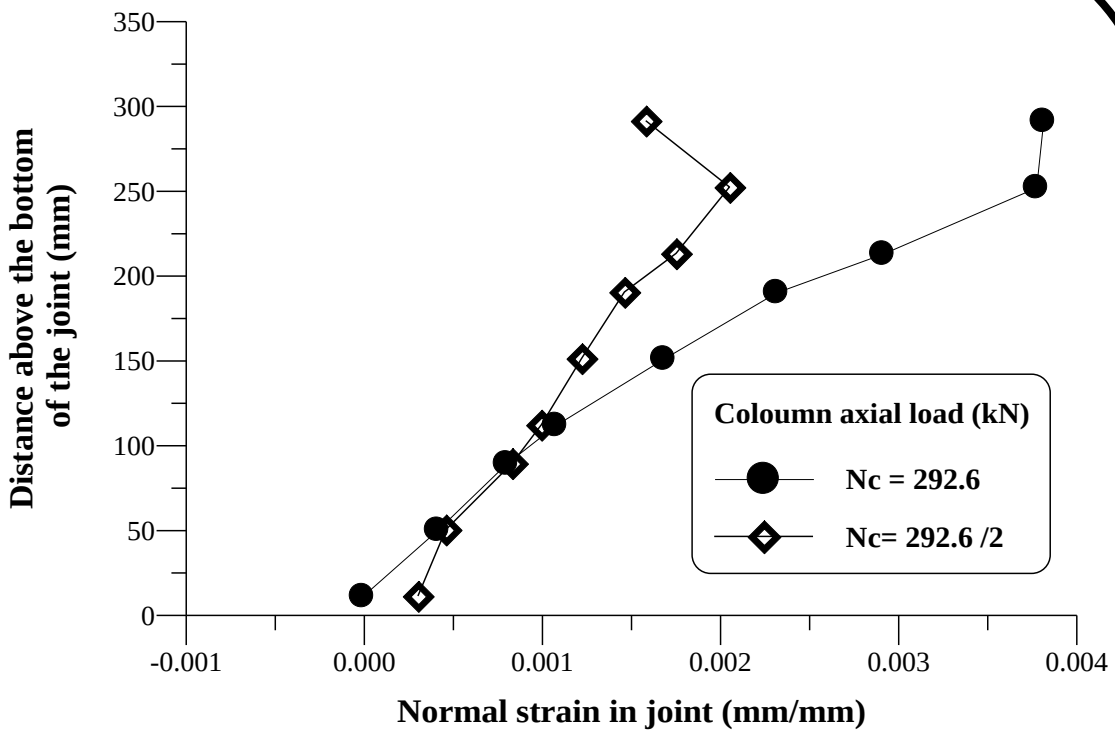

Fig. (٦.١٠) Normal strains distribution in joint

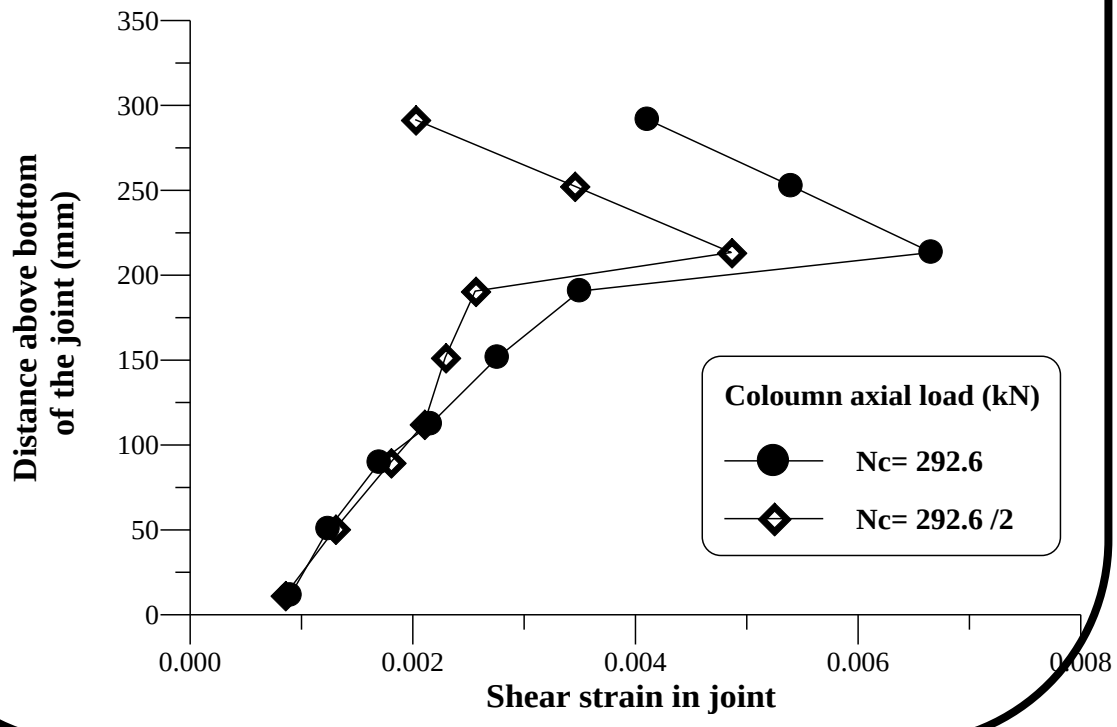

Fig. (٦.١١) Shear strains distribution in joint

٦.٤.٤ The Effect of the Percentage Steel Across the Construction Joint

Three numerical tests have been carried out by using percentages of steel across the construction joint (diameter of the bar) (١٦ mm), (١٨ mm), and (٢٠ mm) for the construction joint at the top level of the beam-column joint, these tests occurred with the original designed specimen. From Fig.(٦.١٢), the deflection decreases with the increase in the steel percentage across the construction joint (column reinforcement) , the contribution in this result is the decreased strains in joint due to increase in dowel stiffness. Figs. (٦.١٣) and (٦.١٤) show the shear and normal strains in joint . It can be notice that these strains decrease with the increase in the steel percentage across the construction joint.

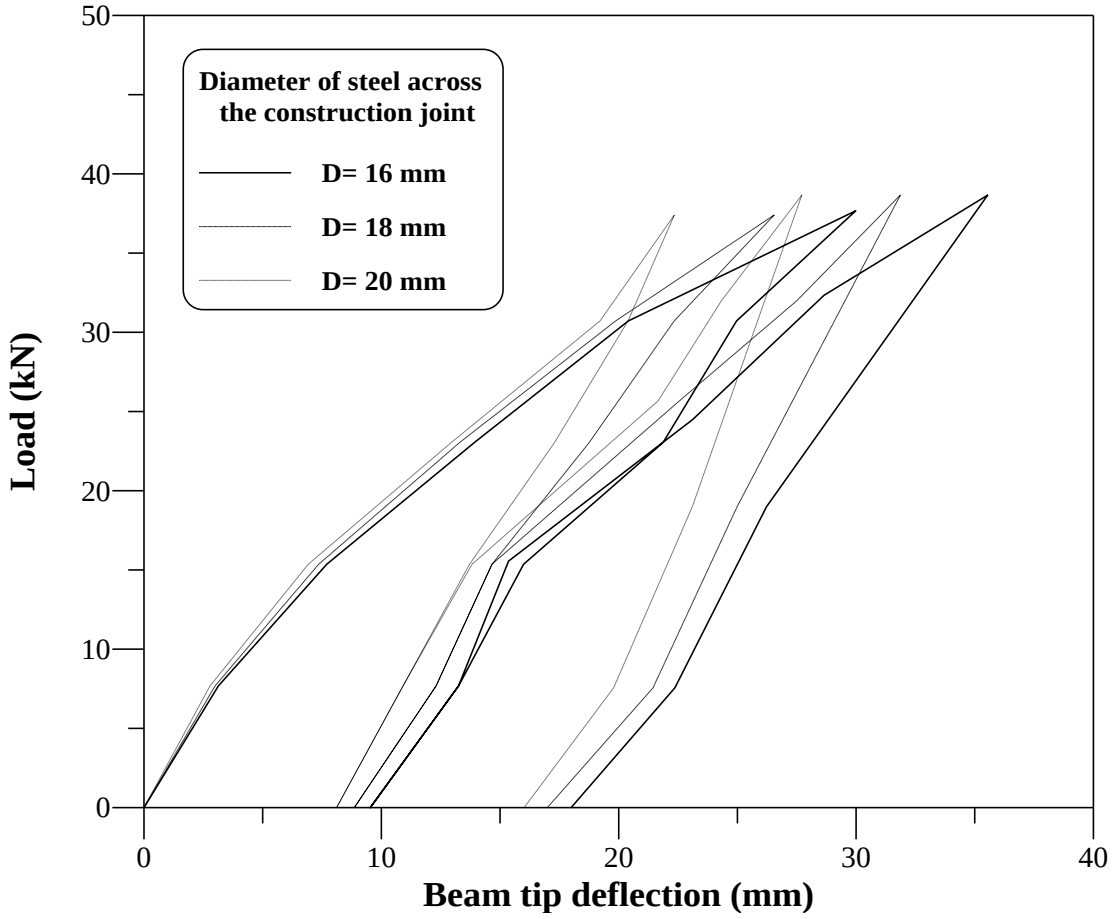

Fig. (٦.١٢) Effect of diameter of crossing steel on the load-beam tip deflection

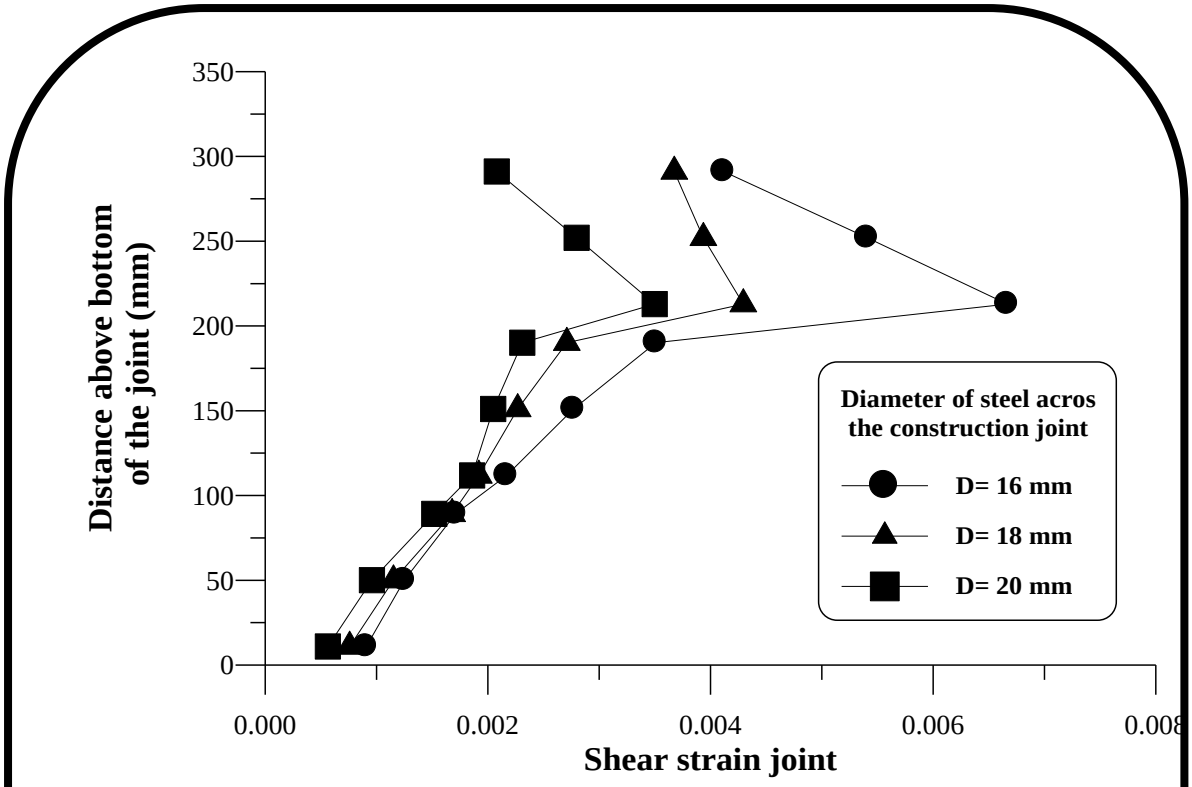

Fig. (٦.١٣) Shear strains distribution in joint

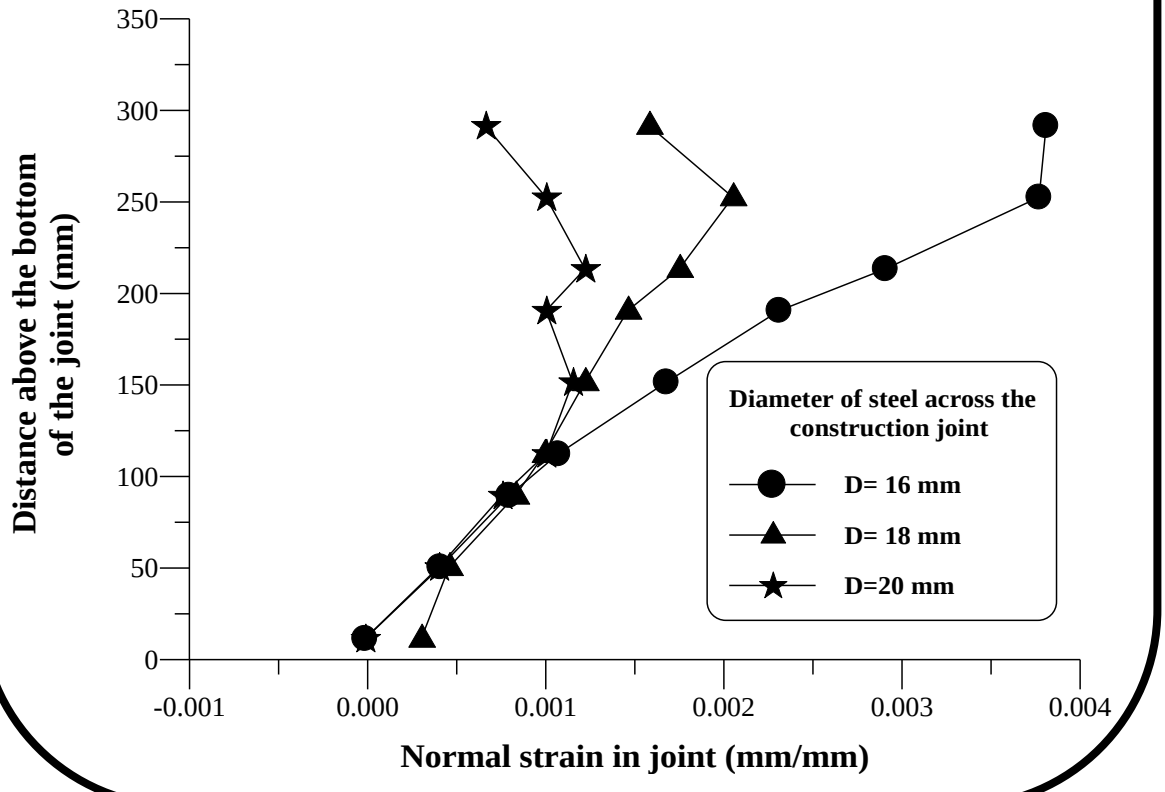

Fig.(٦.١٤) Normal strains distribution in joint

٦.٤.٥ The Effect of the Age of Concrete

The age of concrete pour has an effect on the compressive strength of the concrete . In order to study the effect this age , two tests have been carried out with f'c values equal to ٤٥.٨ , ٤٠ MPa , Fig.(٦.١٥). These values of strengths are for ages approximately equal to ٦٣ , ٣٨ days , respectively for the second pour, including the construction joint. These tests show that the higher concrete compressive strength results in a slight increase in aggregate interlock stiffness of construction joint .

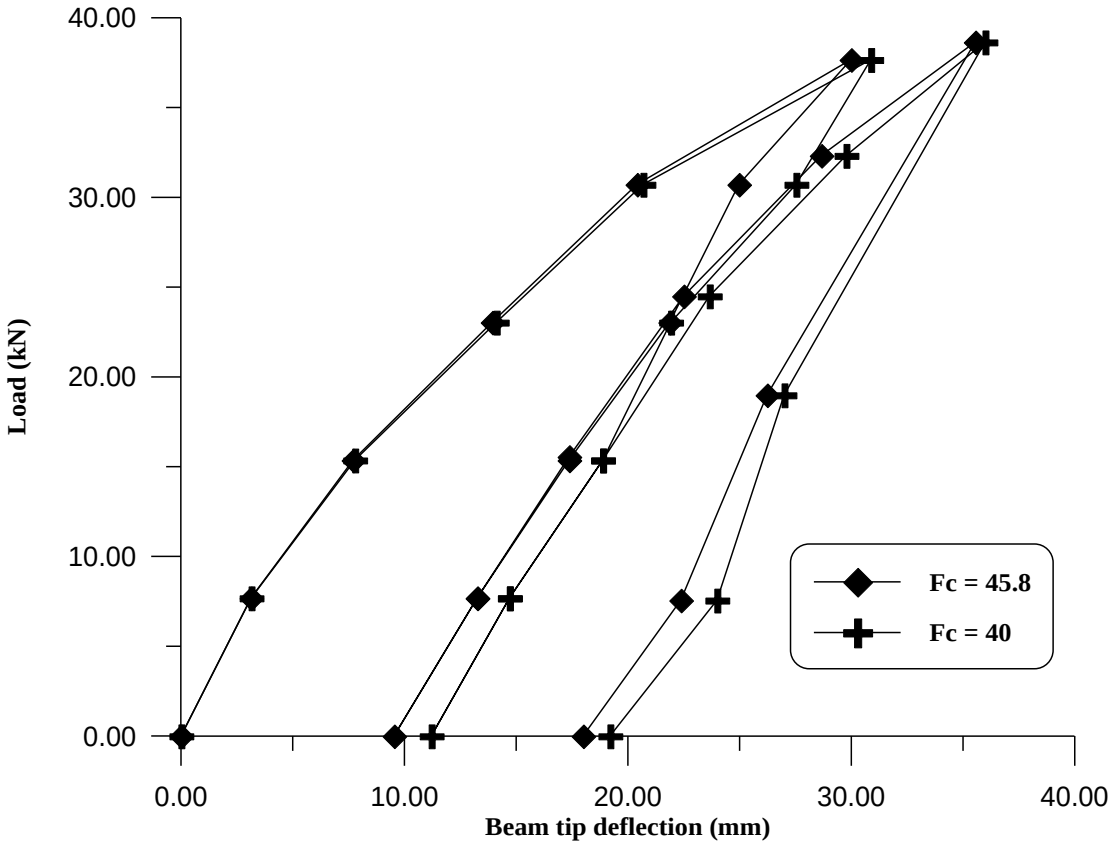

Fig.(٦.١٥) effect of compressive strength on the load-beam tip

Deflection curve for case b (construction joint at the top level of joint)

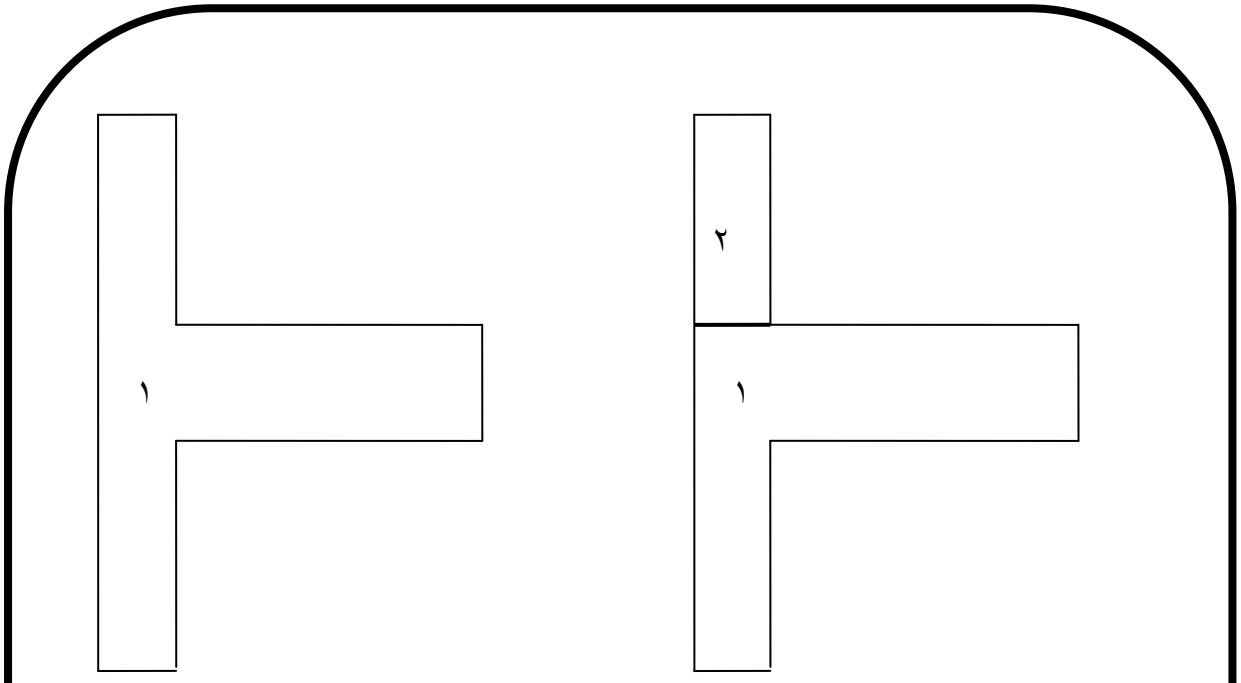

Case (a) Monolithic specimen (without construction

Case (b) Composite specimen (with construction joint at

construction joint)

Fig.(٦.١٦) Cases of construction joints of beam-column joint

٦.٤.٦ The Effect of Position of Construction Joint

In order to study the effect of the position of construction joint (c.j.), a numerical study on four cases have been carried out, Fig.(٦.١٦) , case (a) without c.j. , case (b) with c.j. at the top level of the joint , case (c) with c.j. at the bottom level of the joint , and case (d) with vertical c.j.. These cases were made of two pours (١,٢) of material properties shown in Table (٦.٤) . Fig.(٦.١٧), (٦.١٨) and (٦.١٩) represents load-tip deflection of these cases . As a result of comparison between curves , a soft response occurred for cases with c.j. , the response of case (c) is softer than the response of case (b) , and a softer response of all is observed for case (d) .

Table (٦.٤) Material properties and additional material parameters of Sarsam's control specimens

First pour (١) (age =٦٤ days)		
Material properties		**Material parameters**
Modulus of elasticity , E (MPa)	٣٥٥٠٠	Tension-stiffening parameters :
Compressive strength, f'_c(MPa)	٥٦.٣	α_1=٣٥ , α_2=٠.٣٥
Tensile strength , f_t (MPa)	٤.٥	Shear-retention parameters:
Poisson's ratio , ν	٠.٢*	
Uniaxial crushing strain	٠.٠٠٢٣٨	γ_1=٢٥,γ_2=٠.٥, γ_3=٠.١
Second pour (٢) (age =٦٣ days)		
Material properties		**Material parameters**
Modulus of elasticity , E (MPa)	٣٠٦٠٠	Tension-stiffening parameters :
Compressive strength, f'_c(MPa)	٤٥.٨	α_1=٢٥ , α_2=٠.٢٥
Tensile strength , f_t (MPa)	٣.٩٣	Shear-retention
Poisson's ratio , ν	٠.٢*	

Uniaxial crushing strain	٠.٠٠٣*	parameters: γ ١=٢٥,γ٢=٠.٥, γ ٣=٠.١

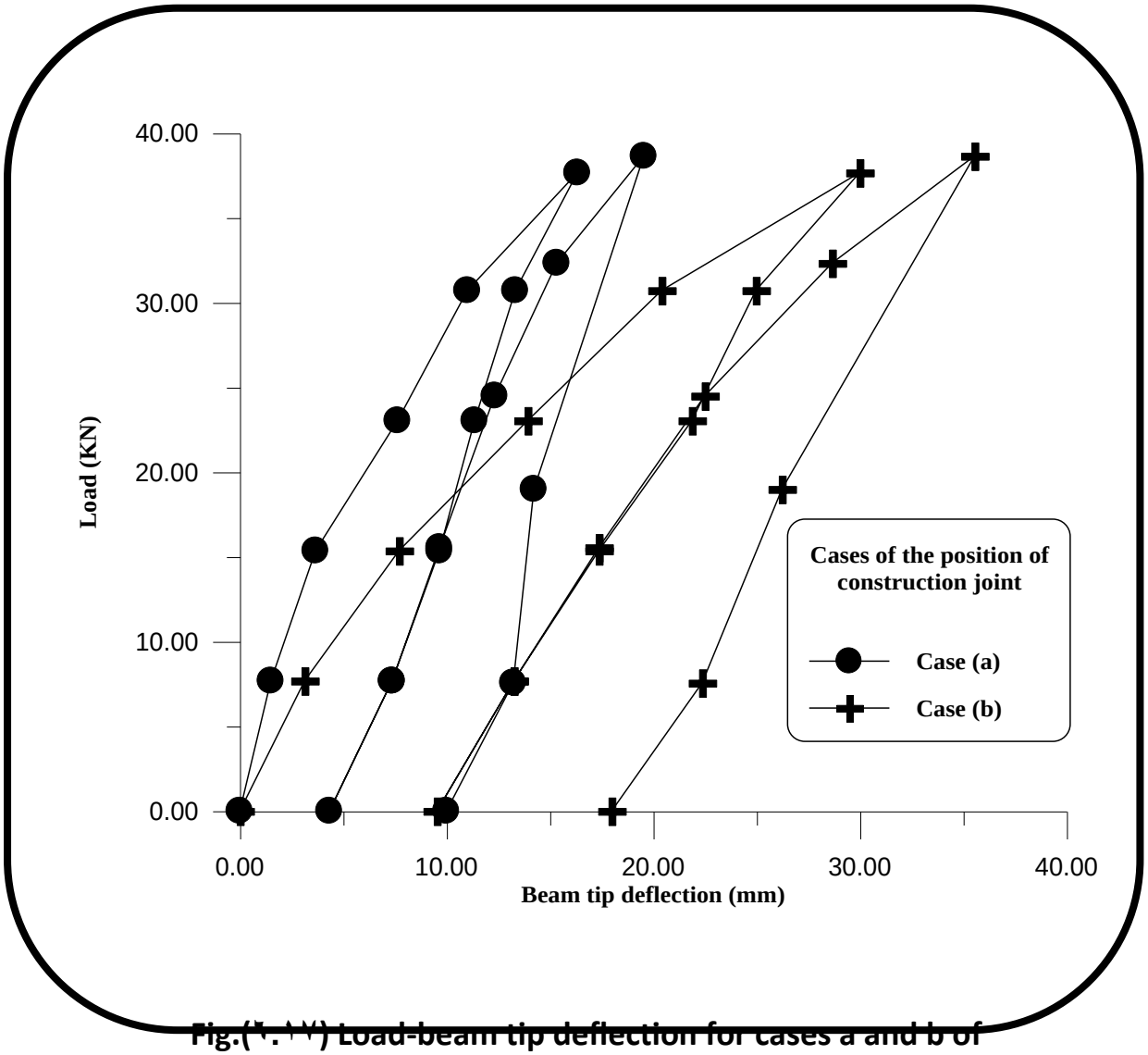

Fig.(٣.٧٧) Load-beam tip deflection for cases a and b of Construction joints

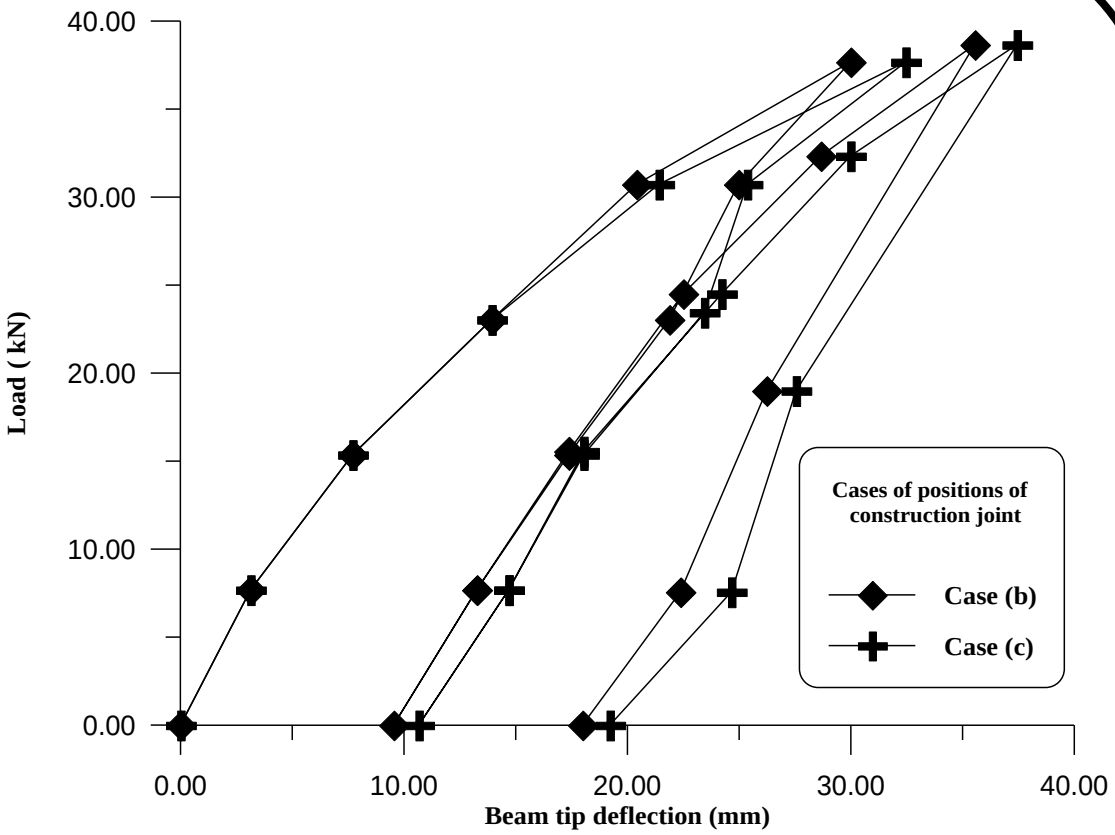

Fig. (٦.١٨) Load-beam tip deflection for cases b and c of Construction joints

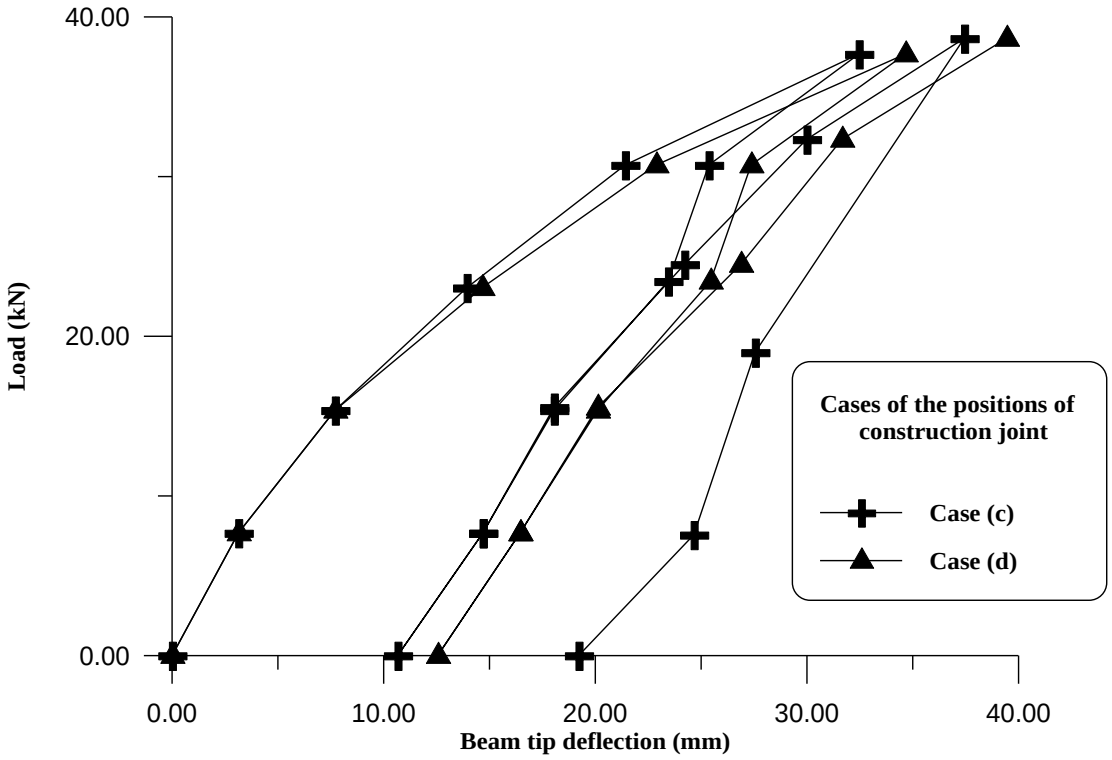

Fig.(٦.١٩) Load-Beam tip deflection for cases c and d of Construction joint

CHAPTER SEVEN

CONCLUSIONS AND RECOMMENDATIONS

٧.١ Conclusions .

The following conclusions can be drawn from the present study :

١. A good assessment can be obtained for the behavior of corner beam-column joints by using the

developed program of the current study (DPACJ) and is suitable to predict the behavior of reinforced concrete under cyclic and repeated loads .

٢. The performance of the interface element , used in this study to model the shear transfer between two concerts cast in different times , is quite good.

٣. A stiff response can be obtained with decrease the thickness of the interface element.

٤. The response of a specimen can be expected within a certain range of thickness of interface element. This range depend on the finite element mesh , nonlinear behavior of material , and the combination of stresses.

٥. The construction joint would affect only on the joint. On the other hand, the mode of failure for the corner beam-column joint in this study is beam hinging, this type of failure conforms with the design requirements.

٦. The presence of column axial load would decrease the aggregate interlock stiffness. However, it secures a good confinement for the beam ,and so as the result of increase it .

٧.The increased of steel percentage across the construction joint would decrease the strains in joint. Consequently, a slightly decrease of deflection occurred.

٧.٢ Recommendations .

١.The extension of the present work to consider bond-slip effects between concrete and steel bars, at that time the material parameters may be varied.
٢.Analysis fibrous reinforced concrete beam-column joint under cyclic load by using finite element model.

٣.Detailed numerical tests on interior beam-column joints are required .

٤.Time dependent effects are needed to be incorporated in this study . These effects include concrete shrinkage , creep , and aging of concrete.
٥.Modification and extension of the present work may be done to investigate dynamic behavior of the beam-column joints .
٦.Study the effect of construction joints at beam-column junctions in the multi story buildings.

ACI Committee ٣١٨, (١٩٩٥). "**Building Code Requirements for Reinforced Concrete (ACI ٣١٨-٩٥)**" American Concrete Institute, Detroit, U.S.A.

Agrawal, G. L. Tulin, L. G. and Gerstle, K. H. (١٩٦٥), **" Response of Doubly Reinforced Concrete Beams to Cycle Loading",** ACI Journal, Vol.٦٢, No٧, July, PP.٨٢٣-٨٣٣.

Al – Shaarabaf, I. A. S. (١٩٩٠). "**Three – Dimentional Nonlinear Finite Element Analysis of Reinforced Concrete Beams in Torsion**" Ph. D. Thesis, University of Bradford, Bradford, England.

AL-Niaemi, Q.A.M., (١٩٩٩), **"Nonlinear Finite Element Analysis of High Strength Fibrous Reinforced Concrete Beam-Column Joint",** M.Sc. Thesis, University of Technology, Iraq, ٣٢٣PP.

AL-Zahrawe R.A.D, (٢٠٠٥) "**Nonlinear Finite Element Analysis of Steel Fiber Reinforced Concrete Beams Subjected To Cyclic Load"** M.Sc. Thesis Al-Nahrain University, Baghdad, Iraq.

Ammar, Y. A., ٢٠٠١, **"Non-Linear Analysis For Behavior of Tensile Reinforcement Lap Splices in Reinforced Concrete Beams"** ,Ph.D. Thesis, University of Baghdad, Iraq.

Bathe, K.J., ١٩٩٦, **"Finite Element Procedures"** Prentice-Hall International, Inc., New Jersey, U.S.A.

Bass, R. A., Carrasquillo. R. L., and Jirsa, J. O. (١٩٨٩). *"Shear Transfer across New and Existing Concrete Interface"* ***ACI Struct. J., Vol. ٨٦, No (٤),pp ٣٨٣- ٣٩٣.***

Bathe, K. J., and Ramaswamy, S. (١٩٧٩). "**On Three – Dimensional Nonlinear Analysis of Concrete Structures**" Nuclear Engineering and Design, Vol. ٥٢, pp. ٣٨٥ – ٤٠٩.

Brown, R .H. and Jirsa, J. O. (١٩٧١), **"Reinforced Concrete Beams Under Load Reversals",** ACI Journal, Vol.٦٨, No٥, May, PP.٣٨٠-٣٩١.

Bresler, B. and Bertero, V. (١٩٦٨), **" Behavior of Reinforced Concrete Under Repeated Load"** Journal of Structural Engineering,(ASCE), Vol.٩٤, NoST٦, June, PP.١٥٦٧-١٥٨٩.

Chen,W.F. , (١٩٨٢), **" Plasticity in Reinforced Concrete"** McGraw-Hill, Inc, NewYork.

Cook, R. D. (١٩٧٤). "**Improved Two-Dimensional Finite Element**" J. Struct. Div., ASCE, ١٠٠(٩), ١٨٥١-١٨٦٣.

Cook R.D.(١٩٨١)**."Concepts and Applications of Finite Element Analysis."**٢nd Edition, John Wiley and Sons, New York.

Darwin, D. and Nmai, C. K. (١٩٨٦), **"Energy Dissipation in RC Beams Under Cyclic Load"** Journal of Structural Engineering,(ASCE), Vol.١١٢, No. ٨, August, PP.١٨٢٩-١٨٤٦.

Dawe, D. J., **"Matrix and Finite Element Displacement Analysis of Structures",** Clarendon Press, Oxford, U. K., ١٩٨٤.

Desai, C. S., Zaman, M. N., Lightner, J. G., and Siriwardane, H. J. (١٩٨٤). "**Thin – Layer Element for Interfaces and Joints**" International Journal for Numerical and Analytical Methods in Geomechanics, Vol. ٨, pp. ١٩ – ٤٣.

Durrani, A.J. and Wight, J.K., (١٩٨٥) , "**Behavior of Interior Column-Beam Connections Under Earthquake-Type Loading"** ACI Journal, May-June, PP.٣٤٣-٣٤٩.

Fronteddu, L., Léger, P., and Tinawi, R. (١٩٩٨). "**Static and Dynamic Behavior of Concrete Lift Joint Interfaces**" J. Struct. Engrg., ASCE, ١٢٤(١٢), ١٤١٨-١٤٣٠.

Hanson, N.W., and Connor, H.W., (١٩٦٧). **" Seismic Resistance of Reinforced Concrete Beam-Column Joints"** , Journal of the Structural Division (ASCE), Vol.٩٣, No.St٥, October, PP.٥٣٣-٥٥٩.

Harajli, M. H. (١٩٨٨), **"Behavior of Partially Prestressed Concrete Joints Under Cyclic Loading",** Journal of Structural Engineering,(ASCE), Vol.١١٤, No. ١١, November, PP.٢٥٢٥-٢٥٤٣.

Hamil, S.J, and Scortt, R.H., (٢٠٠٠), **" Developments in High Strength Concrete Beam-Column Connection Dsign",** Internet.

Hamz, D. M., (٢٠٠٥), "**Analysis Of Corner Beam-Column Junction With Inclusion Of The Effect Of Construction Joints",** M.Sc Thesis, Baghdad University, Iraq, ١١٥PP.

*Hofbeck J.A. ,Ibraham I.O.,and Mattock A.H.(١٩٦٩).**''Shear Transfer in Reinforced Concrete.''**ACI J.,* ٦٦*(* ٢*),* ١١٩-١٢٨.

Irons, B. M. (١٩٧١). "*Quadrature Rules for Brick Based Finite Elements"*

International Journal of Numerical Methods in Engineering, Vol. ٣, pp.

٢٧٥_ ٢٩٠.

Ismail, M. A. F. and Jirsa, J. O. (١٩٧٢), **" Bond Deterioration in Reinforced Concrete Subjected to Law Cycle Loads",** ACI Journal, Vol.٦٩, No٦, June, PP.٣٣٤-٣٤٣.

Jwad, K. R, (١٩٩٢), "**Nonlinear analysis of prestressed concrete frames under cyclic loading"** M.Sc Thesis, Mosul university, Iraq, February.

Kwak, H. G., and Kim, S., (٢٠٠١), *" Nonlinear Analysis of Reinforced Concrete Beam Subjected to Cyclic Loading"*, ***Journal of Structural Engineering, ASCE Vol. ١٢٧, No. ١٢, December.***

*Kupfer H.,Hilsdorf H.K.,and Raush H.(١٩٦٩).''**Behaviour of Concrete under Biaxial Stresses.''**ACI J.,Vol. ٦٦,No(٨),pp ٦٥٦-٦٦٦.*

*Lee Mattock A.H., and Hawkins N.M.(١٩٧٢).''**Shear Transfer in Reinforced Concrete-Recent Research.''**PCI J., ١٧(٢), ٥٥-٧٥, ٥٥-٧٥.*

*Mast R.F. (١٩٦٨).''**Auxiliary Reinforcement in Concrete Connections.''** Proc., ASCE, ٩٤(ST ٦), ١٤٨٥-١٥٠٤.*

Mattock, A. H. (١٩٨١). "**Cyclic Shear Transfer and Type of Interface**" J. Struct. Div., ASCE, ١٠٧(١٠), ١٩٤٥-١٩٦٤.

*Meinheit D.F., Jirsa J.O., (١٩٨١).''**Shear Strength of Reinforc Concrete Beam-Column Connections.''**ASCE, ١٠٧(ST ١١).*

*Mills G.M.(١٩٧٥).**''A Partial Kinking Criterion for Reinforced Concrete Slabs.''** Magazine of Concrete Research ٢٧(٩٠),PP ١٣-٢٢.*

Millard S.G.,and Johnson R.P.(١٩٨٤).**''Shear Transfer across Cracks in Reinforced oncrete due to Aggregate Interlock and to Dowel Action.''** Magazine of Concrete Research,٣٦(١٢٦).

Mohmood. A. K.,(٢٠٠١), "**Nonlinear Finite Element Analysis of Reinforced Concrete Members under Long-Term Loading"** M.Sc Thesis, Baghdad University, Iraq, ١١٥PP.

Moaveni, S. (١٩٩٩). "*Finite Element Analysis Theory and Application with ANSYS" Prentice – Hall, Inc., New Jersey.*

Naji, J. H.,(١٩٨٩) **" Nonlinear Finite Element Analysis of Reinforced Concrete Panels and Infield Frames under Monotonic and Cyclic Loading",** Ph. D. Thesis, University of Bradford, U.K.

Owen, D. R. J., and Hinton, E., (١٩٨٠) **"Finite Element in Plasticity: Theory and Practice"** Pineridge Press, Swansea, U. K.

*Paulay T., and Loeber P.J.(١٩٧٤).**''Shear Transfer by Aggregate Interlock"** . Shear in Reinforced Concrete,Detroit,American Concrete Institute,ACI Special Publication SP ٤٢-١. ١, ١-١٥,(Cited by Millard and Johnson (١٩٨٤)).*

Paulay T., (١٩٨٩)**.''Equilibrium Criteria for R/C Beam-Column Joints" .* ***ACI Structural Journal, Vol. ٨٦, No. ٦, November-December, PP. ٦٣٥-٦٤٣.

Phillips, D. V., and Zienkiewicz, O.C., (١٩٧٦), **" Finite Element Nonlinear Analysis of Concrete Structures"** Proceedings of Institute of Civil Engineers, Vol.٦١, Part ٢, PP.٥٩-٨٨, [mentioned in Al-Shaarabaf (١٩٩٠)].

*Sarsam K.F.(١٩٨٣).**''Strength and Deformation of Structural Concrete Joints.''**Ph.D. Thesis ,University of Manchester.U.K.*

Sarsam, K.F., and Phipps, M.E., (١٩٨٥), **"The Shear Design of In-Situ Reinforced Concrete Beam-Column Joints Subjected to Monotonic Loading",** Magazine of Concrete Research, Vol.٣٧,No.١٣٠,March, PP.١٦-٢٨.

Scanlon, A. (١٩٧١). "**Time Dependent Deflections of Reinforced Concrete Slabs**" Ph. D. thesis, University of Alberta, Edmonton, Alberta, Canada. [mentioned by Al – Shaarabaf (١٩٩٠)].

Sinha, B. P. Gertle, K. H. and Tulin, L. G. (١٩٦٤), **" Response of Singly Reinforced Beams to Cycle Loading" ,**ACI Journal, Vol.٦١, No٨, August, PP.١٠٢١-١٠٣٧.

Tassios T.P.,and Vintzèleou E.N.(١٩٨٧).*''Concrete-to-Concrete Friction.''****J. Struc. Engrg.,ASCE, ١١٤(٩), ٢١٣٣- ٢١٣٦.***

Taplin, G., and Grundy, P., (١٩٩٨) "*Steel-Concrete Composite Beams Under Repeated Loading" ,* ***Department of Civil Engineering, Mnash University (Internet), Department of Civil Engineering, Monash University.***

Ueda, T., Lin, I., and Hawkins, N.M., (١٩٨٦), **" Beam Bar Anchorage in Exterior Column-Beam Connections",** ACI Journal, May-June, PP.٤١٢-٤٢٣.

Verna, J. R. and Stelson, T. E. (١٩٦٢), **"Failure of Reinforced Concrete Under Repeated Loads ",** ACI Journal, Vol.٥٩, No١٠, October, PP.١٤٨٩-١٥٠٣.

Verna, J. R. and Stelson, T. E. (١٩٦٣), **" Repeated Loading effect on Ultimate Static Strength of Concrete Beams",** ACI Journal, Vol.٦٠, No٦, June, PP.٧٤٣-٧٤٩.

*Walraven J.C., and Reinhardt H.W.(١٩٨١).****''Concrete Mechanics, Part A. Theory and Experiments on the Mechanical Behaviour of Cracks in Plain and Reinforced Concrete Subjected to Shear Loading.''****Heron. ٢٦(١A), ١- ٦٨,(Cited by Millard and Johnson (١٩٨٤)).***

Wight D.L., Hanson J.K., (١٩٧٧) ***.''Reinforced Concrete Beam-Column Joints under Large Load Reversals.''*** *Proc ASCE., ١٠٣(ST ١٢).*

Yankelevsky, D. Z. and Reinhardt, H. W. (١٩٨٧), **"Model for Cyclic Compressive Behavior of Concrete"** Journal of Structural Engineering,(ASCE), Vol.١١٣, No. ٢, February, PP.٢٢٨-٢٤٠.

Yankelevsky, D. Z.and Reinhardt, H. W. (١٩٨٩), **"Uniaxial Behavior of Concrete in Cyclic Tension",** Journal of Structural Engineering,(ASCE), Vol.١١٥, No. ١, January, PP.١٦٦-١٨٢.

Zia, P. (١٩٦١). "**Torsional Strength of Prestressed Concrete Members**" ACI J., ٥٧(١٠), ١٣٣٧-١٣٦٠.